Synthesis and Investigation of Reactivity of Alkylated Tripeptides with Metal Ions

Gerður Rún Rúnarsdóttir

Faculty of Physical Sciences
University of Iceland
2016

Synthesis and Investigation of Reactivity of Alkylated Tripeptides with Metal Ions

Gerður Rún Rúnarsdóttir

90 ECTS thesis submitted in partial fulfillment of a
Magister Scientiarum degree in Inorganic Chemistry

Advisor(s)
Dr. Sigríður G. Suman

Faculty Representative
Prof.Dr. Ingvar Árnason

External examiner
Dr. Gissur Örlygsson

Faculty of Physical Sciences
School of Engineering and Natural Sciences
University of Iceland
Reykjavik, June 2016

Synthesis and Investigation of Reactivity of Alkylated Tripeptides with Metal Ions
90 ECTS thesis submitted in partial fulfillment of a *Magister Scientiarum* degree in Inorganic chemistry

Faculty of Physical Sciences
School of Engineering and Natural Sciences
University of Iceland
Dunhagi 3
107, Reykjavik
Iceland

Telephone: 525 4000

Bibliographic information:
Gerður Rún Rúnarsdóttir, 2016, *Synthesis and Investigation of Reactivity of Alkylated Tripeptides with Metal Ions*, Master's thesis, Faculty of Physical Sciences , University of Iceland.

Printing: Háskólaprent ehf.
Reykjavik, Iceland, June 2016

Abstract

Release of greenhouse gases is a great environmental concern in todays world. Carbon dioxide is the thermodynamic end product of combustion of organic compounds and it is one of the most abundant greenhouse gases. CO_2 is known as relatively thermodynamically stable and to have high kinetic barrier.A feasible approach to trap and recycle CO_2 from industrial waste in an economical manner is to reduce it to C1 starting materials such as methanol, methane, or formic acid for the chemical industry. Formation of these C1 products is facilitated when metal based catalysts are employed to lower the kinetic barrier and provide a reaction pathway that may occur under ambient conditions. The long term vision is to synthesize a biodegradable CO_2 copolymer.

In the research presented, synthetic methodology for a novel tripeptide, using liquid phase peptide synthesis, was completed. The tripeptide was employed as a ligand to form a palladium complex that was characterized. Our approach uses alkylated tripeptides as a ligand that can coordinate to a metal ion forming 5 or 6 membered ring chelates which are also the thermodynamically most stable form of chelation and may form a complex that is coordinatively unsaturated. Alkylated glutathione was used as a model tripeptide and its reaction with was investigated.

Útdráttur

Gróðurhúsalofttegundir eru eitt af stærstu umhverfisvandamálum samtímans. Koltvíoxíð (CO_2) myndast við bruna lífrænna efna og er mjög varmafræðilega stöðugt. Endurvinnsla á CO_2 er aðalega fólgin í afoxun CO_2 í eins kolefnis efni (C1) sem síðan eru notuð sem upphafsefni í aðra efnaferla t.d. metanól, metan og formaldehýð. Afoxun CO_2 er orkufrekt ferli sökum hárrar stöðuorku efnisins. Málmhvatar geta þó lækkað virkjunarorku afoxunarinnar og gert afoxun á CO_2 mögulega við mildar aðstæður. Langtímamarkmið verkefnisins er að smíða umhverfisvæna CO_2 fjölliðu sem brotnar niður í náttúrunni.

Rannsóknirnar sem hér eru kynntar sýna samsettar efnasmíðar á nýju trípeptíði með notkun vökvafasa aðferð til peptíðefnasmíða. Trípeptíðið var notað sem tengill til efnasmíða á palladium komplex. Lagt var upp með að nota alkyleruð trípeptíð sem þrítenntan tengil sem gæti myndað komplex og myndað 5 og 6 atóma hringi við málmjónina í byggingu sinni. Alkylerað GSH var einnig notað til að athuga hvort möguleiki væri á myndun komplex með 7 atóma hring tengdann við málmjón í byggingu sinni. Lýst er alkylun glútaþíons og hvarfgirni þess við nokkrar málmjónir.

To my brother in law, that was

a lot on my mind while I wrote this thesis

Table of Contents

List of Figures

List of Schemes

List of Tables

Abbreviations

$CHCl_3$	Chloroform
CHN	Elemental analysis
CH_3CN	Acetonitrile
COD	1,5-Cyclooctadiene
COSY	Correlation spectroscopy
DCM	Dichloromethane
DIC	*N,N′*-Diisopropylcarbodiimide
DIU	*N,N′*-Diisopropylurea
DMF	Dimethylformamide
Ea	Ethyl acetate
EDC	1-Ethyl-3-(3-dimethylaminopropyl)carbodiimide
EDU	1-Ethyl-3-(3-dimethylaminopropyl)urea
EtOH	Ethanol
Fmoc	Fluorenylmethyloxycarbonyl
GABA	Gamma-aminobutyric acid
GSH	Glutathione
GSSG	Glutathione disulfide
HOBt	Hydroxybenzotriazole
i-PrOH	Isopropyl alcohol
IR	Infrared spectroscopy
LPPS	Liquid-phase peptide synthesis

MeOH	Methanol
MS	Mass Spectrometry
NHE	Normal hydrogen electrode
NMR	Nuclear magnetic resonance
O_h	Octahedral
UV-Vis	Ultraviolet–visible spectroscopy
SPPS	Solid–phase peptide synthesis
TEA	Triethylamine
TEAE	Tris(2-amino-ethyl)amine
TEOA	Triethanolamine
T_d	Tetrahedral
TMSCl	Chlorotrimethylsilane

Acknowledgements

First and foremost I would like to thank my supervisor Dr. Sigríður Suman for her guidance, advice and patience throughout my studies. It has been a pleasure and fun working with her and she has taught me a lot.

Secondly I would like to thank my lab partner Lindsey Jean Monger for ALL her help, discussion about glutathione, chemistry in general and her involvement in my project. I also thank present members of the Suman research group; Jóhönnu Margréti Grétarsdóttur, Hafdísi Ingu Ingvarsdóttur and Benedikt Orra Birgissyni as well as former members Þorvaldi Snæbjörnssyni and Philipp Scharf, for all their help and for creating a fun atmosphere in the lab.

At the University of Iceland I would like to thank: Dr. Sigríður Jónsdóttir for NMR and MS measurements and all her help. Svana H. Stefánsdóttir for providing chemicals and her constant willingness to help. Sverrir Guðmundsson for supplying glassware and repairing the glass I broke. I also would like to thank all my coworkers at Raunó for their advice, help and company thoughout my studies. It was a pleasure.

At the University of Debrecen I would like to thank: Prof. Dr. Etelka Farkas for her hospitality during my STSM project and guidance. I had a really great time there and I learned a lot from her. I also want to thank Péter László Parajdi-Losonczi for all his help with potentiometric studies.

Last but not least I would like to thank my wonderful family for their support and patience, especially my boyfriend Magnús Karl Ásmundsson.

1 Introduction

Release of greenhouse gases is a great environmental concern in todays world. Carbon dioxide (CO_2) is the thermodynamic end product of combustion of organic compounds and it is one of the most abundant green house gases. CO_2 is known as relatively thermodynamically stable an to have high kinetic barrier.[1] A feasible approach to trap and recycle CO_2 from industrial waste in an economical manner is to reduce it to C1 starting materials such as methanol, methane, or formic acid for the chemical industry. Formation of these C1 products is facilitated when metal based catalysts are employed to lower the kinetic barrier and provide a reaction pathway that may occur under ambient conditions.[2,3] Reduction reactions of CO_2 to some organic compounds along with their standard reduction potentials (E^0) are shown in Scheme 1.1. Clearly, CO_2 is not a good oxidizing agent.

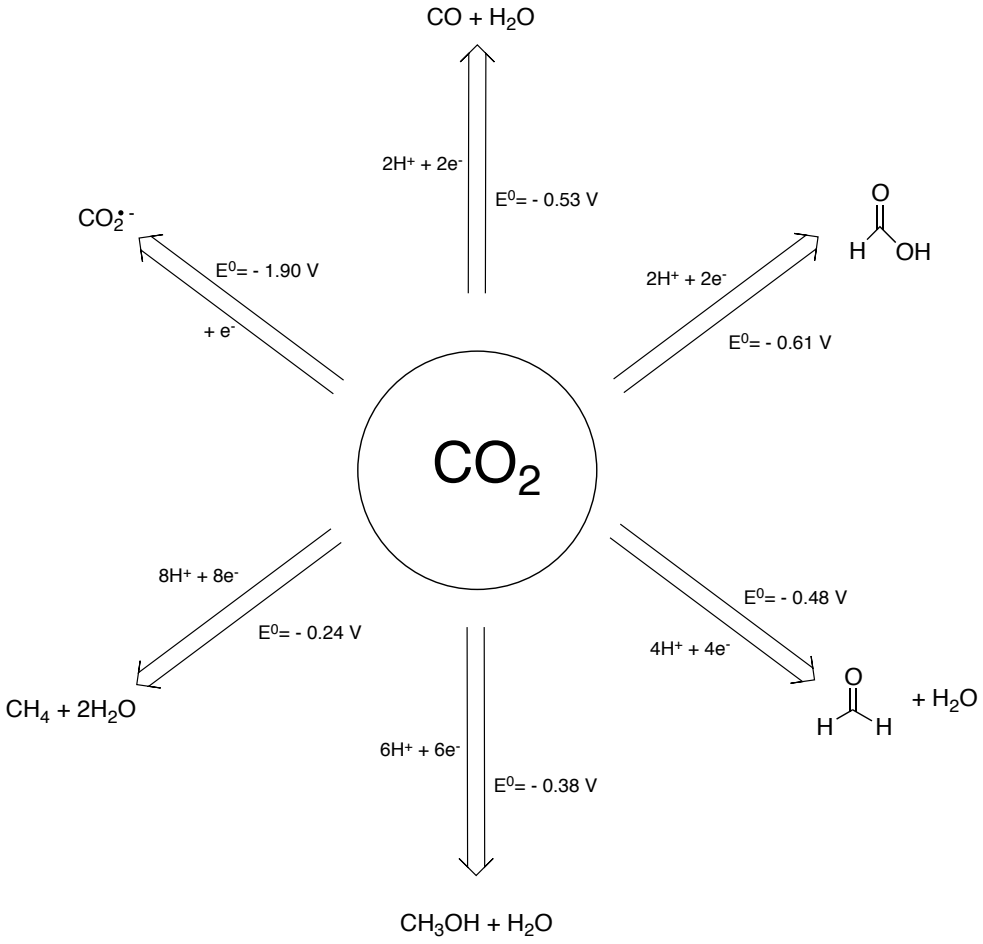

Scheme 1.1: Reduction potentials, $E^{0,}$ of CO_2 using NHE electrode at pH 7, at standard conditions using 1M solutes.[4]

From an industrial point of view there are no efficient routes to introduce CO_2 into organic compounds under ambient conditions. The processes that are now known are neither energy friendly nor atom economic.[1] CO_2 characteristics as a nonpolar compound containing polar bonds that may be exploited to activate it in chemical reactions. The oxygen atoms are nucleophilic while the carbon is electrophilic. However the electrophilicity of the carbon is greater than the nucleophilicity of the oxygen atoms, resulting in CO_2 usually behaving as an electrophile in chemical reactions. Due to these functionality differences bifunctional catalysts are often required for CO_2 activation.[1] CO_2 has strong affinity towards electron donating reagents and nucleophiles (acts as an acid), and reacts with bases. An example of a successful activation of CO_2 is formation of cyclic organic carbonates, from a reaction with epoxy, that then may be used as a substrate for further compound synthesis or may be used as a substrate in manufacturing of polycarbonates, this is a multistep process requiring more than one catalyst, and is expensive from industry point of view.[5]

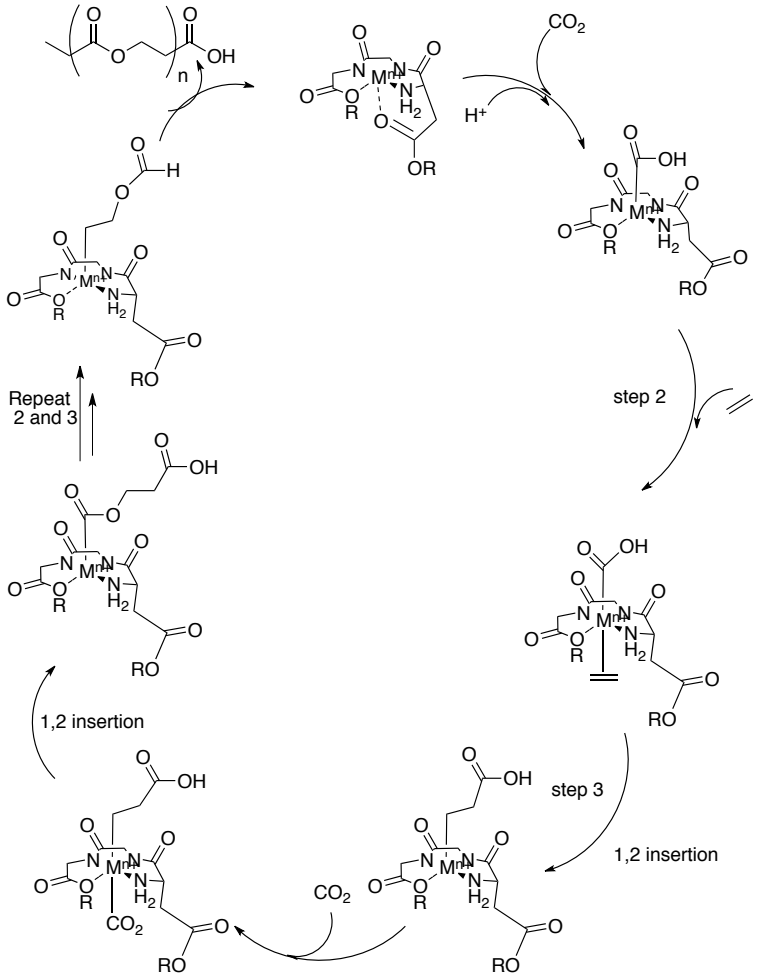

Scheme 1.2 : Proposed catalytic cycle for copolymerization of CO_2 and ethylene. For the coordination of the CO_2 the assumption is made that the metal center has high electron density.

The project long-term vision is to synthesize a highly active catalyst intended for CO_2 and ethylene copolymerization forming a biodegradable CO_2 copolymer at ambient conditions. A possible catalytic cycle is described in Scheme 1.2.

When designing a catalyst for polymerization a lot of features need to be considered to form well-defined, highly active catalysts able to synthesize regularly alternating, high molecular weight, and monodispersed carbon dioxide/ethylene copolymers. For example the competition of the ligands (CO_2/alkene) toward metal coordination needs to be balanced for alternating coordination. Complex deactivation needs to be minimized or prevented, but such deactivation may happen for example by forming a terminal metal oxo complex. Finally, the electron density of the metal center needs to be feasible. The complex also needs to be coordinatively unsaturated so that the ethylene and carbon dioxide can coordinate to the metal ion. Due to these requirements, formation of a complex with a tetrahedral or square planar geometry is probably the best solution, leaving two sites uncoordinated. Also it is possible to form trigonal bipyramidal or square pyramidal geometry where the fifth coordination site is loosely coordinated to the metal ion. This leaves at least one coordination site open for catalytic purposes. Size of the ligand is also important where too bulky ligands can kinetically block the open coordination site by shielding the open coordination site of the metal.[6] Research on Co(II) complexes has shown that some are able to bind CO_2, and Zn(II) complexes are able to catalyze carbon dioxide and epoxide copolymerization producing aliphatic polycarbonates under relatively mild conditions with high activity, therefore these are metals of primary interest.[2,3] Copper and nickel are also interesting due to the complex geometry they support (both T_d and O_h) and their ability to deprotonate amides at pH < 9.[6] Pd(II)-catalysts are also powerful catalysts for copolymerization of CO and alkene forming polyketones.[7]

The research described in this thesis is synthesis of a ligand that can coordinate to a metal without saturating the metal coordination sites. Coordination of peptides to a metal ion has been studied extensively in the literature.[8,9,10] It has been shown on multiple occasions that the formation of 5 membered rings and 6 membered rings is the thermodynamically most stable form of chelation.[8,9,10,11] Coordination of di- and tripeptides with metal ions forming chelates with five membered rings (5,5,5 chelates), and a mixture of six and five membered rings (6,5,5 chelates) form readily under basic conditions with first row transition metal ions, as well as with platinum, and palladium.[8,9,10,11] Our approach is to use alkylated tripeptides as a ligand that could along with metal ion support the geometry and the chelation described above. The goal of this project is to synthesize a novel alkylated tripeptide using a liquid-phase peptide synthesis (LPPS), and to modify a commercially available tripeptide, glutathione (GSH), by alkylating the carboxylate termini and the thiol side group. The aqueous reactivity of the alkylated GSH with metal ions was investigated using potentiometry, and NMR studies. The Pd(II) complex of the novel tripeptide was isolated and characterized.

2 *iso*Asp-Ala-Gly (5)

2.1 Synthesis of 5

Peptides are synthesized by coupling together two amino acids, peptide and amino acid or two peptides. The reaction is a condensation reaction of the carboxylic group of one amino acid and the amine of another resulting in elimination of water and formation of an amide bond. The product is a peptide/oligopeptide. The most common way to synthesize peptides is solid-phase peptide synthesis (SPPS). SPPS is a method where the first amino acid of the sequence is covalently bound to a solid resin particle, and then there is a stepwise addition of protected amino acids to the first amino acid. The elongation of the peptide is toward the N-terminal end. The fact that the peptide is attached to completely insoluble solid resin makes it very easy to remove unreacted reagent and side products by washing and filtering. This method is rapid and eliminates the process intermediates and further work up procedures.[12] The downside of this method is low yield and small-scale reactions. In my research I used LPPS with can be carried out under homogenous conditions. With this method less amount of coupling reagent and amino acid are required compared to SPPS. This makes LPPS more economic and it is better suited in process development for larger scale synthesis of short peptides. The downside to LPPS is long reaction time, time-consuming work up, multiple step reactions with isolation of the intermediates and compatibility complications when synthesizing peptides with dissimilar side chains that are hydrophilic, and hydrophobic. Similarly, LPPS is limited to synthesis of 20 amino acid or shorter.[13,14]

Like described in the Introduction the goal was to synthesize a peptide that would specifically form a 6 membered chelate at the NH_2 terminal, and two 5 membered ring chelates to form overall a four-coordinate complex, optionally with weak axial interaction forming five–coordinate complex. To achieve this, structures of several amino acids were studied to decide what would be a good design for a ligand. After careful consideration synthesis of O^{t}Bu-*iso*Asp-Ala-Gly-OMe with LPPS from glycine(Gly), alanine(Ala) and aspartic acid(Asp) was selected.

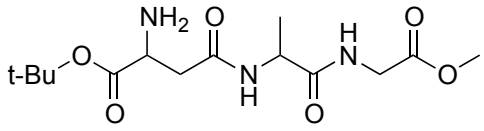

Figure 2.1 : Structure of O^{t}Bu-isoAsp-Ala-Gly-OMe.

Glycine is the smallest amino acid and has a proton as a side chain. Alanine is also a small amino acid containing a methyl group as a side chain. Both of these amino acids contain a side chain generally referred to as non-coordinating and therefore would not chelate to the metal. Aspartic acid has an extra carboxyl group as a side chain, which is referred to as a week coordination side chain meaning that it has no significant effect on the coordination chemistry of complexes. But they still affect their thermodynamic stability.[15] As mentioned before, aspartic acid contains two carboxylic acids. To form O^{t}Bu-*iso*Asp-Ala-Gly-OMe the peptide bond needs to be placed between the amino group of the alanine and the β-

carboxyl group of aspartic acid (*iso*Asp), that is so the complex formed can have (6,5,5 chelates) (Figure 2.2.b) rather than (5,5,5 chelates) (Figure 2.2.a).

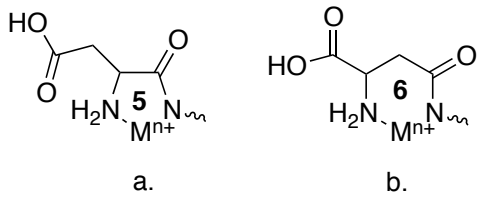

Figure 2.2 : Chelation of peptide to a metal ion containing a) aspartic acid and b)iso-aspartic acid at C-terminal end.

In coupling reactions, aspartic acid has the tendency of forming the peptide though the α-carboxyl group due to its lower pKa value compared the β-carboxyl group. Consequently the α-carboxyl group had to be protected. To couple these amino acids together, protection groups were needed to control the coupling and the sequence. In our synthesis we used Fmoc protection group(Figure 2.3) to protect the amino group of the aspartic acid and alkyl groups; methyl (-CH_3) and *tert*- butyl ($C(CH_3)_3$), to protect the two terminal carboxyl groups.

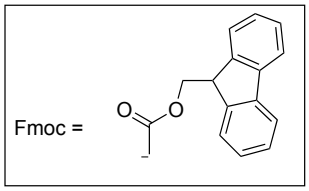

Figure 2.3: Structure of the Fmoc protection group.

2.1.1 Retrosynthesis of 5

O^{t}Bu-*iso*Asp-Ala-Gly-OMe is an unusual peptide due to the fact that it has two alkylated carboxylic acids. Retrosynthetic analysis was performed on the target tripeptide based on commercially available precursors. Two pathways were considered. The first approach is shown in Scheme 2.1.

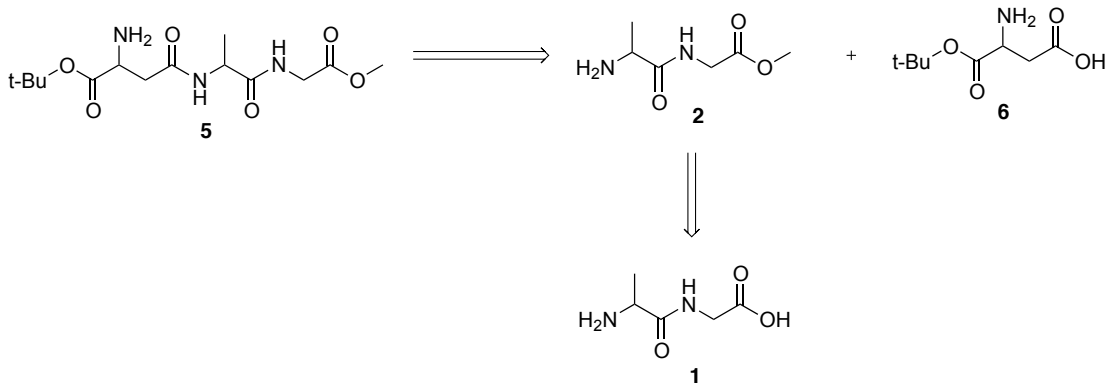

Scheme 2.1 : Retrosynthetis of alkylated isoAsp-Ala-Gly tripeptide without protecting the amino group.

The Scheme 2.1 shows how the target compound **5** is broken down to two compounds, where compound **6** is a substrate while compound **2** is an intermediate formed from esterification of substrate **1.** Both the substrates **1** and **6** are commercially available and can be bought for a reasonable price. The alkyl protection groups on the carboxyl groups have different roles. For the intermediate **2** it is there to ensure the coupling reaction occurs on the amino N-terminal end of the peptide and for substrate **6** it is there to ensure the

coupling reaction occurs on the β −carboxylic group of the amino acid. Asp has two carboxylates, the α- carboxylic group has lower pKa and therefore is more likely to participate in the coupling reaction. But because we want to form 6 membered chelate, through the amino N-terminal and the secondary amine of that peptide bond the peptide coupling has to occur with the the β −carboxylic group of the Asp.

Retrosynthetic analysis for a pathway of coupling reaction is more likely to succeed, when a protection group is present on the amino group of the aspartic acid as is described in Scheme 2.2.

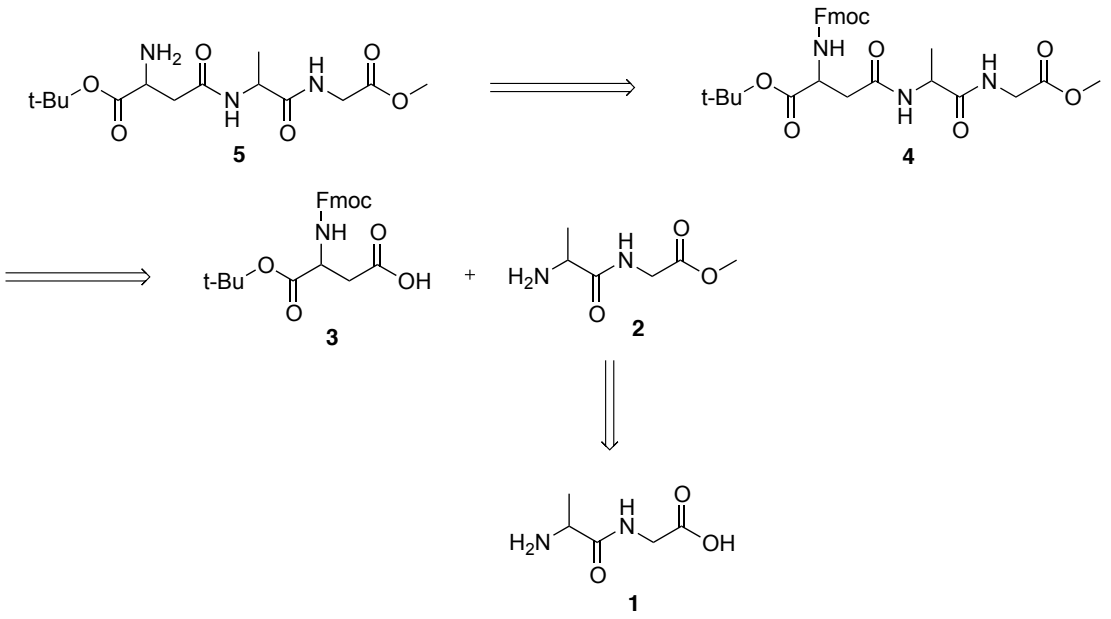

Scheme 2.2: Retrosynthesis of isoAsp-Ala-Gly ligand with protecting the amino group.

The Scheme 2.2 shows how the target compound **5** is broken down into two compounds via intermediate **4.** Compound **3** is a substrate while, as in Scheme 2.1, **2** is an intermediate formed from esterification of substrate **1.** Both the substrates **1** and **3** are commercially available and can be bought for a reasonable price. In this synthesis protection groups are used to control the coupling reaction. The alkyl protection groups have the same purpose as in Scheme 2.1 The Fmoc group on the amine on substrate **3** is introduced to ensure the coupling reaction occurs through amino group of the H-Ala-Gly-OMe instead of the aspartic acid. And also to prevent side reactions that may be, for example, intermolecular reaction.

Both of the synthetic routes from Scheme 2.1 and Scheme 2.2 were tried. As predicted, the Fmoc protecting group is necessary in these reactions. When reacted without the Fmoc group the ^{1}H NMR spectrum of the product showed aromatic protons indicating that intermolecular reaction involving ring closure took place. Therefore it was decided to continue with synthesis shown in Scheme 2.2. The three steps synthesis of O^{t}Bu-*iso*Asp-Ala-Gly-OMe is described below.

2.1.2 Esterification of 1

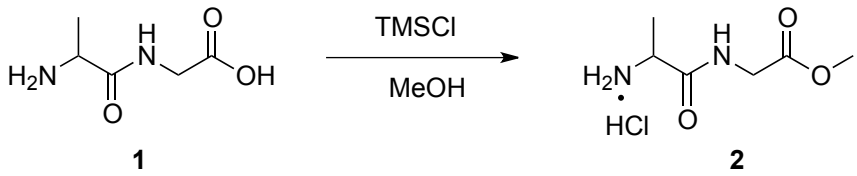

1 **2**

*Scheme 2.3 : Esterification of **1** using MeOH/TMSCl method.*

Methanol(MeOH)/trimethylchlorosilane (TMSCl) esterification method was selected for this reaction.[16] Mainly because it requires mild reaction conditions followed with a fairly simple workup and gives excellent yields. The reaction was carried out in methanol (solvent and a reactant) containing **1** and TMSCl that acts as an acid precursor to form an acid catalyst and a dehydrating agent. Product **2** is formed via silyl ester intermediate. HCl is formed in the reaction resulting in formation of hydrochloride salt of product **2**. The TMSCl was dried over CaH_2 and was used freshly distilled. The reaction condition uses 2 eq. of TSMCl, and the importance of using slightly more than 2 eq was confirmed by experiment. Another important part is that the reactions are carried out in air, rather than inert gas that seemed to slow down the reaction. The reaction is an equilibrium reaction and therefore MeOH is used also as a solvent to push the reaction toward the product, followed by the formation of hexamethyldisiloxane (HMDSO) in an irreversible reaction, pushing the reaction toward the formation of **2.** The product is a hydrophobic white crispy solid formed in almost quantitative yields. The compound was characterized by ^{1}H NMR presented in Appendix A, which showed a singlet at 3.72 ppm for the methyl groups with proper integration. The compound is kept under inert gas since it is hygroscopic.

2.1.3 Coupling reaction of 2 and 3

The method used for this coupling reaction employs carbodiimide as a reagent along with hydroxybenzotriazole (HOBt). HOBt is a base primarily used to avoid competing intermolecular O to N rearrangement. The mechanism of the coupling reaction mechanism is simple but several side reactions complicate the reaction. The mechanism of the reaction and side reactions are shown in Scheme 2.4.

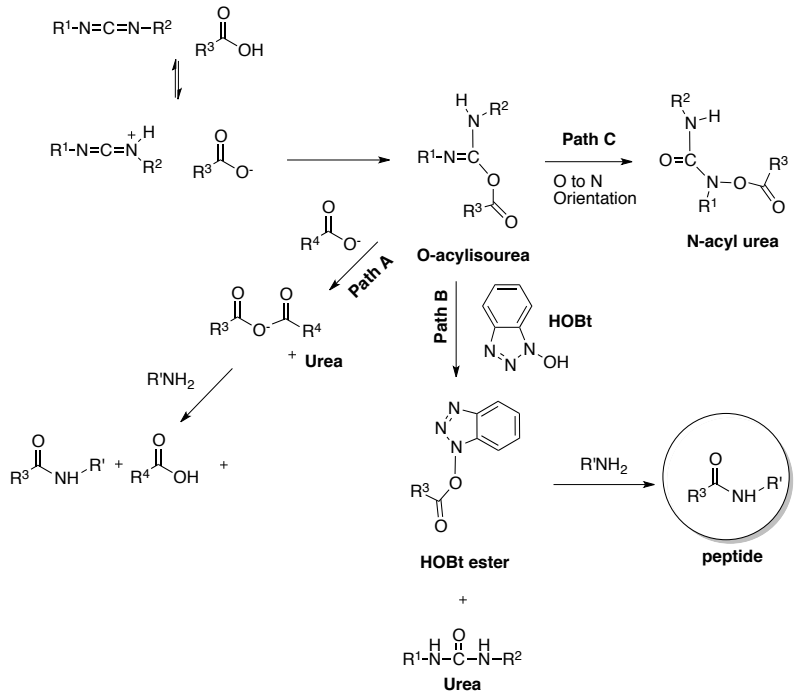

Scheme 2.4 : Mechanism and side reaction in peptide coupling synthesis using carbodiimide as a reagent .[17,18]

The paths referred to in this section are from Scheme 2.4. The first step of the coupling reaction is protonation of the carbodiimide forming a carbocation. The carboxylic acid (after deprotonation) then reacts with the carbocation forming the key intermediate o-acylisourea. Here a competing intermolecular O to N orientation of the carboxylic acid leading to formation of a stable N-acylisourea can occur (Path C). HOBt can inhibit this reaction by nucleophilic attack on the ester of the o-acylisourea which expels this very stable urea as a leaving group forming HOBt ester (Path B).[19] The peptide is formed when a primary amine (non-dissociated nucleophile) attacks the new intermediate resulting in expulsion of HOBT and formation of **4**. In the absence of any added nucleophile another side reaction can happen where the o-acylisourea can react with extra carboxylic acid and form acid anhydride which can then react further with amines and form peptide and urea (Path A).[20] This side reaction also results in the desired product though another mechanism. Due to all these side reactions the reaction conditions need to be controlled very carefully and it is important to use a non-polar solvent to minimize the side products.

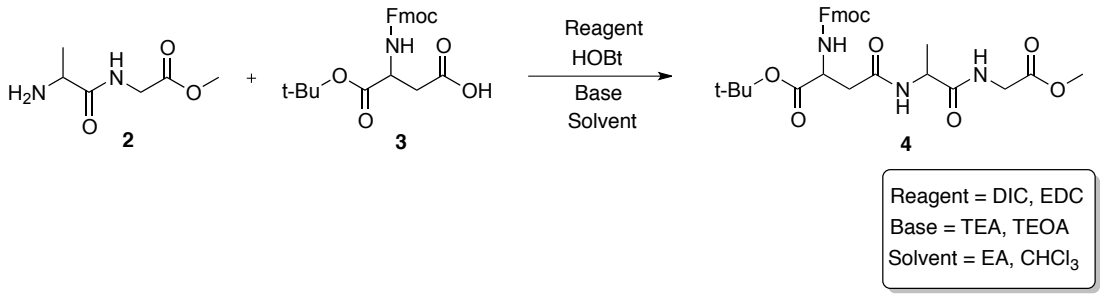

*Scheme 2.5 : The reaction condition of coupling reaction of **2** and **3** to form **4**.*

Several approaches were tried in attempts to synthesize **4.** The first approach was to use DIC as a reagent, triethanolamine (TEOA) as the base and ethyl acetate (EA) as solvent. This did not work well and the ^{1}H NMR of the crude products showed peaks in the aromatic region indicating that intermolecular reaction had taken place probably EA is too polar solvent for the reaction and can fuel the side reactions. Then the solvent was changed to a nonpolar solvent $CHCl_3$ and the rest of the substrates were unchanged. Then the coupling seemed to have occurred but the ^{1}H NMR of the crude product showed the alkyl protection groups of the ester were absent. The solution was probably too acidic, which can cause acid catalyzed hydrolysis, so a stronger base, triethylamine (TEA, pka ~ 10), was tried next and all other substrates kept unchanged. ^{1}H NMR showed coupling reaction was successful, however the separation of the DIU and the product was impossible because it had the same solubility in all solvents as the product. Then the carbodiimide was changed to 1-ethyl-3-(3-dimethylaminopropyl)carbodiimide hydrochloride (EDC) which worked well resulting in an easy separation with silica gel chromatography affording a clean product **4**. The reaction took 24 hours resulting in white powdery solid in 55% yield. Compound **4** was characterized using ^{1}H NMR, ^{13}C NMR, COSY, IR, MS and CHN analysis, the spectra are shown in Appendix B.

2.1.4 Cleavage of the Fmoc group of 4

The Fmoc group is the most common protection group for amine groups in peptide synthesis, due to its stability under acidic conditions. The cleavage of Fmoc is usually carried out by a base though β- elimination that exploits the acidity of the proton on the β-carbon on the Fmoc group. The base reagents usually used are aqueous ammonia, ethanolamine, piperidine, pyridine, morpholine, or tris(2-amino-ethyl)amine (TAEA), TEA.[21,22,23]

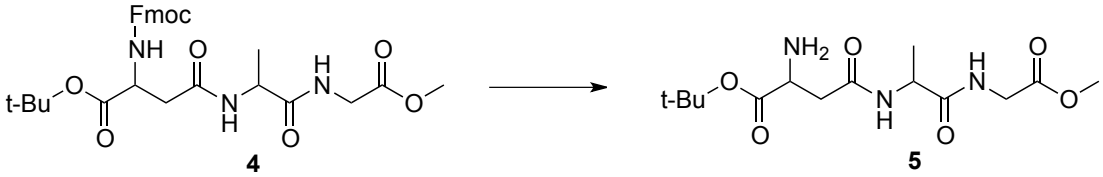

*Scheme 2.6 : Cleavage of the Fmoc group from **4;** formation of **5**.*

Four different reagents were explored for the cleavage reaction to form **5** (Scheme 2.6). The first attempt used piperidine as a base and DMF as the solvent. This reaction was tried over several different timeframes. Some of these attempts led to cleavage of the Fmoc group and also to intermolecular ring closure. Then another base and solvent were tried, TEA as the base and pyridine (distilled) as the solvent. This approach led to formation of an insoluble compound, and a tiny amount of that white compound, but too little to analyze, even with NMR spectroscopy. If this product had been the desired product, the yield would have been unacceptably small, so this method was eliminated. Third method involved using TAEA in dichloromethane (DCM) which lead to cleavage of the Fmoc and also to the intermolecular reaction. The intermolecular ring closure in the reactions above is most likely promoted by deprotonation of the amine carried out by the base. It was concluded this side reaction is happening because the base is too strong. Final trial was using a mild base like DMF which can act as a Lewis base and by heating the reaction to ~

120°C to increase the base behavior of the DMF. DMF was also used as the solvent so it is in excess. Reaction was run over several different timeframes. The best results were observed after 4-5 hours of stirring that resulted in yellow oil in about 65% yields. The oil was purified using chromatography on silica gel. This compound is hygroscopic and was stored under inert gas. The compound was characterized using ^{1}H NMR, ^{1}H COSY ^{13}C, IR and MS. The spectra are shown in Appendix C.

2.2 Synthesis of palladium complexes 8 and 9

In our laboratory we are exploring coordination of tripeptides to different metal ions as a part of synthesis of complexes that can catalyze CO_2 copolymerization as described in the Introduction. The modified tripeptide O^{t}Bu-*iso*Asp-Ala-Gly-OMe has three possible nitrogen coordination sides. They are the amine group of the aspartic acid and two amides in the backbone of the peptide (peptide bonds). Also the oxygen atoms of the terminal esters could weekly interact with the metal. Pd(II) complexes usually have square planar geometry, distorted octahedral Pd(II) complexes have been reported but they are rare.[24] Therefore Pd(II) complexes are unlikely to support higher coordination geometry as described in the Introduction. However Pd(II) complexes are known to catalyze copolymerization of CO and organic alkenes to form highly regular polyketone polymers.[7] Pd(II) can deprotonate amide groups at moderate pH and it has been reported that Pd(II) can form metal amide bond at around pH ~ 2.[25] Because of these properties, Pd(II) is an interesting metal ion to use in our investigation of chelation of the novel alkylated tripeptide. The O^{t}Bu-*iso*Asp-Ala-Gly-OMe was employed as a ligand to form a palladium complex that was characterized using MS and IR

In a reaction of potassium tetrachloro palladate (K_2PdCl_4) and **5** there are at least three possible species that could form theoretically. All these chelations are shown in Scheme 2.7. For example, formation of a dimeric complex with two bridging chlorine atoms as shown marked **7** in Scheme 2.7 having κ^2 (NH_2, N^-) chelation of the peptide. Formation of **7** can either have *cis*- or *trans*- configuration. Isomer shown in Scheme 2.7 is the *trans-isomer* and would be more likely to be formed due to steric effects.. Monomeric complex can also be formed with κ^3(NH_2, $2N^-$) chelation with one chloride still attached to the metal as shown marked **8** in Scheme 2.7 or κ^4 (NH_2, $2N^-$,O) chelation as shown marked **9** in Scheme 2.7.

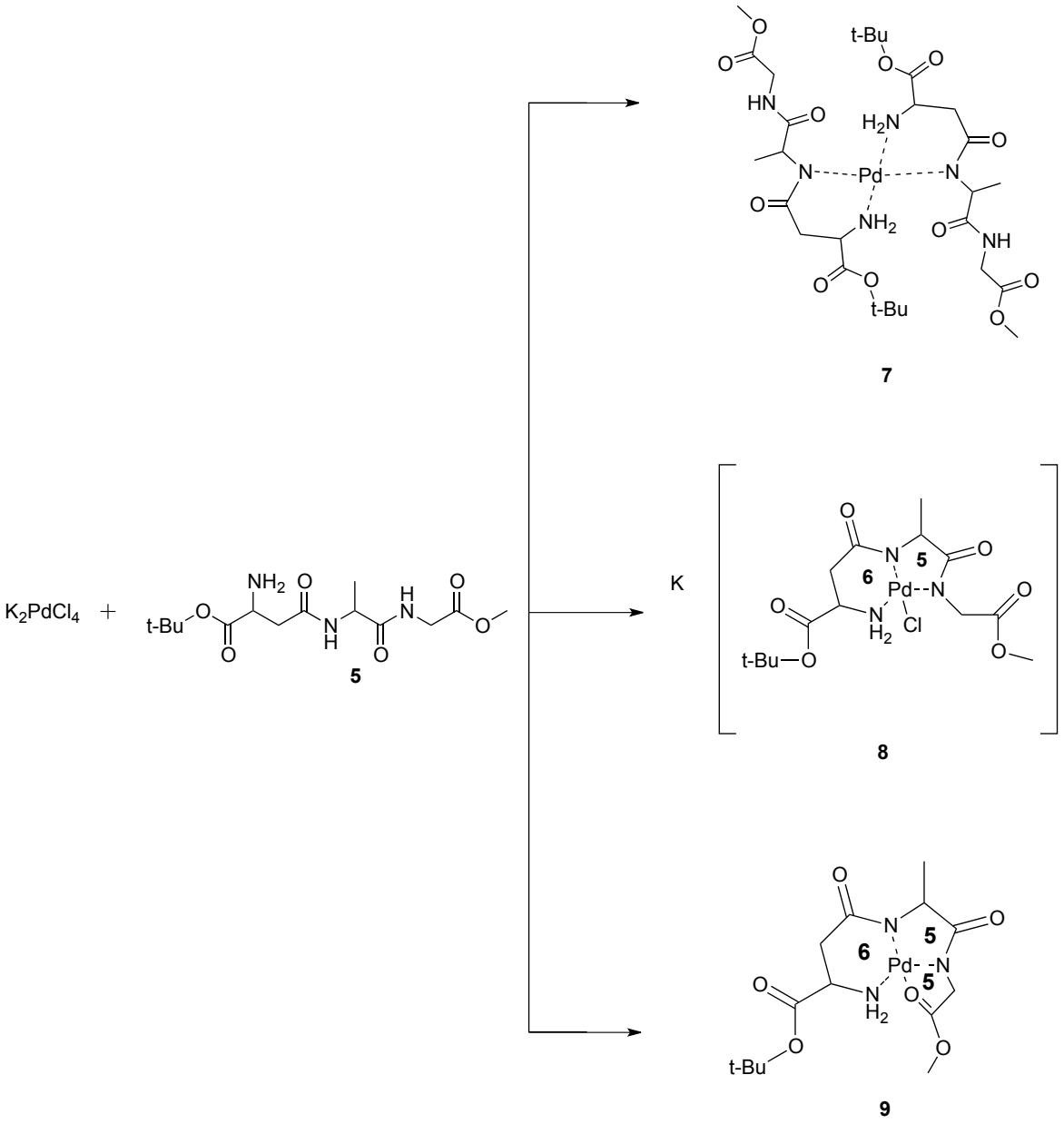

*Scheme 2.7 : Three possible chelation of **5** to Palladium (II).*

As described above, Pd(II) can deprotonate amine at pH ≥ 2. That is why this reaction is carried out in H_2O under inert gas (N_2) without adding base or other reagents. The reaction was monitored by UV-Vis spectroscopy, the shift of the d-d transition peak from 420 nm (K_2PdCl_4) to 333 nm indicates that a reaction took place. The peak did stop moving after 4 hours indicating that the reaction takes about 4hr. The yellow complex formed was isolated and analyzed by UV-Vis, IR and MS, spectra are shown in Appendix D. The product formed in this reaction is a mixture of complex **8** and complex **9** where the **8** is the major product.

2.3 Results

2.3.1 OtBu-Fmoc-*iso*Asp-Ala-Gly-OMe (4)

^{1}H NMR of the compound along with COSY shows a shift of the protons that are located next to amides and carboxyl groups that form the peptide bond the spectra are shown in Appendix B. The β- protons of the aspartic acid is no longer attached to the carboxylic acid but to a peptide bond instead with has lower electronegativity resulting in upfield shift of the peak. The α- proton of the alanine shifts since it is now attached to secondary amine in place of a primary amine. The molecule is now more sterically strained, resulting in a downfield shift of the ^{1}H NMR peak. This combined with m/z value determined by MS ($C_{29}H_{35}N_3NaO_8^+$; m/z = 576,2316) and the results from elemental analysis confirmed formation of **4**.

2.3.2 OtBu-*iso*Asp-Ala-Gly-OMe (5)

A suitable synthetic methodology was developed for **5.** The most difficult task for this synthesis was the work-up procedures for **4** and **5.** That was an expected consequence from using LPPS. The yields for the synthetic route of **4** and **5** were not as high as expected but nevertheless higher than for a coupling reaction employing solid phase peptide synthesis (SPPS). Upon deprotection of the amine, the molecule is not as sterically strained as before. The α- and β- protons of the aspartic acid located near the amine show an upfield shift and the shape of these peaks also changed. ^{1}H NMR of the compound along with ^{1}H COSY shows the absence of the Fmoc group protons, the spectra are shown in Appendix C. This combined with m/z value determined by the MS ($C_{29}H_{35}N_3NaO_8^+$; m/z = 576,2316) confirmed formation of **5**. Several attempts were made to dry **5** and improve its air stability, washing with solvents such as ether, toluene, and hexane did not help. Recrystallization from acetone/water or water removal using toluene in a Dean Stark method did not show improved physical properties. Recrystallization from acetone/hexane mixture formed a white sticky compound, which upon contact with air resulted in formation of the same yellow oil. None of these attempts above resulted in drier or less air sensitive compound **5** leading to the conclusion this is the best physical form obtainable at this point. The future improvement for the synthesis of **5** could be to modify the work-up to obtain higher yields. A likely possibility for modification is in the silica gel chromatography of compound **4**, where the polarity of the solvent system may be increased in smaller steps to improve the separation. The reaction time of the coupling reaction could as well be extended which could lead to increased yields. Also it may be a good idea to form the hydrochloride salt of the ligand to make it more air stable, easier to handle and work with.

2.3.3 K[Pd(*iso*Asp-Ala-Gly)Cl] (8) and [Pd(*iso*Asp-Ala-Gly] (9)

The ligand **5** was employed to form a palladium complex that was characterized sufficiently to confirm its composition. The reaction was carried out under mild conditions. The complexes show coordination of amine and both amides forming the expected (6,5,5) membered ring chelation. MS was mainly used to characterize these compounds. The spectra were run in the negative mode in MeOH. The m/z value found were ($C_{14}H_{24}N_3O_6Pd$; m/z = 436.0705) confirming formation of [Pd(*iso*Asp-Ala-Gly], **9,** and ($C_{14}H_{24}N_3O_6PdCl^-$; m/z = 472.0365) confirming the presence of the anion K[Pd(*iso*Asp-Ala-Gly)Cl] of **8**. IR also verified presence of the esters accompanied with a shift to lower wavenumber confirming that the O-carboxylate is weakly coordinated at least for **9.** No shift to lower wavenumber was observed for the peptide backbone carbonyl stretch. The ^1H NMR is complicated to analyze due to presence of the two species in the sample and poor resolution of the signals. The future work remaining for **8** and **9** is to separate the compounds by some kind of chromatography or react the mixture further forming a single species. That could likely be achieved in a reaction of silver nitrate ($AgNO_3$) with the mixture, abstracting the chloride by forming an insoluble silver chloride (AgCl) precipitate. The prediction is that will leave an open coordination site for weak coordination of a carboxylate and forming a pure product **9**. Like described above Pd-complexes are known to catalyze polymerization,[7] once pure product **9** is formed the next step would be to try the complex as a catalyst in a polymerization reaction.

2.3.4 Conclusion

A synthetic methodology for a novel *iso*Asp-Ala-Gly, using LPPS, was completed. This method is a three step process and is quite affordable synthesis The yields are around 65% which are fair for coupling reactions with LPPS, however, there is always room for modification of the method to increase the yields. The downside of this synthesis is long reaction time. The novel *iso*Asp-Ala-Gly was employed as a ligand to form a palladium complex. Characterization thereof implies formation of (6,5,5) membered ring chelation as I set out to synthesize. The reaction still needs to be developed further. However it was shown that novel *iso*Asp-Ala-Gly chelates to Pd(II) forming two different complexes under ambient condition in a short period of time. This complex formation underpins that it may be possible to use novel *iso*Asp-Ala-Gly to form complex intended for copolymerization of CO_2 and alkene. Therefore further investigation of novel *iso*Asp-Ala-Gly and it's reactions with different metal ions will make an interesting project for further research.

3 $GSH(OMe)_2(SMe)$ (12)

GSH is a naturally occurring tripeptide consisting of glutamate(Glu), cysteine(Cys) and glycine(Gly). GSH plays a digenetic part in biological processes in our cellular homeostasis. It participates in following processes: antitoxic, antioxidant, pro-oxidant and as a modulator which all are extremely important functions for us to stay alive.[26] The pathways are shown in Scheme 3.1.

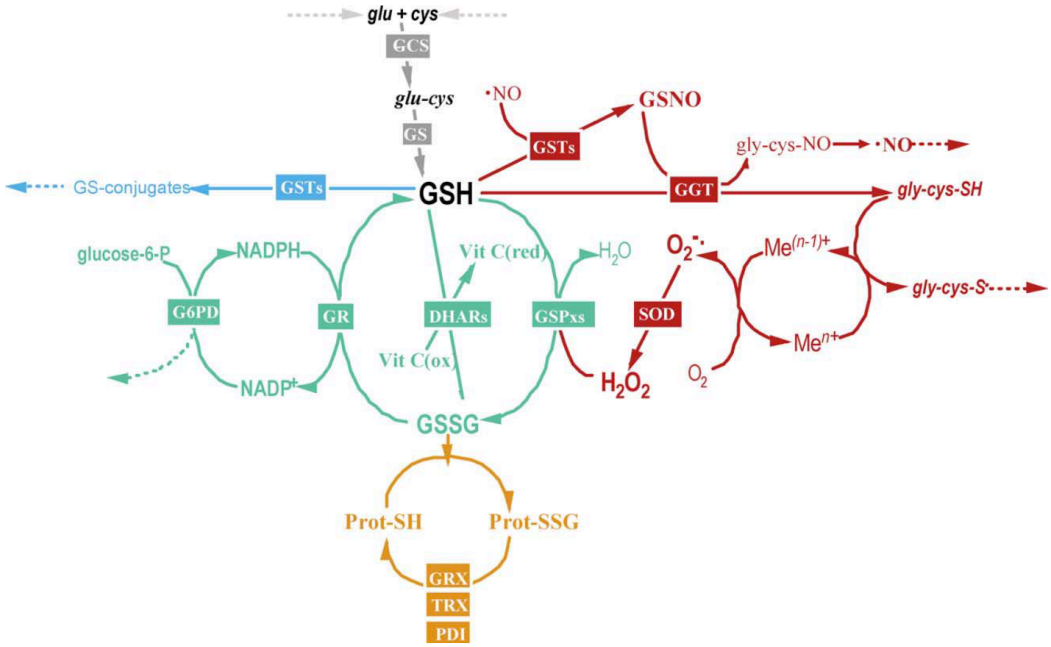

Scheme 3.1 : Pathways of GSH in biological processes: antitoxic(blue), antioxidant (green), pro-oxidant (red) and modulator (yellow).[26]

Studies of the coordination chemistry of GSH show a great variety of complex structures that can form.[27] GSH can coordinate to a metal ion through eight different donor atoms, amine –N (primary or secondary), thiol-S and carboxylate –O.[15] To control the modes of coordination, a modification of the GSH was introduced. Our research plan was to use GSH as a model ligand without exploring sulfur and carboxylate coordination and therefore control the coordination. We set out to modify the GSH by alkylating both terminal carboxylates and the thiol group (Figure 3.1.a). By doing that this way we expect coordination to take place primarily with nitrogens and avoid interference from the redox active thiol and competition from the carboxylates with the nitrogens for coordination with the metal.

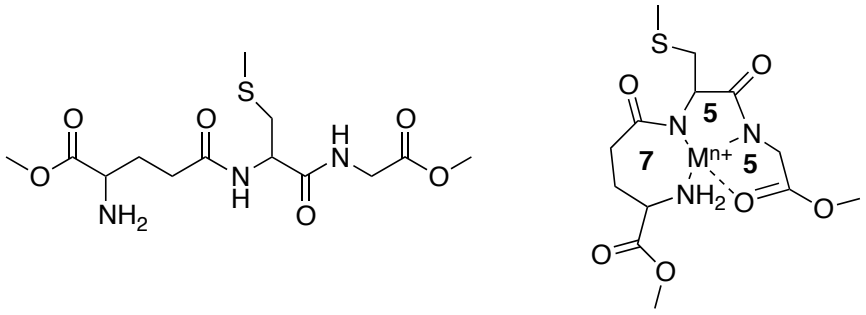

Figure 3.1 : a) Structure of the modified GSH –> {GSH(OMe)$_2$(SMe)}. b) Possible chelation of {GSH(OMe)$_2$(SMe)} with metal ion.

Thiol has high coordination affinity towards metal ions along with redox properties in presence of redox active metal ions. It is extremely important to avoid the redox of the thiol. The oxidized GSH glutathione disulfide (GSSG) is twice as big as the ligand GSH and therefore has more coordination sides. In addition it has completely different properties and is known to form loop structures and polynuclear complexes upon coordination to metal ions.[28] Consequently the complexes would be expected to have completely different properties than the targeted complex.

After modification {GSH(OMe)$_2$(SMe)} has three coordination sides, amino N-terminal, and the two amides of the backbone. The three GSH nitrogen and carboxylate-O if coordinated, could form 7, 5, 5 chelate systems with a metal ion capable of supporting such coordination geometry (Figure 3.1.b). {GSH(OMe)$_2$(SMe)} was used as a model ligand to investigate if formation of 7,5,5 membered ring chelation is possible with selected metal ions. This result would tell us if a synthesis of a peptide that would support that chelation would be worth a try There are two synthetic routes that are possible for this modification of **10**, as shown in Scheme 3.2. The routes and the steps referred to in this section are from that Scheme. The use of other alkyl groups like ethyl (Et) and isopropyl (iPr) would be preferred since they are more stable towards hydrolysis. The reaction of these alkyl groups and GSH were studied in our group and they showed much slower reaction that never led to complete alkylation. Therefore we used methyl group only as a protecting group in the modification of the GSH.

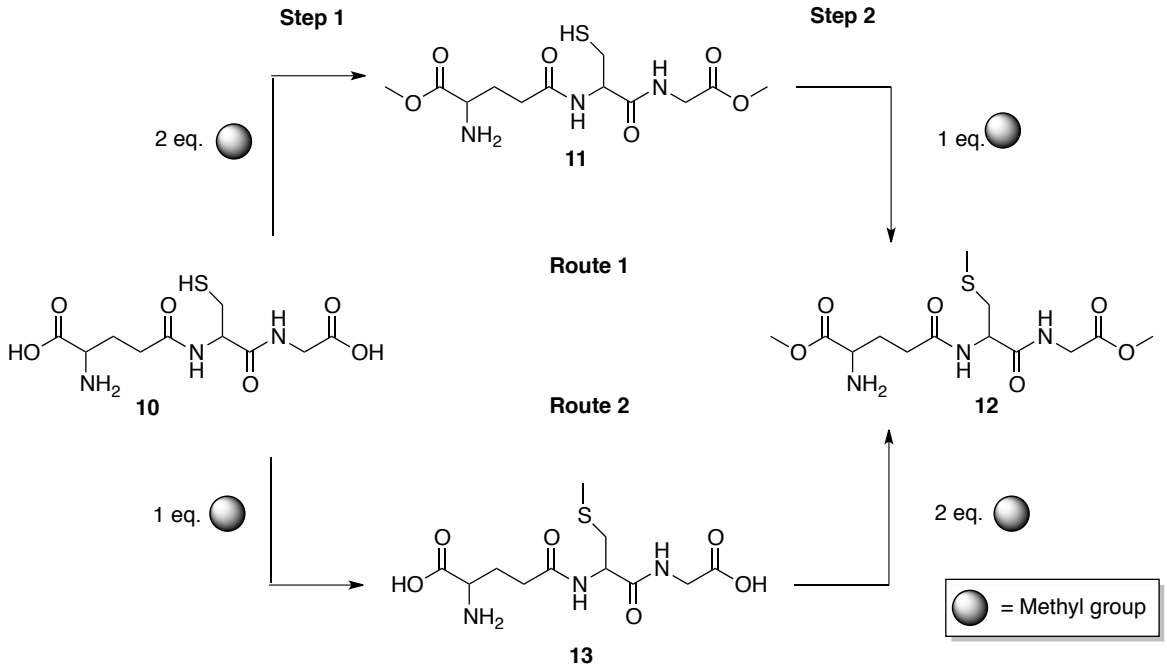

Scheme 3.2 : The two routes explored for modification of GSH.

The coordination affinity towards metal ions of $GSH(O\text{-}Me)_2(S\text{-}Me)_2$ was investigated in aqueous solution through potentiometric studies and ^1H NMR. Copper(II) and nickel were the metal ions used in the potentiometric study. Mainly because of the Irving-Williams Rule stating that Cu(II) and Ni(II) are the transition metal ions that form the most stable complexes. Palladium (II) was chosen for the NMR experiment due to the ability of the metal ion to deprotonate amides in lager pH range and it has been reported that Pd(II) can form metal amide bond at around pH ~ 2.[25] The theory behind these experiments will be described later in the thesis.

3.1 Modification of GSH

For the modification of GSH two routes were explored. The routes are reversed process of each other and will be described as follows.

3.1.1 Synthesis of 12; route 1

In this route the first step is to synthesize the methyl ester of the GSH (step 1) and then alkylation of the thiol is executed (step 2).

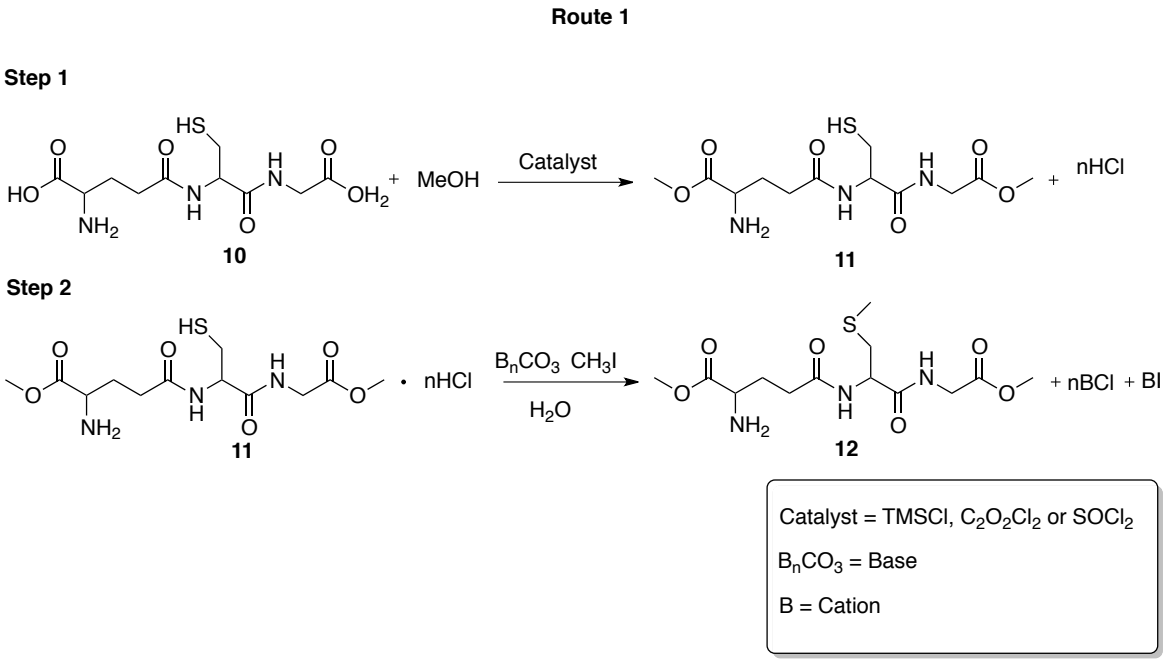

Scheme 3.3 : The reaction and conditions for modification of GSH using route 1.

First attempt was to use the same method described in section 2.1.1. MeOH/ TMSCl esterification method.[16] Mainly because it requires mild reaction conditions followed by fairly simple workup and gives excellent yields. The reaction was carried out in methanol (solvent and a reactant) containing **10** and TMSCl with acts as a acid precursor where the acid formed (HCl) is then used as catalyst and a dehydrating agent. Product **11** is formed via silyl ester intermediate. HCl is formed in the reaction resulting in formation of hydrochloride salt of the product **11**. The TMSCl was dried over CaH_2 and used freshly distilled. Characterization by ^1H NMR of that compound shows that complete alkylation did not occur. Second attempt used oxalyl chloride ($C_2O_2Cl_2$) as acid precursor where the acid formed (HCl) is then used as catalyst and a dehydrating agent similarly to the MeOH/ TMSCl esterification method. Methanol acts as a solvent and a reactant, containing **10** and $C_2O_2Cl_2$. Product **11** was formed via dimethyl oxalate intermediate, which results in final formation of oxalic acid. Characterization of this compound showed that complete alkylation did not occur. The third attempt employed thionyl chloride in a reaction that is also similar to the MeOH/TMSCl esterification method. Methanol was the solvent and a reactant $SOCl_2$ acts as an acid precursor where the acid formed (HCl) acts as a catalyst and also as a dehydrating agent. Product **11** was formed via dimethyl sulfite intermediate that

reacts further to form stable sulfurous acid. Characterization of this compound showed that complete alkylation was not achieved. Although none of the reactions showed 100% alkylation it was decided to complete purification of the final product.

The thioether formation reaction was carried out in H_2O, using CH_3I as the alkylating agent forming the methyl ester in a S_N2 reaction mechanism. In this reaction, the base plays an important role, it can affect the rate, yields, and controls which salt product is formed (Scheme 3.3). Three different salts were tested as a base for this reaction. These three salts all contained carbonate (CO_3^{2-}) but had different cations. The cation forms a side product with the halogens in the solution. The separation of these side products from the product was a challenge, resulting in experimenting with three different salt. The dissociation of these salts in water is shown in Scheme 3.4. First attempt was using 1 eq of Na_2CO_3. The side product is CO_2 that is released from the reaction as a gas. For route 1, sodium ion will react with the iodide that is the leaving group in the alkylation reaction forming NaI and the chloride (from HCl) forming NaCl. With this base complete alkylation was never reached as was confirmed first in potentiometric studies (Figure 3.3), and then later by ^{1}H NMR. Cs_2CO_3 was tried due to its solubility in methanol so the reaction could rather be carried out in methanol instead of water, and by that avoid the hydrolysis of the methyl esters formed in step 1 of Scheme 3.3 That was not successful, the product formed lost a methyl group of one ester. The last base tried was ammonium bicarbonate. It forms NH_4Cl and NH_4I as side products like Scheme 3.3 and 3.4 shows. It is possible to remove the NH_4Cl by a gentle heating, and excess of NH_4CO_3 can also be removed by heating (Scheme 3.4.B). NH_4I is then easily removed from **13** with flash chromatography on silica gel. However, this reaction also did not show complete alkylation as was confirmed by ^{1}H NMR.

A.

$$Na_2CO_{3(aq)} \rightleftharpoons 2Na^+_{(aq)} + CO_3^{2-}{}_{(aq)} \quad (1)$$

$$CO_3^{2-}{}_{(aq)} + H_2O \rightleftharpoons CO_{2\,(g)} + 2OH^-_{(aq)} \quad (2)$$

B.

$$NH_4HCO_{3\,(aq)} \rightleftharpoons NH_4^+{}_{(aq)} + H^+_{(aq)} + CO_3^{2-}{}_{(aq)} \quad (3)$$

$$CO_3^{2-}{}_{(aq)} + H_2O \rightleftharpoons CO_{2\,(g)} + 2OH^-_{(aq)} \quad (4)$$

$$NH_4^+{}_{(aq)} + X^-_{(aq)} \rightleftharpoons NH_4X \quad (5)$$

$$NH_4Cl_{\,(aq)} \underset{\triangle}{\rightleftharpoons} NH_{3\,(g)} + HCl_{\,(g)} \quad (6)$$

$$NH_4HCO_{3\,(aq)} \underset{\triangle}{\rightleftharpoons} NH_{3\,(g)} + H_2O + CO_{2\,(g)} \quad (7)$$

C.

$$Cs_2CO_{3(aq)} \rightleftharpoons 2Cs^+_{(aq)} + CO_3^{2-}{}_{(aq)} \quad (8)$$

$$CO_3^{2-}{}_{(aq)} + H_2O \rightleftharpoons CO_{2\,(g)} + 2OH^-_{(aq)} \quad (9)$$

Scheme 3.4 : Aqueous reactions of salts used in modification of the GSH shown along with reactions of side products formed.

This route 1 seemed not to be a good fit mostly because the second step is carried out in water and therefor hydrolysis of the esters formed in step 1. Therefore complete alkylation was never observed for route 1.

3.1.2 Synthesis of 12; route 2

This route is route 1 reversed. So first the thioether is formed (step 1) and then the esterification reaction is performed (step 2). Compound **13** is also commercially available but it is very expensive for the desired quantity, so the synthesized compound was used mostly in the synthesis, although purchased compound was used to finish up the last experiments.

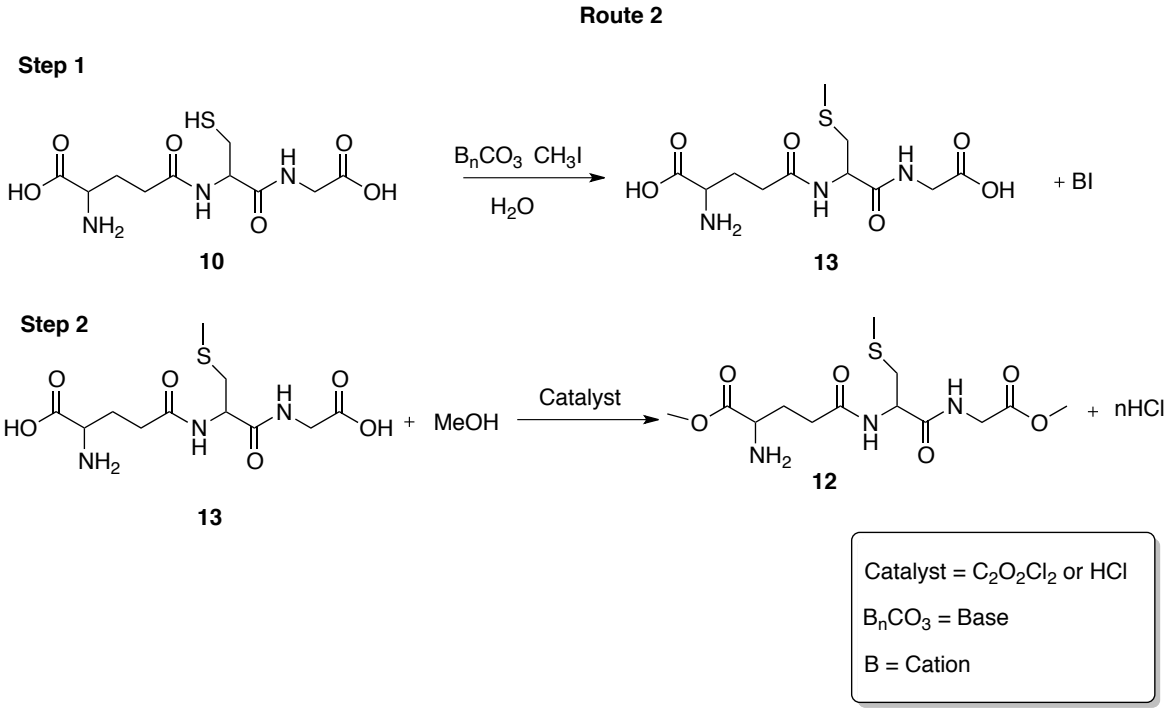

Scheme 3.5 : The reaction and conditions for modification of GSH using route 2.

The same methodology was used for the thioether formation in both route 1 and route 2. The reaction was carried out in water, using CH_3I as an alkylating agent as before. The three basic salts that were tried before were also tried here. First attempt was using 1eq of Na_2CO_3. Sodium ion will react with the iodine forming NaI. Using this base the reaction complete alkylation was never reached in either route and the side product NaI has the same solubility as the ligand so their separation was impossible. Cs_2CO_3 was again tried due to its solubility in methanol. The proton of the α-carbon of the glutamate and the proton of the α-carbon of the glycine showed distorted irregular peaks in ^1H NMR, indicating structural changes of the compound. Finally ammonium bicarbonate was tried as a base and forming NH_4I as a side product. As before the excess of NH_4CO_3 is possible to get ride of by gentle heating. NH_4I is then easily removed from **13** with silica cartography. This reaction showed complete alkylation forming a white solid in 97% yields. Compound

13 was characterized by ^{1}H NMR, ^{13}C NMR, COSY, IR, and MS. The spectra are shown in Appendix E.

First attempt of carboxylate esterification used oxalyl chloride as an acid catalyst and a dehydrating agent similarly to route 1. The second attempt used acidic Fishers alkylation. The method is a nucleophilic acyl substitution where eletrophilicity of the carbonyl carbon is used to attract nucleophilic alcohol. This process is kinetically slow without use of an acid catalyst such as hydrochloric acid. First there is a protonation of carbonyl carbon from the acidic catalyst. This increases the electrophilicity of the carbonyl carbon and makes it more suitable for nucleophilic attacks from the oxygen of the alcohol. Then there is a 1,2, addition forming an oxonium ion. An intermolecular proton transfer occurs followed by a 1,2 elimination of water. A deprotonation of the carbonyl oxygen by chloride from the acid leaves an ester. The mechanism for acid catalyzed esterification is shown in Scheme 3.6.

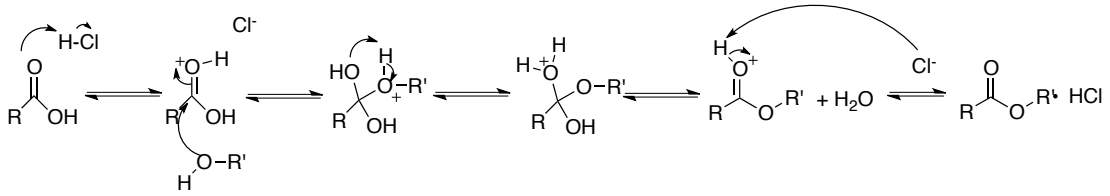

Scheme 3.6 : Mechanism for reaction for acid catalyzed esterification.

After 1,2 addition of the alcohol all the steps are in equilibrium since the alcohol is usually the reactant and the solvent in this reaction (e.g. in large excess) pushing the reaction toward formation of the hydrochloride salt of **12**. This reaction formed light yellow hygroscopic crystals in 95% yields. The compound **12** was characterized by ^{1}H NMR, ^{13}C NMR, IR and ^{1}H COSY, spectra are shown in Appendix F.

3.2 Results

3.2.1 Characterization of 13

When the GSH is partially alkylated there are three species in the solution **10, 11, 13, 12** and GSSG. These species are similar but do not have identical ^{1}H NMR but they overlap, obscuring the peaks and give inaccurate integration. When the ^{1}H NMR shows sharp regular peaks the odds are that the alkylation is completed, which was confirmed by integration of the ester singlet formed at 2.18 ppm compared to the backbone protons. The α- and β- protons of the cysteine are closest to the sulfur and are therefore most affected by the alkylation. These proton environments change as a result in peak coupling changes. The α- proton gave triplet ($^{3}J_{HH}$= 5.6 Hz) before but now shows a quartet ($^{3}J_{HH}$= 3.2 Hz, $^{3}J_{HH}$= 5.2 Hz) and has shifted downfield, while the β- proton gave a quartet (obsc) before but now shows a quartet of doublets (obsc.), a part of the spectra is presented in Figure 3.2.

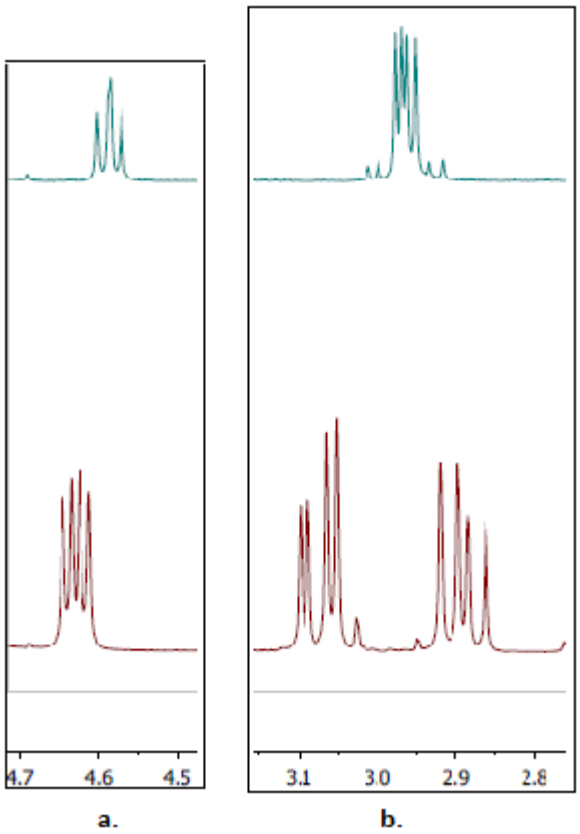

Figure 3.2 : Shift of protons in ^{1}H NMR a) α- $proton_{Glu}$ b) β- $proton_{Cys}$ Blue (GSH) and Red {GSH(SMe)}.

CHN analysis of these compounds showed that 1mol eq. of NH_4OH, formed unexpectedly in the reaction. Because of that the solution prepared for NMR is more basic then the GSH precursor resulting in a small upfield shift of the protons located next to the amides. The compound is too hygroscopic to get good IR spectra but the absence of a sharp stretch from SH at 2535 cm^{-1} was confirmed a along with mass spectral data, MS ($C_{11}H_{19}N_3O_6SNa^+$; m/z = 344.0887) supports the product composition.

3.2.2 Characterization of 12

Analysis of **12** was mainly performed using ^{1}H NMR. The greatest indication that the esters were formed are the two singlets forming at 3.90 ppm and 3.80 ppm and the integration of the ester signals relative to the backbone protons provided information to the level of alkylation of the GSH, the spectrum is presented in Appendix F. Compound **12** is formed as hydrochloride salt, meaning that if the NMR solution is acidic, then the proton near the amide in the GSH(SMe) precursor shifts downfield. The peak representing α-protons of the glutamate showed a quartet in the salt free compound but in the hydrochloride salt it is a multiplet due to the fact the solution is more acidic and therefore the amino group has an extra proton resulting in increased splitting of the α- $protons_{Glu}$

peak. MS confirmed the composition with m/z values corresponding to the alkylated GSH ($C_{13}H_{24}N_3O_6S^+$; m/z = 350.1380). The sample was sent to two different services for CHN analysis, however the analysis was not successful do to the hygroscopicity of the compound.

3.2.3 Conclusion

Several different reactants were tried in the esterification reactions. Characterization of the compounds in most cases showed the alkylation reaction did not go to completion. In ^{1}H NMR, the integration of the ester resonances compared to the backbone proton resonances were not consistent, and that along with two sets of peaks from some of the backbone protons confirmed that there was still some unreacted compound present. The average alkylation yield for these reactions was 70%. Purification of the crude product by flash chromatography was tried with different ratio of elution. The right elution for separation was not achieved. As described before alkyl groups like ethyl (Et) and isopropyl (iPr) would be preferred since they are more stable towards hydrolysis. Characterization of these compounds showed lower yield of alkylated compounds than for the methyl esters. Therefore alkylated GSH is not a feasible ligand for aqueous studies under conditions that may promote ester hydrolysis.

3.3 Potentiometric studies of 12 with Cu(II) and Ni(II)

3.3.1 Introduction

Potentiometric studies are one of the oldest instrumental analytic methods, where rapid development of new, more sensitive and more accurate electrodes have expanded the analytical ranges and properties of the method.[29] Potentiometric studies involve measuring the potential of an electrochemical cell in the absence of noticeable currents. Potential of an ion sensitive membrane electrode provides the ion concentration of the system. That kind of electrode is practically free from interference and provides an agreeable way for quantification of numerous anions and cations. Potentiometry equipment is composed of a reference electrode, indicator electrode and a simple and inexpensive potential measuring device. The reference electrode is a half-cell potential electrode with known constant concentration and is entirely insensitive to the studied solution. The criterion the reference electrode has to obey are; the Nernst equation, be reversible, exhibit constant potential over time and exhibit low hysteria with temperature cycling. Still no electrodes meet all of the requirements above but there are several that come close.[30] Silver/silver chloride electrode ($Ag\left|AgCl(sat'd),KCl(xM)\right|\left|\right.$) is the most widely used reference electrode and it is commonly used in potentiometric studies. One of the advantages of the silver/silver chloride electrode is that it operates at a temperature higher then 60°C.[30] The

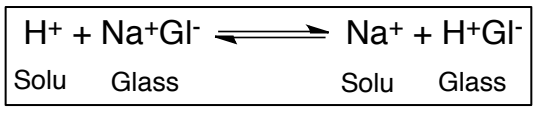

Scheme 3.7 : Ion –exchange reaction of sodium and hydrogen ions.

membrane electrode that was used is a glass electrode. The main components in the glass are silicone and oxygen in SiO_2. The presence of singly charged cation mobile in the structure causes the electrical conduction within the membrane. In aqueous solution the cation and H^+ undergo ion-exchange reaction. Usually the glass membrane is made from silicic acid (H^+Glass^-, or H_2SiO_3) due to its large equilibrium constant for the ion exchange process. Except if the concentration of hydronium ions (H^+) is low in the solution, the equilibrium shifts towards (Na^+Gl^-) as predicted by Le Chatelier's principle (Scheme 3.7). For the membrane to work it has to be hydrated or the pH measurements are not accurate. The membrane interacts with both the analytical solution as well as the internal solution of the reference electrode. The boundary potential developed across the membrane (E_b) is made up by the hydronium ion activity and dissociation taking place. The potential difference is the analytical parameter for the pH measurement in the potentiometer. The reference electrodes provide electrical constant with the solution, making it possible to measure the boundary potential (Scheme 3.8).

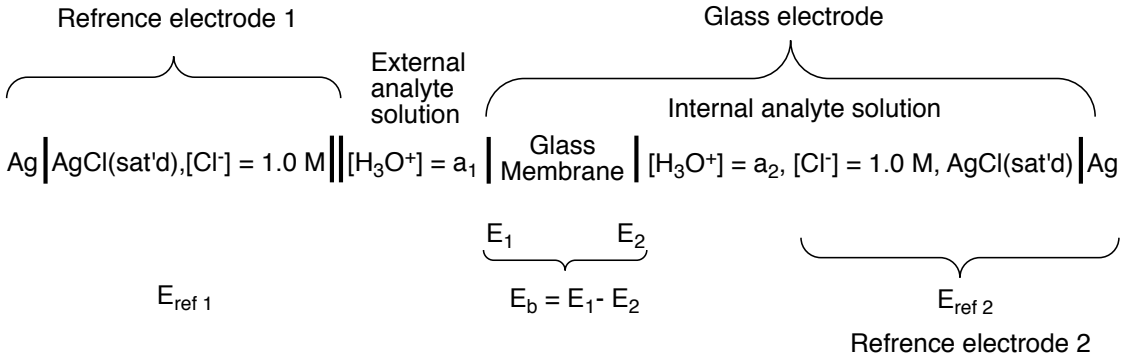

Scheme 3.8 : Diagram of potential of a glass electrode.[30]

Alkaline error is something that needs to be considered. Glass electrode as described above responds not only to H^+ but also to singly charged cations in basic solutions. Sodium is more likely to form the alkaline error than potassium due to more similarity in size to the hydrogen compared to potassium. That is corrected by introduction of selectivity coefficient.[30] Acid error can also exist at pH of under pH 0,5, but that is far from the value measured in our experiment so no precaution was needed for that.

Potentiometric titration is similar to titration of a redox reaction, but does not need an indicator. A solution with fixed concentration of electrolytes, ligand and metal salt is titrated with base of known concentration. A small volume of the titrant (base) is added to the analyte stepwise until the reaction reaches the end point. Meanwhile the potential is measured across the electrolyte solution with the potentiometric equipment described above. Bjerrum showed in 1941 that a ligand is a conjugate base of a weak acid and the pH measurements with glass electrode of several solutions containing known total concentration of a metal salt and the ligand acid can give information and value of the stepwise equilibrium constants for complex formation and therefore also provide the overall equilibrium constant.[31]

3.3.2 Potentiometric titration setup

The pH meter was calibrated by measuring the exact concentration and equilibrium point of KOH, and HCl by a Gran method.[32] First KH-phtalate is titrated with the base and the equilibrium point determined. Then HCl is titrated with KOH and the equilibrium point is also determined. The equivalent point is determined with Gran method by plotting ΔV/ ΔpH, or ΔV/ΔE versus V, and this way the equivalent point is determined very accurately in the potentiometric titration.[32] The water ionization constant K_w may be calculated from the basic region (after the eq point) where the pH is determined from the titrant excess. The K_w is then used in the calculations of the equilibrium constant in the potentiometric titration. First the titration of the pure ligand was performed in aqueous solution, containing fixed amount of electrolyte (KCl) and at a fixed starting pH value. The program SUPERQUAD was used to calculate and fit the experimental curve to a calculated one, the calculations can estimate the equilibrium points of the ligand along with the exact concentration of the peptide stock solution.[33]

The pH-potentiometric titrations were performed in 15 ml samples in the metal ion concentration range of 0.668 - 3.47 mmol L^{-1} for metal ion:ligand ratios 1:1 1:2 and 1:6. A stock solution of copper(II) chloride and nikcel(II) chloride were prepared from analytical grade reagent metal salts. All measurements were carried out at 25°C and at an ionic strength of 0.2 M (KCI). During the titration, argon was bubbled through the samples to ensure the absence of oxygen and carbon dioxide and to agitate the solutions. The measurements were taken with an automatically controlled Radiometer DL50 Graphix (METTLER TOLEDO) titration system containing a pH-meter and automatic burette and equipped with a 51109503 combined silver/silver chloride electrode (METTLER TOLEDO). The number of experimental points reached around 30-40 data (ml– pH) for each titration curve. The pH readings were converted into hydrogen ion concentration as described earlier.[31] Protonation constants of the ligands and the overall stability constants ($\log_{MA}$) of the complexes were calculated by general computational programs, PSEQUAD and SUPERQUAD like described above.[33,34]

3.3.3 Potentiometric Study of GSH derivatives

Titration curves for three "free" GSH derivatives were measured for {GSH(OMe)$_2$(SMe)}, {GSH(OEt)$_2$(SEt)}, {GSH(OiPr)$_2$(SEt)} and the equilibrium points along with exact concentration where calculated. The two ligands, {GSH(OEt)$_2$(SEt)} and {GSH(OiPr)$_2$(SEt)} were synthesized by a PhD student in the Suman group, Ms. Lindsey J. Monger.

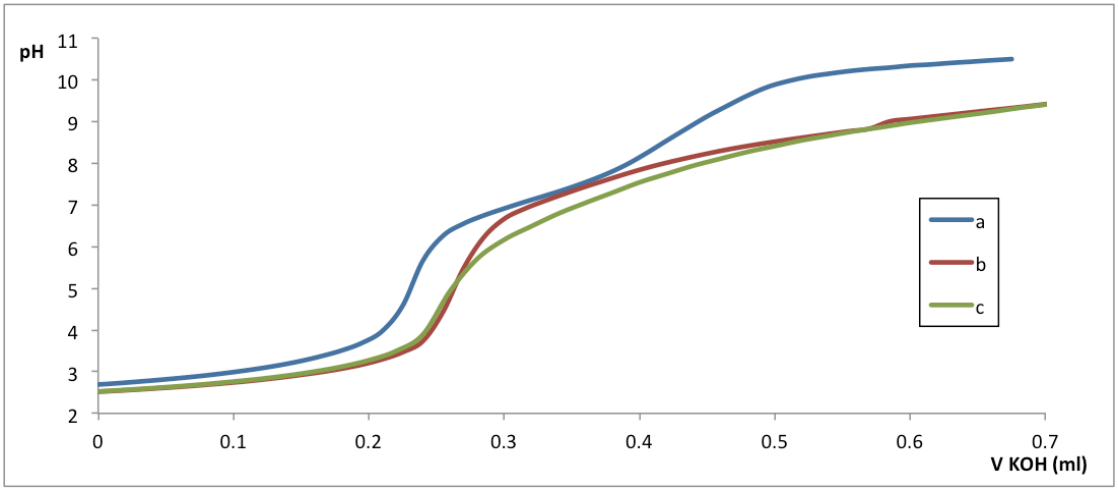

Figure 3.3 : pH-Metric titration curve a) "free", {GSH(OMe)$_2$(SMe)} ($c_{\{GSH(OMe)2(SMe)\}}$ =3.38 mmol L^{-1}). b) "free", {GSH(OEt)$_2$(SEt)}) ($c_{\{GSH(OEt)2(Set)\}}$ =4.10 mmol L^{-1}). c) "free", {GSH(OiPr)$_2$(SEt)}) ($c_{\{GSH(OiPr)2(SEt)\}}$ =4.10 mmol L^{-1}). At 25°C and at an ionic strength of 0.2M (KCI).

The titration curves (Figure 3.3) show that none of the derivatives is fully alkylated. The expectation was to see a titration curve with a single big jump at the pH of neutralization. However, the {GSH(OMe)$_2$(SMe)} (blue curves) show a characteristic profile of weak acids indicating that either the hydrolysis of the ester is rapid or that the compound synthesized are not fully alkylated. Later on it was confirmed with ^{1}H NMR that the synthesized compounds were not fully alkylated. The {GSH(OMe)$_2$(SMe)} (blue line) also shows a second jump indicating that it was also not 100% thioether. The {GSH(OEt)$_2$(SEt)} (red curve) and {GSH(OiPr)$_2$(SEt)}(green curve) show a sharper curve and have less weak acid characteristic indicating these samples have larger ratio of alkylated product, the jump is however low implying the ligand has two amine groups. That may be explained by GSH oxidation forming GSSG, with is a much bigger ligand with different physical properties then the GSH. The fitting in SUPERQUAD confirmed this when the calculated curve did not match the observed curve. It confirmed that the carboxylic acid was not fully alkylated, also indicated that the thiol was not completely on thioether form. This means as mentioned in section 3.2.1, that the sample is possibly a mixture of five species **10**, **11**, **12**, **13**, and GSSG, and that there is no way of knowing the mixture's correct ratio. Potentiometric studies of these ligands would result in inaccurate results. The results from the Potentiometric titration of the GSH derivatives inspired the change of synthetic route 1 to route 2.

3.3.4 Potentiometric Study with GABA

GABA (gamma- aminobutyric acid) (Figure 3.4.1) is a γ amino acid and therefore could chelate to a metal through the primary amine and the carboxylic group to from a seven membered ring (Figure 3.4.2) Although it is known that carboxylic groups have higher tendency to coordinate to metals than a peptide carbonyl-O donor, the GABA is still an adequate model for comparison allowing us to draw a conclusion about the ability of the GSH derivative coordination. The GABA was used as a model for coordination ability of copper and nickel in supporting 7 membered ring chelate (Figure 3.4.2). Thermodynamics of the complexes of GABA with copper and nickel ions are presented.

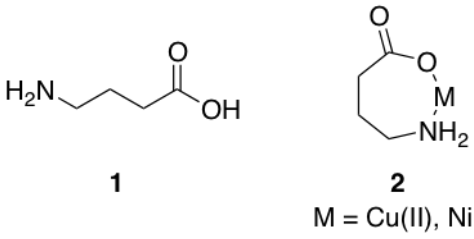

Figure 3.4 : a) Structure of GABA b) and its coordination to metal ions.

Copper(II):GABA

First the pH-Metric titration curve for pure GABA was measured and the equlibrium points and concentration calculated.

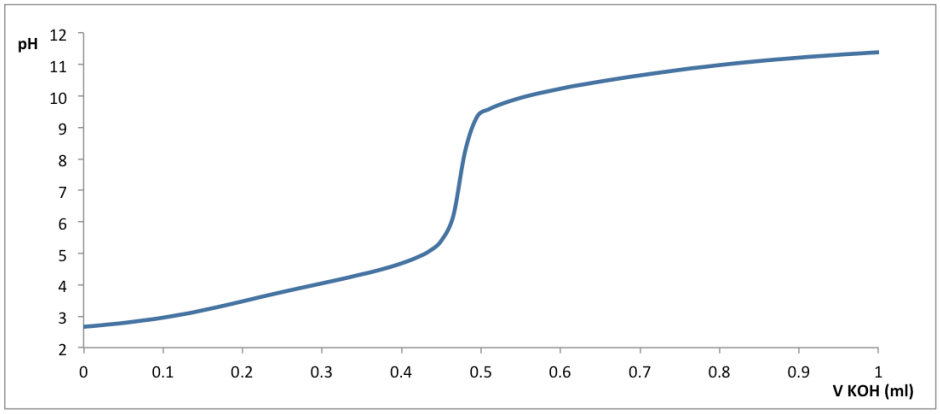

Figure 3.5 : pH-Metric titration curve of "free" GABA (c_{GABA}) =4.10 mmol L^{-1} at 25°C and at an ionic strength of 0.2M (KCI).

Titration curve for free GABA (Figure 3.5) shows weak acid (COOH) strong base(NH_2) titration curve like expected. SUPERQUAD was used to calculate and fit the experimental curve.[33] The fit was almost identical to the experimental curve.

The calculated values:

n_{GABA}; 0.06048 mmol (my calculation 0.0615 mmol 1.6% error)

n_{H+}= 0.1582 mmol (my calculation 0.1607 mmol 1.5% error)

β_1: 10.33 (pKa NH_3^+ 10.43)

β_2: 14.40 (pKa COOH 4.23)

pH-Metric titration were performed on three solutions using different ratio of metal ion:ligand where Cu(II):GABA used was (1:1), (1:2), and (1:6).

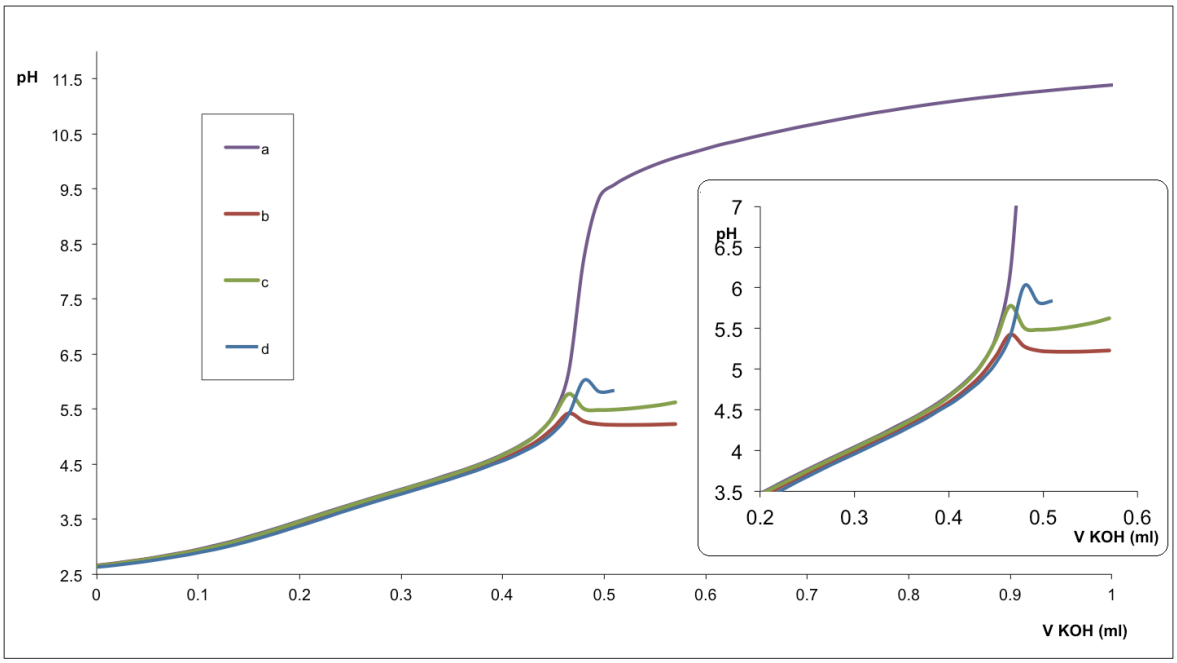

Figure 3.6 : pH-Metric titration curve of Cu^{II}-GABA. a) "free" GABA, b) 1:1 ratio (c_{cu}=3.47 mmol L^{-1}, c_L =4,10 mmol L^{-1}), c) 1:2 ratio (c_{cu}=1.60 mmol L^{-1}, c_L =4.10 mmol L^{-1}), d) 1:6 ratio (c_{cu}=0.668mmol $L^{-1,}$ c_L =4.10 mmol L^{-1}).

Figure 3.6 clearly shows how the complex formation is about to start at around pH 4.55 or around the same value as hydrolysis of copper starts; the formation of $Cu(II)(OH)_2$ was confirmed by a visible formation of a blue green precipitate at around pH 5.5. Stability constant calculations were performed using the program PSEQUAD[34] which provided following overall stability constants:

$\log \beta_{MAH}$= 11.89 (STD 0.04)

$\log \beta_{MA}$= 5.30 (STD 0.37)

(M = metal ion, A = ligand, H = dissociable proton)

Evaluation of the stepwise stability constants: The species of MAH is, most likely a carboxylate-coordinated complex, in which the amino group is still in ammonium form, containing the dissociable proton. β_{MAH} is the overall stability constant for formation of MAH that involves not only the β_{MAH}, which relates to the metal-ligand interaction but protonation constant of the amino group also needs to be considered. The stepwise constant (K) for the M + HA process is calculated. Following are the complex formation reactions and the equations for their stability constants.

$$M + A + H \rightleftarrows MAH \qquad \beta_{MAH} = \frac{[MAH]}{[M][A][H]} \tag{1}$$

$$M + HA \rightleftarrows MAH \qquad K = \frac{[MAH]}{[M][HA]} \tag{2}$$

$$H + A \rightleftarrows HA \qquad \beta_{HA} = \frac{[HA]}{[A][H]} \tag{3}$$

Then equation of stability constants β_{MAH} and β_{HA} are inserted into equation (2) ; and K may be calculated.

$$K = \frac{[MAH]}{[M][HA]} = \frac{\beta_{MAH} * \cancel{[M][A][H]}}{\cancel{[M]} * \beta_{HA} * \cancel{[A][H]}} = \frac{\beta_{MAH}}{\beta_{HA}} \tag{4}$$

$$logK = \log \beta_{MAH} - log\beta_{HA} \tag{5}$$

The titration curve of GABA gave $log\beta_{HA}$ =10.33 (*see on page 27*). So the stepwise equilibrium constant for MAH species may be calculated as:

$LogK$ = 11.90 – 10.33 = 1.57

For the MA species the stepwise equilibrium constant obtained is:

$$logK = \log \beta_{MA} = 5.30 \tag{6}$$

The results show that the complex formation is just about to start around 4.5, which is around the same value as blue green precipitate is detected where copper hydroxide is formed. First there is a weak monodentade interaction and then a weak bidentade interaction of the ligand with the copper. The bidentate interaction is more stable than the monodentate interaction, but it is not stable compared to a five-membered or even a six-membered amino acid type chelate.[35] Even with large ligand excess there was no increase in the complex formation. The interactions of GABA and copper were so weak that the $Cu(OH)_{2\,(s)}$ was the favored reaction product.

Nickel (II):GABA

First the pH-Metric titration curve for pure GABA was measured and the equlibrium points and concentration calculated as before.

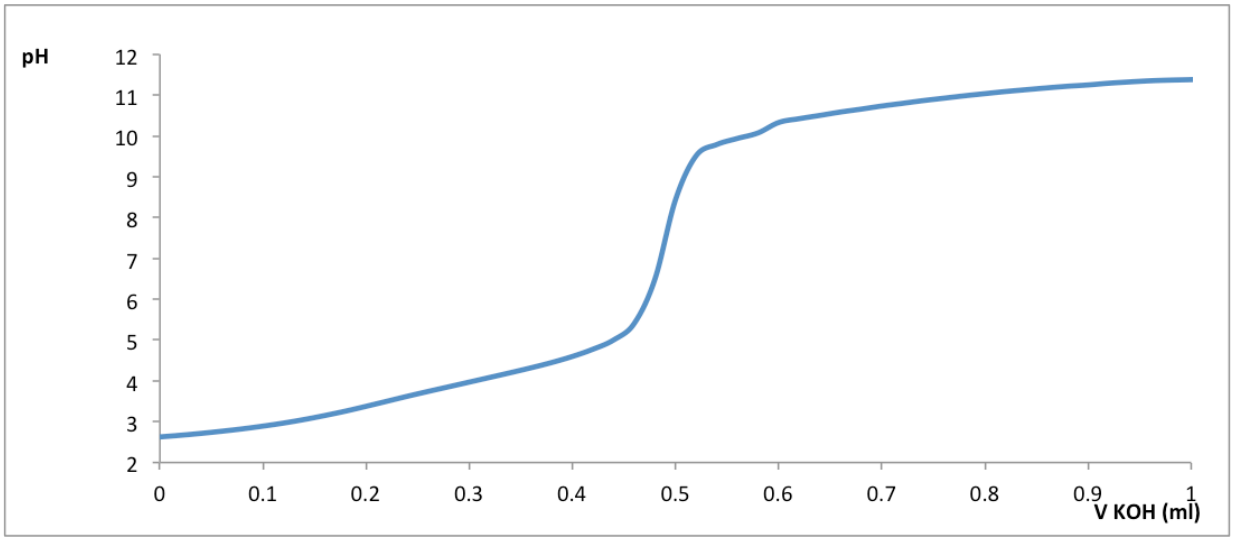

Figure 3.7 : pH-Metric titration curve of "free", GABA (c_{GABA}) =4.10 mmol L^{-1} at 25°C and at an ionic strength of 0.2M (KCI).

Like before the titration curve on GABA (Figure 3.7) showed weak acid (COOH) strong base (NH_2) titration curve. SUPERQUAD was used to calculate and fit the experimental curve.[33] The fit was almost identical.

The calculated values:

n_{GABA}; 0.0593 mmol (my calculation 0.060 mmol 0.9 % error)

n_{H+}=0.1605 mmol (my calculation 0.159 mmol 0.9 % error)

β_1: 10.54 (pKa NH_3^+ 10.43)

β_2: 14.64 (pKa COOH 4.23)

pH-Metric titration were performed on three solutions using different ratio of metal ion:ligand where Ni(II):GABA) used was (1:1), (1:2), and (1:6).

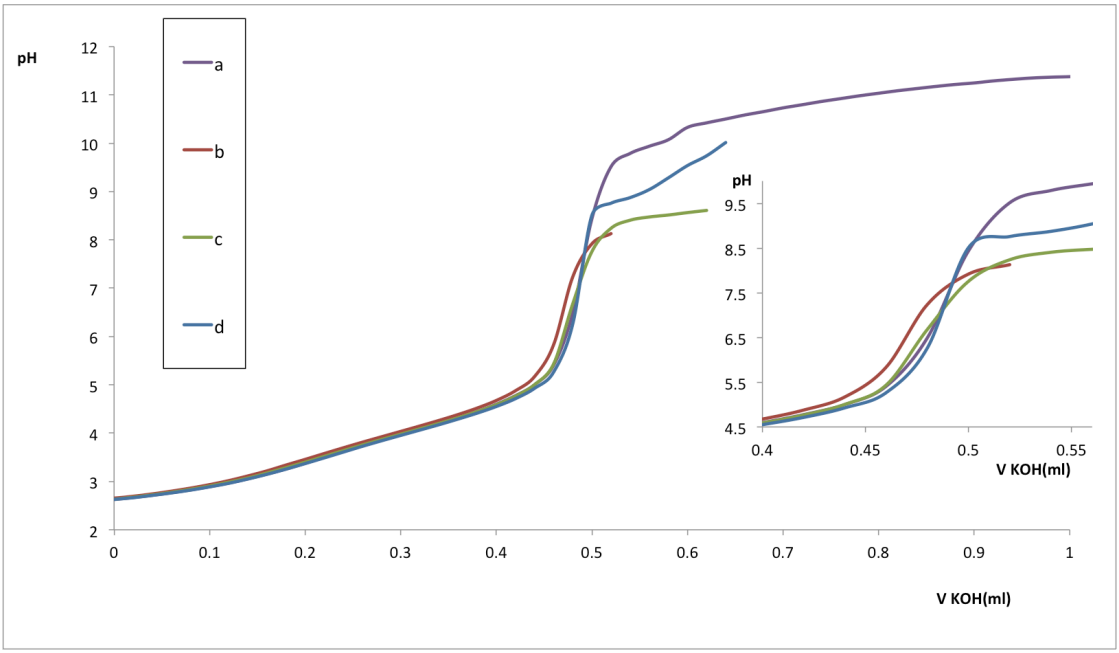

Figure 3.8 : pH-Metric titration curve of Ni^{II}-GABA. a) "free" GABA, b) 1:1 ratio (c_{Ni} = 3.61 mmol L^{-1}, c_L =3.99 mmol L^{-1}), c) 1:2 ratio (c_{Ni} = 1.66 mmol L^{-1}, c_L = 3.99 mmol L^{-1}), d) 1:6 ratio (c_{Ni} = 0.555 mmol $L^{-1,}$ c_L = 3.99 mmol L^{-1}).

Figure 3.8 stated that the complex formation starts around pH of 8 which is around the same value as the hydrolysis of nickel starts, the formation of Ni(II)$(OH)_2$ was confirmed by visible formation of a white precipitate at around pH of 8-9, where $Ni(OH)_2$ forms. Stability constant calculations were performed using the program PSEQUAD[34] which gave following over all stability constants:

$\log \beta_{MAH}$= 11.96 (STD 0.22)

$\log \beta_{MA}$= 3.99 (STD 0.30)

(M = metal ion, A = ligand, H = dissociable proton

Evaluation of the stability constants. As for the copper, the species of MAH is most probably, a carboxylate-coordinated complex, in which the amino group is still on the ammonium form, containing the dissociable proton. β_{MAH} is the overall stability constant for formation of MAH involves not only the β_{MAH}, which relates to the metal-ligand interaction but the protonation constant of the amino group also needs to be considered. The stepwise stability constant (K) for the M + HA process is calculated. The derivation of the stepwise stability constant is exactly the same as for the Cu(II):GABA described above (eq. 1 to 4). Leaving the equation for log K as follows:

$$log_K = \log \beta_{MAH} - log\beta_{HA} \qquad (5)$$

The titration curve of GABA gave $log\beta_{HA}$ = 10.43 (*see on page 30*). So the stepwise equilibrium constant for MAH species may be calculated.

$logK$ = 11.96 – 10.43 = 1.425

For the MA species the stepwise equilibrium constant is therefore:

$logK = \log \beta_{MA} = 3.99$ (6)

The calculations show that the complex formation is just about to start at around pH of 8 which is around the same value as white precipitate is detected where nickel hydroxide is formed. The conclusion was that a weak monodentate formation was observed. The interactions are so weak that hydrolysis of the nickel to the hydroxide is the favored reaction. The experimental results agree that there is a weak monodentate interaction followed by a weak bidentate interaction of the ligand and the nickel. The bidentate interaction is more stable than the monodentate interaction, but it is not stable compared to a five-membered or even a six-membered amino acid type chelate.[35] Even whith large ligand excess there was no increase in complex formation. The interactions of GABA and nickel were so weak that the $Ni(OH)_{2(s)}$ was the favored reaction product.

3.3.5 Conclusions

The GSH derivatives were either not fully alkylated or pure enough for the potentiometric studies to give good and accurate results for stability constants with metals. Gamma-aminobutyric acid was used as a model to learn the potentiometric technique and to see if the formation of a seven membered ring is possible with the two selected metal ions. Potentiometric studies of GABA showed that the chelating of GABA to copper and nickel is weak. As the pH is increased, first a monodentate interaction though the carboxylic moiety occurs in an almost negligible amount of intermediate species. In parallel, the coordination of the primary amine starts, and the seven-membered chelate formed this way has a moderate stability. The over all stability constant calculated for Cu(II):GABA system were $\log\beta_{MA}$= 5.30 and for Ni(II):GABA system were $\log\beta_{MA}$= 3.99. The constant is much lower compared to a chelate what would be formed with α - or β - amino acids (DL-Alanine–Cu(II) $\log_{MA2}$=15.85).[36] The seven membered ring formation is slightly stronger with copper than nickel, but only slightly. The formation of hydroxide complexes of these metal ions could not be prevented under the investigated conditions. It was also observed that the stability constant of the chelates follows the Irving-Williams Rule: Cu(II) > Ni(II) as expected. The rule describes the stability of complexes formed with divalent first-row transition metals ions. And states that the stability of these complexes generally increase across the period to a maximum stability at copper.[11] Cu(II) and Ni(II) are the two of the more stable divalent first-row metal ions and were for that reason most likely candidates for success in this experiment. The experimental results show that first row transition metal ions interact weakly with peptides that require them to form 7-membered rings upon coordination rendering the peptide chelate effects ineffective.

3.4 Reactivity of 12 with Pd(II)

3.4.1 Introduction

Sulfur-containing amino acids are known to interact with Pd(II) and Pt(II) initially through the sulfur that then promotes further chelation in aqueous solutions.[37,38] For sulfur-containing amino acids there is a competition between the sulfur and the amino group for coordination to palladium. Sulfur has a great tendency toward bond forming with Pd(II) and Pt(II) as explained by the HSAB (hard/soft acid/base) theory that sulfur is a soft Lewis base and the metals are soft Lewis acids.[39] The coordination of the sulfur is therefore not pH dependent. The NH_2 also has a strong tendency toward bond formation with Pd(II) and with Pt(II). That coordination is however pH dependent, at low pH the amino group is protonated (NH_3^+) so there is a competition between binding to H^+ and the metal ion. Pd(II) and Pt(II) can deprotonate amine groups at moderate pH and it has been reported that Pd(II) can form metal amide bond at around pH ~ 2.[25] The coordination of **12 (**alkylated GSH**)** to the Pd(II) though all eight different donor atoms, amine–N (primary or secondary), thiol-S and carboxylate–O is possible.[15] Investigation of interactions of $[Pd(en)(H_2O)_2]^{2+}$ with **12** in the range of pH 2.5-10 over 45 h was studied and characterized with ^1H NMR. The complex, $[Pd(en)(H_2O)_2]^{2+}$ has two open coordination sites where **12** may chelate.

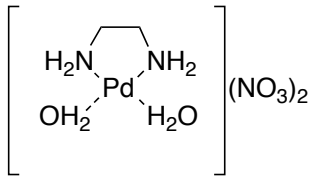

Figure 3.9 : Structure of $[Pd(en)(H_2O)_2](NO_3)_2$.

3.4.2 NMR Studies

The ligand, **12** was synthesized as described in section 3.1.2. The complex $[PdCl_2(en)]$ was prepared according to literature procedure.[40] The $[Pd(en)(H_2O)_2]^{2+}$ was then prepared by stirring $[PdCl_2(en)]$ in aquous solution with 2 eq. $AgNO_3$ for 24 h in the dark resulting in $[Pd(en)(H_2O)_2]^{2+}$ and insoluble AgCl, that was removed by filtration (spectra are presented in Appendix G). The solvent used was D_2O. All the samples contained KNO_3 in 4x ligand concentration as an electrolyte. NaOD (1.0 mmol L^{-1}) and DCl (1.0 mmol L^{-1}) were used to adjust the pH. Three solutions were prepared at pH 2.3, 5.9 and 9.5. ^1H NMR spectroscopy was used to determine the species distribution in the $[Pd(en)(H_2O)_2]^{2+}$- **12** system, at 25°C over 45h after ten different time periods.

3.4.3 NMR results

The results are from measurements of three samples pH 2.3, 5.9 and 9.5. The structure of **12** can be seen in Figure 3.10 with the protons numbered. In this section the referenced numbers refer to this outline.

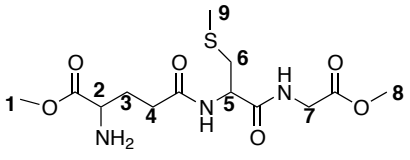

*Figure 3.10 : Structure of **12** with numbere protons for identification*

.

Measurements at pH 2.3

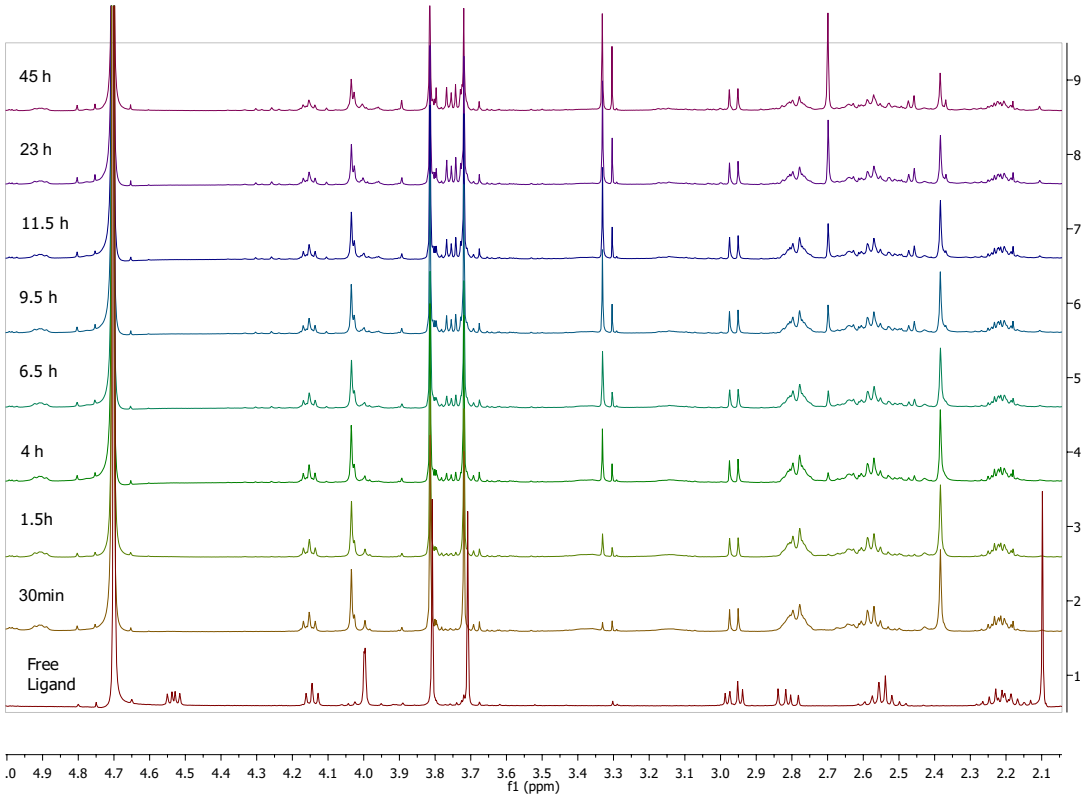

Figure 3.11 : ^{1}H NMR spectra of a solution at pH 2.3 at 25°C. $c_{Pd(en)}$=10 mmol L^{-1}, c_{12}=10 mmol L^{-1}, c_{KNO3}=40 mmol L^{-1}. Over 45h time period.

After adding the complex $[Pd(en)(H_2O)_2]^{2+}$ to the mixed solution, a white precipitate formed. Evaluation of the species formed at pH 2.3 is based on spectra taken over a period of time (Figure 3.11). The reaction of $[Pd(en)(H_2O)_2]^{2+}$ with **12** at 1:1 molar ration forms two major products over 45h period κ^1(S) (Figure 3.12.a) and κ^4 (NH_2, 2N, S) (Figure 3.11.b) complexes. First there is a coordination of the thioether to the metal that is confirmed by the marked downfield shifts of the protons 9, 5 and 6. Singlet of proton 9 shiftes form 2.2 ppm to 2.5ppm, quartet represented by proton 5 shifts from 4.6 ppm to 5.0 ppm and becomes obscured and the obscured peak for proton 6 shifts from 2.6 ppm to 3.3 and becomes broad. As time progresses, the resonance for free ethylenediamine at 2.7 ppm appears in the spectrum and the signal from the ethylendiamine – Pd multiplet around 2.8 ppm decreases. That indicates that the ethylendiamine is released from the Pd and the secondary amines of the ligand are also coordinated to the Pd. That is confirmed by the shift of protons 2 (4.2 ppm), 5 (5.0 ppm) and 7 (4.0 ppm) upfield to 3.7-3.8 ppm region. Additionally, hydrolysis of the esters is observed through formation of MeOD. Further chelation of the ligand to the Pd motivates thioether cleavage based on reduction in the SMe integral, along with increased formation of MeOD at 3.3 ppm.

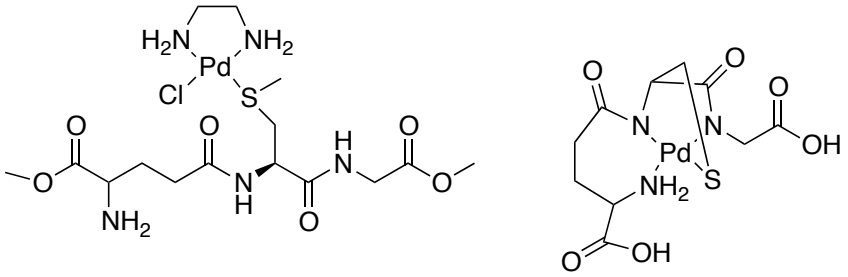

Figure 3.12 : Structures formed at pH 2.3 at 25°C. $c_{Pd(en)}$*=10 mmol* L^{-1}*,* c_{12}*=10 mmol* L^{-1}*,* c_{KNO3}*=40 mmol* L^{-1}*. Over 45h time period a)* κ^1(S) complex and b) κ^4 (NH_2, 2N, S) complex.

Measurements at pH 5.9

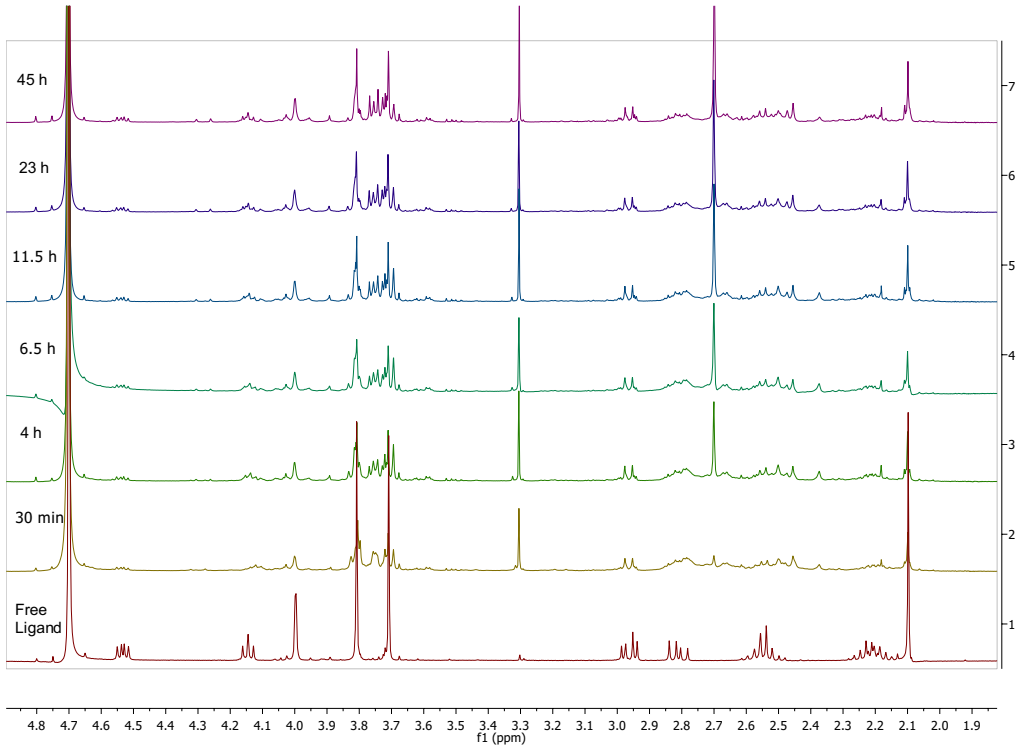

Figure 3.13 : ^{1}*H NMR spectra of a solution at pH 5.89 at 25°C.* $c_{Pd(en)}$*=10 mmol* L^{-1}*,* c_{12}*=9.9 mmol* L^{-1}*,* c_{KNO3}*=39 mmol* L^{-1}*, over 45h time period.*

After adding the complex $[Pd(en)(H_2O)_2]^{2+}$ to the mixed solution, a white precipitate formed. The evaluation of the species formed at pH 5.9 is based on spectra taken over period of time (Figure 3.13). The reaction of $[Pd(en)(H_2O)_2]^{2+}$ with **12** at 1:1 molar ration forms two major products over 45h period; *a* κ^1(S)(Figure 3.12.a) and a κ^3 (NH_2, 2N) (Figure 3.14.a) complexes. The κ^3 (NH_2, 2N) is the major product but a little bit of the κ^1(S) complex is observed by a small singlet of SMe at 2.4 ppm. When the pH increases, the resonance from proton 2 moves upfield due to deprotonation of NH_3^+ to NH_2.[41] The

formation of the complex κ^3 (NH_2, 2N) takes place over a long period of time displacing the ethylendiamine. This is observed by appearance of a singlet at 2.7 ppm and a decrease of the multiplet integral representing Pd-ethylendiamine at 2.8 ppm. Chelation of the amides is observed by shifts of the proton resonances for 2 (4.2 ppm), 5 (4.5 ppm) and 7 (4.0 ppm) upfield to 3.7-3.8 ppm region; these protons are all located next to the amides. Hydrolysis of the esters was observed by formation of MeOD and is greater than at lower pH, and now there is an increased possibility that that coordination to the metal encourages even more rapid hydrolysis.[41] Consequently there is some free carboxyl –O in the solution that can loosely coordinate to the palladium and stabilize the complex(Figure 3.14.b). The ligand is not very soluble in H_2O, but the complex is. So as more ligand dissolves, it displaces more of the ethylenediamine from the Pd and the intensity of the free ethylenediamine peaks becomes greater and the intensity of signal from the Pd-ethylendiamine multiplet around 2.8 ppm decreases. As mentioned above the sulfur coordinated complex is also observed in the spectra, since the proton resonances of that species are visible in the spectrum, but in small quantities. Rough estimate after 45 h by integration over the S-Me peaks indicates about 20% of the formed complexes are $a\ \kappa 1(\mathrm{S})$ species. The solution is not sufficiently basic to form 100% the κ^3 (NH_2, 2N) complex.

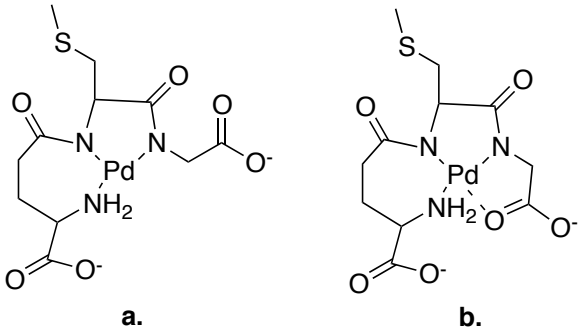

Figure 3.14 : Structures formed at pH 5.9, $c_{Pd(en)}$=10 mmol L^{-1}, c_{12}=9.9 mmol L^{-1}, c_{KNO3}=39 mmol L^{-1} and at pH 9.5,$c_{Pd(en)}$=9.9 mmol L^{-1}, c_{12}=9.6 mmol L^{-1}, c_{KNO3}=38 mmol L^{-1}. Obtained at 25°C over 45h time period. a)κ^3 (NH_2, 2N) complex and b) κ^4 (NH_2, 2N, O) complex.

Measurements at pH 9.5

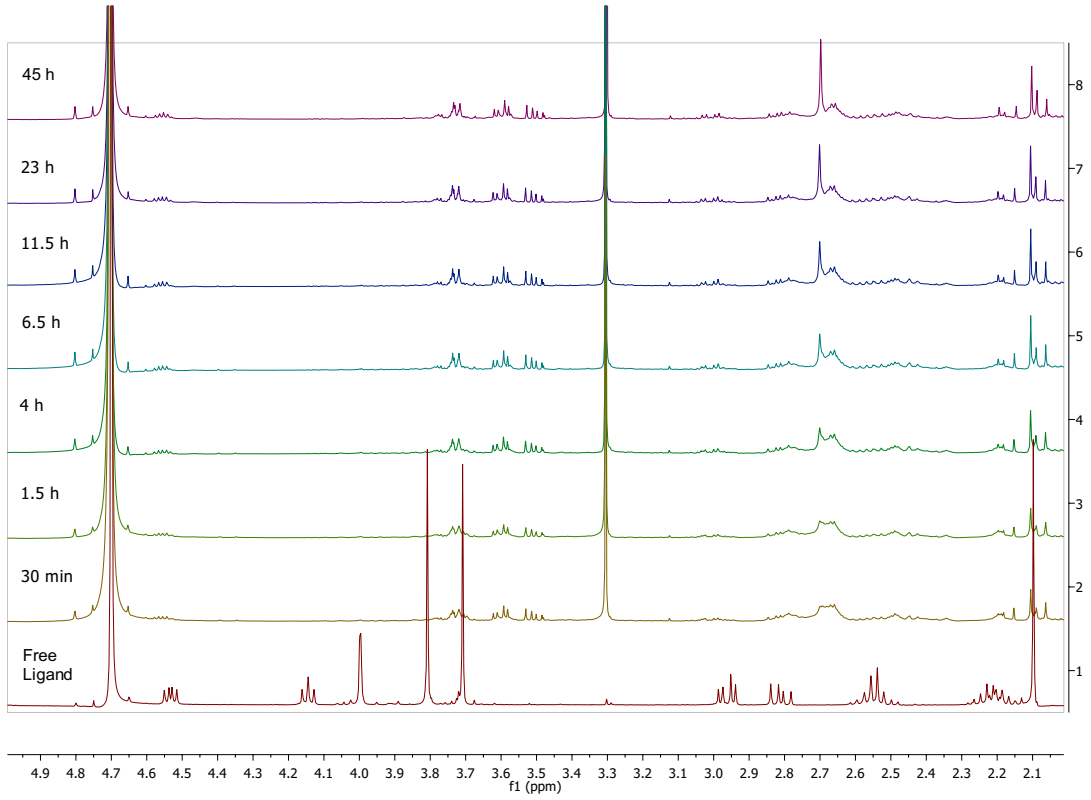

Figure 3.15 :^{1}H NMR spectra of a solution at pH 9.5 at 25°C. $c_{Pd(en)}$=9.9 mmol L^{-1}, c_{12}=9.6 mmol L^{-1}, c_{KNO3}=38 mmol L^{-1}, over 45h time period.

After adding the complex $[Pd(en)(H_2O)_2]^{2+}$ to the mixed solution, a white precipitate formed. The evaluation of the species formed at pH 9.5 is based on spectra taken over period of time (Figure 3.15). The reaction of $[Pd(en)(H_2O)_2]^{2+}$ with **12** at 1:1 molar ration forms a single product over 45h, κ^3 (NH_2, 2N) (Figure 3.14.a) or κ^4 (NH_2, 2N, O) (Figure 3.14.b) complex. When the pH increases, the resonances from proton 2 moves upfield due to changes of NH_3^+ to NH_2.[41] Formation of the complex, κ^3 (2N,NH_2) takes place over a long period of time displacing the ethylendiamine from the Pd in parallel. This is observed by appearances of a singlet at 2.7 ppm and decrease of the multiplet representing Pd-ethylendiamine at 2.8 ppm. Chelation of the amides is observed by shift of the protons 2 (4.2 ppm) and 7 (4.0 ppm) upfield to 3.5-3.8 ppm region , these protons are located next to the amide connected. Proton nr. 5 which is also next to an amide nitrogen does not shift upfield but it becomes a quintet ($^3J_{HH}$ = 4.4 Hz) instead of a quartet ($^3J_{HH}$ = 3.2 Hz, $^3J_{HH}$ = 5.2 Hz). The hydrolysis of the esters is 100% and is observed by formation of MeOD and absence of two singlets for methylgroups 1 and 8. Here it is also a possibility the coordination to the metal encourages hydrolysis in parallel to base catalyzed hydrolysis. The free carboxyl –O that can loosely coordinate to the Pd(II) and stabilize the complex. The complex formation drives dissolution of the ligand. So as more ligand dissolves, it displaces more of the ethylenediamine and the intensity of the free ethylenediamine peaks becomes greater and the intensity of signal from the Pd-ethylendiamine multiplet around 2.8 ppm decreases.

The precipites formed at all three pH values were isolated and dissolved in DMSO-d_6 and ^{1}H NMR recorded. In these spectra only resonances from the ligand were present and barely identified, but further or accurate characterization was prevented by their low concentration. The most likely explanation for the precipitation is reduced solubility of the free ligand in the mixture. The ligand is not as soluble in H_2O/D2O as the $[Pd(en)(H_2O)_2]^{2+}$ and due to high concentration of the mixed solution, the addition of the $[Pd(en)(H_2O)_2]^{2+}$ caused precipitation of a portion of the ligand.

3.4.4 Conclusions

Our present studies indicate the amide chelated species will suppress sulfur coordinated species in a $[Pd(en)^{2+}$ complex of **12** at a basic pH. At pH 5.9 only about 20 % is still sulfur coordinated species. The Pd(en)-**12** complexes are less thermodynamically stable than κ^3 [Pd-**12**] complex at all three pH. That is confirmed by formation of free ethylenediamine over time. The timeframe of the experiment may need to be longer to complete the reactions, since all the samples are still mixtures. Future work could be to repeat this experiment over extended timeframe. At this point a better idea of at what pH exactly the amide chelation suppresses the sulfur coordination and it would be interesting to measure samples at pH 2.5, 4.5, 6.5-7 and at 9.5. Another interesting experiment would be to repeat this experiment with another complex, [Pd(dien)Cl]Cl, I already synthesized according to literature procedures.[42] This complex has only one coordination site available and the dien is tridentate, and it is therefore interesting to investigate for comparison.

4 Experimental Section

4.1 General considerations

All solvents used were purchased from Sigma-Aldrich and were used without further purification, unless otherwise noted. Methanol for GSH modification was distilled under inert atmosphere and stored over molecular sieves.

H-Ala-Gly-OH and Fmoc-Asp-O^{t}Bu were purchased from Bachem. Other starting materials were purchased from Sigma-Aldrich and were used without further purification, unless otherwise noted. Triethylamine (TEA) for novel *iso*Asp-Ala-Gly synthesis was distilled under inert atmosphere and stored over molecular sieves. Trimethylchlorosilane (TMSCl) used in esterification was dried over CaH_2 and used freshly distilled. Thin layer chromatography (TLC) plates, with glass backing were purchased from Silicycle (250μm, F-245) along with silica gel for flash column chromatography (G60 60-200μm). $[Pd(en)Cl_2]$,[40] $[Pd(en)(H_2O)_2](NO_3)_2$,[43] [Pd(dien)Cl]Cl,[42] were all prepared by modification of published procedures.

^{1}H, COSY and ^{13}C nuclear magnetic resonance spectra were recorded on a Bruker Avance 400 MHZ spectrometer at 400 and 101 MHz, respectively. The spectra were all measured at ambient temperature. Solvents used were D_2O, $CDCl_3$ and DMSO-d_6. In ^{1}H NMR spectrum the singlet from residual $CHCl_3$ in $CDCl_3$ at δ 7.26 ppm was used as a reference, similarly for the singlet from residual of H_2O in D_2O at δ 4.79 ppm as well as the quintet form residual DMSO in DMSO-d_6 at δ 2.50 ppm. Chemical shifts (δ) are quoted in parts per million (ppm) and the coupling constants (*J*) in Hertz (Hz). Infrared spectra were recorded on a Nicolet Avatar 360 FT-IR (E.S.P.) spectrophotometer using KBr pellets. The spectra were obtained using 32 scans and 4 cm^{-1} resolution, over the 480-4000 cm^{-1} range. Uv-Vis spectra were recorded on Perkin Elmer, Lambda 25, UV/Vis spectrometer. The spectra were obtained over the 200-1100 nm range. Mass spectra were recorded by Dr. Sigríður Jónsdóttir at the University of Iceland Science Institute on a micrOTOF-Q spectrometer, equipped with E-spray atmospheric pressure ionization chamber (ESI). Spectra were measured in positive ion mode and negative ion mode as appropriate. pH measurements were performed with Mettler Toledo pH and conductivity meter. Potentiometric studies were performed in collaboration with Prof. Dr. Etelka Farkas at the University of Debrecen, Hungary and were executed in her laboratory. The potentiometric studies were performed with Radiometer DL50 Graphix (METTLER TOLEDO) titration system containing a pH-meter and automatic burette and equipped with a 51109503 combined silver/silve chloride electrode (METTLER TOLEDO).

The numbers of the compounds referred to in this section are as in sections 2 and 3.

4.2 Methods

H-Ala-Gly–OMe (2): Dried chlorotrimethylsilane (2.61ml, 20.56 mmol) was added dropwise to dry H-Ala-Gly-OH (1.500g, 10.26 mmol) resulting in white muddy mixture. Then MeOH (11ml) was added to the stirring solution and a drying tube attached. Stirring of the mixture was continued for 25h at room temperature. Evaporation of the solvent and of the side product yielded the H-Ala-Gly–OMe(**2**) as 1.992g of the white hydrochloride salt (99% yield). ^{1}H NMR (D_2O): δ, ppm 4.17 (q, $^{3}J_{HH}$ = 7.2 Hz, 1H, α-H_{Ala}), 4.10 (d, $^{3}J_{HH}$=2 Hz, 2H, α-H_{Gly}), 3.79 (s, 3H, O=C-O-**C**$H_{3\ Gly}$), 1.58 (d, $^{3}J_{HH}$= 7.2, 3H, β-H_{Ala}). ^{13}C-{*H*} NMR(D_2O) δ, ppm: 171.84 (R(O=**C**)-O-$CH_{3\ Gly}$), 171.38 (C=O_{Ala}) 52.93 (O=C-O-**C**$H_{3\ Gly}$) 49.05(α-C_{Ala}) 41.20 (α-C_{Gly}) 16.43(β-C_{Ala}).

O^{t}Bu-Fmoc-*iso*Asp-Ala-Gly-OMe(4):1-ethyl-3-(3-dimethylaminopropyl)-carbodiimide hydrochloride(EDC) (521 mg, 2.72 mmol) was added to a stirred suspension of Fmoc-Asp-O^{t}Bu (1017mg, 2.47 mmol) and hydroxybenzotriazole t∗H_2O(418 mg, 2.73 mmol) dissolved in $CHCl_3$ (10ml) at 0°C (ice/H_2O). After addition the ice bath was removed and the solution was stirred for five minutes, when the suspension started to dissolve. Then (**2)** (487mg, 2.47mmol) was added to the mixture followed by slow dropwise addition of triethylamine (0.345 ml, 2.47mmol) dissolved in 3ml of $CHCl_3$. The reaction was stirred for 24h. Then the solvent was removed under reduced pressure, resulting in a yellow paste. The resulting yellow paste was stirred in H_2O (25ml) for 2h forming a white suspension and a yellow solution. The white suspension was collected by filtration. The crude product was purified by flash chromatography (neutral silica gel) using Dichloromathane (DCM):MeOH as the elutent in a stepwise elution (1:0, 99:1, 98:2) to give pure product O^{t}Bu-Fmoc-*iso*Asp-Ala-Gly-OMe **(4)**, after evaporation of solvent under reduced pressure, as 749 mg of a white powder (55% yield). ^{1}H NMR ($CDCl_3$): δ ppm 7.75 (d, $^{3}J_{HH}$= 7.6 Hz, 2H, C-H-Ph_{Fmoc}), 7.61 (d, $^{3}J_{HH}$= 7.6 Hz, 2H, C-H-Ph_{Fmoc}) 7.39 (d, $^{3}J_{HH}$= 7.2 Hz, 2H, C-H-Ph_{Fmoc}) 7.30 (d, $^{3}J_{HH}$= 7.2 Hz, 2H, C-H-Ph_{Fmoc}) 6.77(s, 1H, NH_{Gly}), 6.31 (s, 1H, NH_{Ala}), 6.13 (s,1H, NH_{Asp}), 4.57(m, 1H, α-H_{Ala}), 4.51(m, 1H, α-H_{Asp}) 4.36(q, $^{3}J_{HH}$=8 Hz, 2H, $CH_{2\ Fmoc}$) 4.22(t, $^{3}J_{HH}$=7.2 Hz, 1H, CH_{Fmoc}) 4.01 (qd ,$^{2}J_{HH}$= 18 Hz, $^{3}J_{HH}$= 5.2 Hz, 2H, α-H_{Gly}) 3.70 (s, 3H, O=C-O-**C**$H_{3\ Gly}$) 2.83 (q, $^{2}J_{HH\ =}$ 36.8, $^{3}J_{HH\ =}$ 18.0, 2H, β-H_{Asp}) 1.47(s, 9H, $OtBu_{Asp}$), 1.40 (d, $^{3}J_{HH\ =}$7.2 Hz, 3H, β-H_{Ala}). ^{13}C {*H*} NMR($CDCl_3$): ppm 172.15 (R(O=**C**)-O-CH_{3Asp}), 170.20 (C=O_{Asp}), 169.85 (C=O_{Ala}), 143.90, 141.28, 127.71, 127.09, 125.22, 119.96 (C-H Ph_{Fmoc}) 82.51 (α-C_{Asp}), 67.21 ($CH_{2\ Fmoc}$), 52.42 (**C**$(CH)_{3\ Asp}$), 48.72 (C=O_{Fmoc}), 47.17 (α-C_{Gly}), 41.14 (α-C_{Ala}), 38.30 (β-C_{Asp}), 27.96(C(**C**$H)_{3\ Asp}$), 18.15(β-C_{Ala}). IR (KBr, cm^{-1}): 3385(m, N-H, R_2-NH) 3271(m, N-H, R_2-NH), 3315(m, N-H, R_2-NH) 3067(w), 3044s(w) 2986(w), 2952(w) (C-H,) 1752(s, C=O, RCOOR'), 1725(s, (C=O, RCOOR')) 1690(s, CO), 1647(s, CO). CHN-Anal. Calcd. For $C_{29}H_{35}N_3O_8$: C, 62.69; H, 6.71; N, 7.56. Found: C, 62.58; H, 6.46; N, 7.62. MS (ESI/positive): M ($C_{29}H_{35}N_3O_8$) 553.60 g/mol -m/z found(calc.) = 576,2316 (576,2319) [M-Na^{+}].

O^{t}Bu-isoAsp-Ala-Gly-OMe (5): OtBu-Fmoc-isoAsp-Ala-Gly-OMe (**4**) (380 mg, 0.686 mmol) was dissolved in DMF (25ml) forming a clear solution. A drying tube was added and the mixture heated to ~120 °C and stirred for 5h. The resulting mixture was a yellow solution. It was placed in the freezer overnight. The DMF was evaporated in vacuo (max

heat 50°C) forming two separate compounds; a white film and a yellow paste. The product was stirred in MeOH (~30ml) for 1h resulting in a yellow solution and a white precipitate. The precipitate was removed by filtration. The crude product was purified by flash chromatography (neutral silica gel) using DCM :MeOH (92:8) for elution to afford the pure product O^{t}Bu-isoAsp-Ala-Gly-OMe(**5)**, that after evaporation of solvent formed 161 mg of a yellow film (65% yield). Compound **5** is hydroscopic and was kept under inert gas. ^{1}H NMR (D_2O): δ ppm 4.40 (q, $^{3}J_{HH}$= 7.2Hz, 1H, α-H_{Ala}), 4.06 (s, 2H α-H_{Gly}), 3.79 (s, 3H R(O=C)-O-$CH_{3\ Gly}$) 3.78 (t, $^{3}J_{HH}$= 6.0 Hz, 1H, α-H_{Asp}) 2.74(q, $^{3}J_{HH}$= 3.2 Hz, 2H, β-H_{Asp}), 1.49 (s, 9H, $OtBu_{Asp}$), 1.44(d, $^{3}J_{HH}$= 7.2 Hz, 3H, β-H_{Ala}).^{13}C {H} NMR(D_2O): ppm 175.57 (R(O=**C**)-O-CH_{3Asp}), 174.37 (R(O=**C**)-O-$OtBu_{Asp}$), 172.49 (C=O_{Asp}), 171.90 (C=O_{Ala}), 83.42 (α-C_{Asp}), 52.78 (R(O=C)-O-**C**$H_{3\ Gly}$), 51.49 (R(O=C)-O-**C**$(CH)_{3\ Asp}$), 49.45 (α-C_{Gly}), 41.10 (α-C_{Ala}), 38.84 (β-C_{Asp}), 27.11(C(**C**$H)_{3\ Asp}$), 16.74(β-C_{Ala}). IR (KBr, cm^{-1}): 3374(ms) 3307(ms) (N-H, R_2-NH), 3126 (m, N-H, R-NH_3^+) 2981(m), 2935(m) (C-H) 1740 (s, C=O, RCOOR') 1655 (s, C=O). MS (ESI/positive):M ($C_{14}H_{25}N_3O_6$) 331.36 g/mol -m/z found(calc.) = 332.1816 (332.1814) [M-H$^+$].

Pd-O^{t}Bu-isoAsp-Ala-Gly-OMe (8) and (9): K_2PdCl_4 (55 mg, 1.69 mmol) was dissolved in H_2O (5ml) and stirred for 15 minuets. The suspension was then filtrated. To the filtrate was added dropwise, a solution of O^{t}Bu-isoAsp-Ala-Gly-OMe (**5**) (55 mg, 1.66 mmol) dissolved in H_2O (7ml). The color of the solution changed from yellow to brown. The reaction was monitored by UV-vis and was stirred for 5h. By that time the solution had turned yellow. The solvent was removed by rotary evaporation resulting visibly in two precipitates, white and yellow. The solid was treated with acetonitrile (20 ml) resulting in a white precipitate and a yellow solution. The precipitate was removed by filtration and the solvent evaporated from the solution forming a yellow solid [Pd-O^{t}Bu-isoAsp-Ala-Gly-OMe].(yield; 55mg). The yellow solid proved to be a mixture of two Pd complexes with O^{t}Bu-isoAsp-Ala-Gly-OMe(**5**). IR (KBr): 3374 cm^{-1}(m), 3306 cm^{-1}(m), 3126 cm^{-1}(w), 2981 cm^{-1}(m), 2935 cm^{-1} (m), 1739 cm^{-1}(s), 1654 cm^{-1}(ms). (MS (ESI/negative):M ($C_{14}H_{23}ClKN_3O_6Pd$) 510.32 g/mol -m/z found(calc.) = 471.0360 (471.04) [M-H$^+$]. M ($C_{14}H_{25}N_3O_6Pd$) 435.77 g/mol -m/z found(calc.) = 436.0711 (436.0746) [M-H$^+$]

GSH(SMe) (13): Ammonium bicarbonate (413 mg, 5.23mmol) was added to a solution of glutathione (535 mg, 1.74 mmol) in H_2O(20ml) (degassed).The solution was stirred for 20 minuets and formation of bubbles was observed. Then iodomethane(CH_3I) (0.110 ml, 1.77 mmol) was added and the flask fitted with a drying tube, after which the mixture was stirred for 4h. The solvent was removed by rotary evaporation resulting in a clear oil. This oil was redissolved in H_2O (20ml) (degassed) and the reaction was repeated. Then ammonium bicarbonate (413 mg, 5.23mmol) was added to the solution and stirred for 20 minuets and formation of bubbles was observed. Then CH_3I (0.110 ml, 1.77mmol) was added and the mixture stirred for 4h as before. The solvent was removed resulting in clear oil that solidified into a white solid after drying in vacuo. The salts were removed from the crude product by flash chromatography (neutral silica gel) using Acetonitil(CH_3CN): H_2O as elutent in stepwise elution (9:1 and 1:1) to give pure product GSH(SMe)(**13)**, after evaporation of solvent and drying in vacuo 778mg of a white solid was collected (95% yield). ^{1}H NMR (D_2O): δ ppm 4.63 (q, $^{3}J_{HH}$= 4.0 Hz, $^{3}J_{HH}$= 4.8 Hz, 1H, α-H_{Cys}), 3.84 (s, 2H, α-H_{Gly}), 3.82 (t, $^{3}J_{HH}$= 6.4 Hz 1H, α-H_{Glu}) 2.98 (obsc. 2H, β-H_{Cys}) 2.58 (Sex, $^{3}J_{HH}$= 4.0

Hz, 2H, γ-H_{Glu}), 2.20 (qt, $^3J_{HH}$= 6.4 Hz, 9H, β -H_{Glu}), 2.17(s, 3H, SMe).$^{13}C\{H\}$ NMR (D_2O): ppm 175.93 (α-$C{=}O_{Glu}$) 174.99(α-$C{=}O_{Gly}$) 173.96 (α-$C{=}O_{Cys}$) 172.25 (γ-$C{=}O_{Glu}$) 54.10(α-C_{Gly}) 52.70 (α-C_{Cys}) 35.02(α-C_{Glu}) 35.02 (β-C_{Cys}) 31.36 (S-CH_3) 26.18(γ-C_{Glu}) 14.62 (β-$C{=}O_{Glu}$). MS (ESI/Positive):M ($C_{11}H_{19}N_3O_6S$) 321.35 g/mol -m/z found(calc.) = 344.0887 (344.0884) [M-Na^+].

{GSH(OMe)$_2$(SMe)} (12): Hydrochloric acid(HCl) gas was formed by dropwise addition of $H_2SO_{4\ conc}$ to ammonium chloride. The HCl gas formed was fed into a flask containing stirred suspension of GSH(SMe)(132mg, 0.411mmol) in distilled MeOH (60ml). This mixture was stirred for 4h, with constant $HCl_{(g)}$ flow at 0°C(ice/H_2O). Then the solvent was removed in vacuo, resulting in a white powder. The powder was redissolved in distilled MeOH (10ml) and again the mixture was stirred with constant $HCl_{(g)}$ flow for 1.5h. Then the solvent was removed in vacuo resulting in the hydrochloride salt of the product {GSH(OMe)$_2$(SMe)} (**12**)**.** The product was collected as 152 mg of a light yellow powder (94% yield). Compound **12** is hydroscopic and was stored under inert gas. ^1H NMR (D_2O): δ ppm 4.62 (q, $^3J_{HH}$= 3.2 Hz, $^3J_{HH}$= 5.2 Hz, 1H, α-H_{Cys}), 4.24 (t, $^3J_{HH}$= 6.8 Hz 1H, α-H_{Glu}), 4.09(s, 2H, α-H_{Gly}) 3.989 (s, 3H $RCOOCH_{3\ Glu}$) 3.80 (s, 3H, $RCOOCH_{3\ Gly}$) 2.98 (obsc. 2H, β-H_{Cys}) 2.64 (o, $^3J_{HH}$= 7.6 Hz 2H, γ-$H_{\ Glu}$) 2.30 (m, 2H β -H_{Glu}), 2.19(s, 3H, SMe). $^{13}C\{H\}$ NMR (D_2O): ppm 174.15 (α-C=O-(Glu)) 173.06 (α-$C{=}O_{Gly}$) 171.76 (α-$C{=}O_{Cys}$) 170.14 (γ-$C{=}O_{Glu}$) 53.65 (O=C-O-**C**H_{3Glu})52.79(O=C-O-**C**$H_{3\ Gly}$) 52.62(α-C_{Gly}) 52.16(α-C_{Cys}) 41.20 (α-C_{Glu}) 34.87 (β-C_{Cys}) 30.65 (S-CH_3) 25.26 (γ-C_{Glu}) 14.63 (β-$C{=}O_{Glu}$). IR (KBr, cm^{-1}): 3396(ms), 3257(ms) (N-H, R_2-NH), 3059(ms, N-H, R-NH_3^+), 2954(ms), 2926(ms) (C-H), 1748 (s, C=O, RCOOR'), 1645(s, C=O). MS (ESI/Positive):M ($C_{13}H_{24}N_3O_6S$) 349.40 g/mol -m/z found(calc.) = 350.1380 (350.1370) [M-H^+].

[Pd(en)Cl$_2$]: K_2PdCl_4(1.003g, 3.07 mmol) was dissolved in H_2O (12ml) and stirred for 15 minutes. The solid formed was removed by filtration. To 5 ml of the brown filtrate, 1.5 M ethylenediamine solution (2.1ml) was added dropwise. The color of the solution changed to salmon pink. The resulting solution was heated to boiling(~ 85°C) for 1.5h during which the color changed to yellow. The solution was cooled to 10°C (ice/H_2O) and the remaining K_2PdCl_4 solution was added. Formation of salmon pink precipitate was observed. The pink precipitate was collected by filtration and washed with cold H_2O (ice/H_2O) (2x10ml). To a suspension of the pink precipitate in H_2O (10ml), 2 drops of 12 M HCl was added, and the resulting mixture was heated to ~100°C and stirred in the dark for 2h. After that time the suspension had partly turned yellow. Then 2 more drops of 12M HCl was added along with H_2O (5ml). The solution was stirred and heated (~100°C) in the dark for additional 45 minutes. Then the suspension had all turned yellow. The mixture was cooled in ice bath for 10 minutes. The precipitate was collected by filtration and washed with cold H_2O. The precipitate was dried in a desiccator for two days, resulting in 506mg of a yellow solid (70% yield). ^1H NMR (DMSO-d^6): δ ppm 4.88 (s, 4H, NH_2), 2.33 (s, 4H, CH_2). IR (KBr,): 3289 cm^{-1}(s), 3259 cm^{-1}(s), 3209 cm^{-1}(s), 3109 cm^{-1}(m)1563 cm^{-1}(ms), 1099 cm^{-1}(ms),1056 cm^{-1}(s)

$[Pd(en)(H_2O)_2](NO_3)_2$: $AgNO_3$ (147 mg, 0.842 mmol) was added to a stirred suspension of $[Pd(en)Cl_2]$ (100 mg, 0.421mmol) in H_2O (25ml). The mixture was stirred for 20h in the dark. A white suspension formed immediately. The solvent was removed by rotary evaporation forming a yellow film that was washed with ether (20ml) and dried in vacuo overnight resulting in 137,2 mg of a yellow solid (95% yield). ^1H NMR (D_2O): δ ppm 5.14 (s, 1H, NH_2), 2.59 (s, 4H, CH_2). IR (KBr): 3433 cm^{-1}(w) 3305 cm^{-1}(ms), 3242 cm^{-1}(ms), 3142 cm^{-1}(m) 2999 cm^{-1}(vw) 2961 cm^{-1}(vw), 2895 cm^{-1}(vw) 1577cm^{-1}(ms), 1499 cm^{-1}(s), 1474 cm^{-1}(s), 1384 cm^{-1}(s), 1300 cm^{-1}(s), 1277 cm^{-1}(s),1099 cm^{-1}(ms),1056 cm^{-1}(ms)

[Pd(dien)Cl]Cl: $PdCl_2$ (1.000 g, 6.64 mmol) was dissolved in H_2O (17ml) and HCl_{Conc} (3ml) and stirred for 1h. The solid formed was removed by filtration. Diethylendiamine (5.65mmol) was added slowly dropwise (exothermic) to the burgundy red filtrate resulting in formation of yellow precipitate. The mixture was stirred for 19h. More precipitate had formed which was collected by filtration and dried in vacuo. The compound was recrystallized from highly concentrated aqueous solution by addition of ethanol forming yellow brown precipitate that was dried in vacuo over night to yield 476 mg of a solid (30% yield). ^1H NMR (DMSO-d_6): δ , ppm: 9.997 (s, 1H, NH_2), 8.304 (s, 3H, N-CH_2), 3.215 (d, $^3J_{HH}$= 22.4 Hz, NH_2-CH_2). IR (KBr): 3175 cm^{-1}(s), 3012 cm^{-1}(s), 2973 cm^{-1}(s), 2816 cm^{-1}(s), 1589cm^{-1}(m), 1563 cm^{-1}(m), 1491 cm^{-1}(s), 1473 cm^{-1}(s), 1442cm^{-1}(m),1016cm^{-1}(s).

Potentiometric studies: For each metal:ligand pH Metric titration it is important that the same stock solutions for all chemicals is used thoughout the experiment. Mixtures of the measured solutions used in potentiometric studies on copper(II):GABA systems is displayed in table 4.1 All stock solutions were prepared using H_2O as a solvent. The solution containing the metal was always the last added.

Table 4.1: Composition of the solutions used in potentiometric studies of copper(II):GABA systems

PMT solution*	**GABA (0.123mM)**	**KCl (1.00M)**	**HCl (0.198M)**	**$CuCl_2$ (0.0401M)**	**H_2O**	**V_{total}**
GABA	5.00ml	3.00ml	0.50ml	-	6.50ml	15.00ml
Cu:GABA(1:1)	5.00ml	3.00ml	0.50ml	1,30ml	5.20ml	15.00ml
Cu:GABA(1:2)	5.00ml	3.00ml	0.50ml	0.60ml	5.90ml	15.00ml
Cu:GABA(1:6)	5.00ml	3.00ml	0.50ml	0.25ml	6.25ml	15.00ml

*PMT solution : Solution used in potentiometric studies.

Mixing of the measured solutions from stock solutions used in potentiometric studies on nickel(II):GABA systems is displayed in table 4.2. All stock solutions were prepared using H_2O as a solvent. The solution containing the metal was always the last added.

Table 4.2 Composition of the solutions used in potentiometric studies of nickel(II):GABA systems

PMT solution*	GABA (0.119mM)	KCl (1.00M)	HCl (0.198M)	$NiCl_2$ (0.0416mM)	H_2O	V_{total}
GABA	5.00ml	3.00ml	0.50ml	-	6.50ml	15.00ml
Ni:GABA(1:1)	5.00ml	3.00ml	0.50ml	1,30ml	5.20ml	15.00ml
Ni:GABA(1:2)	5.00ml	3.00ml	0.50ml	0.60ml	5.90ml	15.00ml
Ni:GABA(1:6)	5.00ml	3.00ml	0.50ml	0.25ml	6.25ml	15.00ml

*PMT solution : Solution used in potentiometric studies.

HCl method was used for titration curve of the pure GABA. Titration addition: incremental, dV[ml] = 0.015, measured = time incremental, dt[s]=90sek, Termination (at potential at 11.5)

Ru method was used for pH-Metric titration curve of metal(II):GABA systems. dV[ml] = 0.015, measured mode = equilibrium control, de[mV] = 0.015, dt[s] = 11, t(min) = 120, t(max) = 300, pH potential 7-10 (depending on the ration).

NMR Experiments: All the samples were mixed the same way. {$GSH(OMe)_2(SMe)$} (**12)** and $[Pd(en)H_2O](NO3)_2$ were synthesized as described above. First the **12** was added to D_2O with dose that did not completely dissolve. Then the KNO_3 was added. Last the $[Pd(en)H_2O]$ was added to the solution and formation of precipitate and a yellow solution was observed. Finally the pH was adjusted with NaOD (2.13 mol L^{-1}) and DCl (2.05mol L^{-1}). 1 ml of each mixture was transferred to NMR tube. Mixing of the measured solutions used in NMR experiment for palladium(II):**12** systems is displayed in table 4.3. No stock solution were made due cost of D_2O.

Table 4.3 Composition of the solutions used in NMR studies of palladium(II):**12** systems.

pH	$\{GSH(OMe)_2$-(SMe)}(12)(mg)	$[Pd(en)H_2O]$-$(NO3)_2$ (mg)	KNO_3 (mg)	NaOD (μl)	DCl (μl)	H_2O(ml)	V_{total} (ml)
2.331	7.7	6.7	8.0	-	-	2.000	2.000
5.983	7.7	6.7	8.0	20	-	2.000	2.020
9.512	7.8	6.8	8.1	80	20	2.000	2.100

5 Conclusion

In my studies as a M.Sc. student in chemistry department of the University of Iceland Science Institute various experiments were executed with different degree of success. Progress was made on some projects during studies on synthesis and investigation of reactivity of alkylated tripeptides with metal ions but there are still quite a few question left unanswered which are an interesting project for future researchers. In this thesis I also left out work I performed unrelated to this project to help out with other projects in Suman's group.

A synthetic methodology for a novel *iso*Asp-Ala-Gly, using LPPS, was completed. This method is a three step process and is quite affordable synthesis The yields are around 65% which are fair for coupling reactions with LPPS, however, there is always room for modification of the method to increase the yields. The downside of this synthesis is long reaction time. The novel *iso*Asp-Ala-Gly was employed as a ligand to form a palladium complex. Characterization thereof implies formation of (6,5,5) membered ring chelation as I set out to synthesize. The reaction still needs to be developed further. However it was shown that novel *iso*Asp-Ala-Gly chelates to Pd(II) forming two different complexes under ambient condition in a short period of time. This complex formation underpins that it may be possible to use novel *iso*Asp-Ala-Gly to form complex intended for copolymerization of CO_2 and alkene. Therefore further investigation of novel *iso*Asp-Ala-Gly and it's reactions with different metal ions will make an interesting project for further research.

A synthetic methodology for modification of GSH was presented. That process was complicated and the optimization of the method was time consuming. That is probably no coincidence because of its importance in biological processes. The plan was to use $\{GSH(OMe)_2(SMe)\}$as a model ligand to see if seven membered ring chelation was possible for Cu(II) and Ni(II). That plan did not work out due to ester hydrolysis of the alkylated compounds, and GABA was used instead. The results from potentiometric titration of GABA with Cu(II) and Ni(II) indicates that seven membered ring chelation is possible but it is not as stable as five and six membered ring chelation. The $\{GSH(OMe)_2(SMe)\}$was also employed as a ligand for Pd(II) complexes in an NMR experiment studying the complex formation at three different pH values. The result show that a (7,5,5) membered ring chelation is possible with Pd(II). The chelation mode of the ligand differs over the pH range. In acidic pH the chelation through the thioether is favored and as the solution becomes more alkaline the NH_2 coordination is favored. The chelation to the Pd(II) has a larger formation constant than the Pd(en) complex which is considered quite stable. This conclusion applies both kinetically and thermodynamically to this system. The results from potentiometric titration and NMR studies showed that 7-membered ring chelation is possible but it is not as stable as 5 and 6 membered ring chelation for first row transition metals ion. Palladium can however support 7 membered ring chelation in aqueous soluions, Pd(II) is a lager metal ion then Cu(II) and Ni(II) and can there for support larger ring chelations.

My project provided solid training in synthesis and in solving synthetic problems while working towards a specific goal of making a potential catalyst for utilization of a waste greenhouse gas. At the end of the project I leave two such catalysts for the next steps.

References

1. Aresta. M. Carbon Dioxide Reduction and Uses as a Chemical Feedstock in : Tolman, W. B(Ed.), Activation of Small Molecules, edition WILEY-VCH Verlag GmbH & Co. KGaA, Minneapolis, 2006, p. 1.

2. Cheng, M., Lobkovsky, E. B., Coates, G. W. Catalytic Reactions Involving C1 Feedstocks : New High-Activity Zn(II)-Based Catalysts for the Alternating Copolymerization of Carbon Dioxide and Epoxides. *J. Am. Chem. Soc.* **120,** 11018–11019 (1998).

3. Fujita, E., Creutz, C., Sutin, N., Szalda, D. J. Carbon-Dioxide Activation By Cobalt(I) Macrocycles - Factors Affecting CO_2 and CO Binding. *J. Am. Chem. Soc.* **113,** 343–353 (1991).

4. Benson, E. E., Kubiak, C. P., Sathrum, A. J. & Smieja, J. M. Electrocatalytic and homogeneous approaches to conversion of CO_2 to liquid fuels. *Chem. Soc. Rev.* **38,** 89–99 (2009).

5. Sakakura, T., Choi, J., Yasuda, H. Transformation of Carbon Dioxide. *Chem. Rev.* **107,** 2365–2387 (2007).

6. Miessler, G., Fischer, P.Tarr, D. A. *Inorganic Chemistry*, 4th edition, Pearson Education Limited, 2014.

7. Durand, J., Milani, B. The role of nitrogen-donor ligands in the palladium-catalyzed polyketones synthesis. *Coord. Chem. Rev.* **250,** 542–560 (2006).

8. Siebert, A. F. M., Sheldrick, W. S. pH-Dependent competition between N,S and N,N chelation in the reaction of $[Pt(en)(H_2O)_2]^{2+}$(en = $H_2NCH_2CH_2NH_2$) with methionine-containing di- and tri-peptides. *J. Chem. Soc. Dalt. Trans.* 385–393 (1997).

9. Ágoston, C. G., Jankowska, T. K., Sóvágó, I. Potentiometric and NMR studies on palladium(II) complexes of oligoglycines and related ligands with non-coordinating side chains. *J. Chem. Soc. Dalt. Trans.* 3295–3302 (1999).

10. Nagy, Z., Fábián, I., Sóvágó, I. Thermodynamic, kinetic and structural studies on the ternary palladium(II) complexes of thioether ligands. *J. Inorg. Biochem.* **79,** 129–138 (2000).

11. Irving, H., Williams, R. J. P. The stability of Transition-metal Complexe. *J. Chem. Soc.* 3192–3210 (1953).

12. Merrifield, R. Solid Phase Peptide Synthesis. I. The Synthesis of a Tetrapeptide. *J. Am. Chem. Soc.* **85,** 2149–2154 (1963).

13. Takahashi, D., Yamamoto, T. Development of an efficient liquid-phase peptide synthesis protocol using a novel fluorene-derived anchor support compound with Fmoc chemistry; AJIPHASE. *Tetrahedron Lett.* **53,** 1936–1939 (2012).

14. Fujishima, A., Honda, K. Liquid Phasa Synthesis og Peptides. *Nature.* **237,** 512–513 (1972).

15. Sóvágó, I., Kállay, C., Várnagy, K. Coordionation chemistry reviews. *Coord. Chem. Rev.* **256,** 2225–2233 (2012).

16. Li, J., Sha, Y. A convenient synthesis of amino acid methyl esters. *Molecules.* **13,** 1111–1119 (2008).

17. Sheehan, J., Hess, G. A new method of forming peptide bonds.(carbodiimide). *J. Am. Chem. Soc.* **77,** 1067-1068 (1955).

18. Chan, L. C., Cox, B. G. Kinetics of Amide Formation through Carbodiimide / N-Hydroxybenzotriazole (HOBt) Couplings. *J. Org. Chem.* **72,** 8863–8869 (2007).

19. Clayden, J., Greeves, N., Warren, S., Peter, W. *Organic synthesis*, Oxford university Press, 2001.

20. Iwasawa, T., Wash, P., Gibson, C., Rebek, J. Reaction of an introverted carboxylic acid with carbodiimide. *Tetrahedron.* **63,** 6506–6511 (2007).

21. Gioeli, C., Chattopadhyaya, J. B. The Fluoren-9-ylmethoxycarbonyl Group for the Protection of Hydroxy- groups; Its Application in the Synthesis of an Bctathymidylic Acid Fragment. *J. Chem. Soc. Chem. Commun.* 672–674 (1982).

22. Carpino, L. A., Sadat-Aalaee, D., Beyerman, M. Tris(2-aminoethy1)amine as a Substitute for 4-(Aminomethy1)piperidine in the FMOC/Polyamine Approach to Rapid Peptide Synthesis. *J. Org. Chem.* **55,** 1673–1675 (1990).

23. Höck, S., Marti, R., Riedl, R., Simeunovice, M. Thermal cleavage of the fmoc protection group. *Chimia (Aarau).* **64,** 200–202 (2010).

24. Takeda, N., Shimizu, D., Tokitoh, N. Synthesis and Structure of a Distorted Octahedral Palladium (II) Complex Coordinated with a Tetrathioether Ligand Tethered with Bulky Substituents. *Inorg. Chem.* **44,** 8561–8568 (2005).

25. Ágoston, C. G., Jankowska, T. K., Sóvágó, I. Potentiometric and NMR Studies on palladium(II) complexes of oligoglycines and related ligands with non-co-ordinating side chains. *J. Chem. Soc., Dalt. Trans.* 3295–3302 (1999).

26. Pompella, A., Visvikis, A., Paolicchi, A., De Tata, V., Casini, A. F. The changing faces of glutathione, a cellular protagonist. *Biochem. Pharmacol.* **66,** 1499–1503 (2003).

27. Krężel, A., Bal, W. Coordination chemistry of glutathione. *Acta Biochimica Polonica.* **46,** 567–580 (1999).

28. Várnagy, K., Sóvágó, I., Kozlowski, H. Transition metal complexes of amino acids and derivatives containing disulphide bridges. *Inorganica Chim. Acta.* **151,** 117–123 (1988).

29. Serjeant, E. P. Practical Applications of Potentiometry Potentiometry. *Anal. Chem.* **57,** 711–712 (1985).

30. Skoog, D. A., Holler, F. J., Nieman, T. A. *Principles of Instrumental Analysis*, 5th edtion, Thomson Learning Inc, USA, (1998), p. 591.

31. Irving, H., Miles, M. G., Pettit, L. D. A Study of Some Problems in Determining the Stoichiometric proton dissociation constants of complexes by potentiometric titrations using a glass electrode. *Anal. Chim. Acta.* **8,** 475–488 (1967).

32. Gran, G. Determination of the Equivalent Point in potentiometric Titrations. *Acta Chem. Scand.* 559–577 (1950).

33. Gans, P., Sabatini, A., Vacca, A. SUPERQUAD: An Improved General Program for Computation of Formation Constants from Potentiometric Data. *J. Chem. Soc., Dalt. Trans.* ***6,*** 1195–1200 (1985).

34. Zékány. I., Nagypal. I. in: D.J. Legget(Ed.), Computational Methods for Determination of Formation Constants, Plenum Press, New York, 1985.

35. Berthon, G. Critical evaluation of the stability constants of metal complexes of amino acids with polar side chains (Technical Report). *Pure Appl. Chem.* **67,** 1117–1240 (1995).

36. Dogan, A., Köseoglu, F., Kilic, E. The Stability Constants of Copper(II) Complexes with Some alfa -Amino Acids in Dioxan–Water Mixtures. *Anal. Biochem.* **295,** 237–239 (2001).

37. Norman, E., Ranford, J. D., Sadler, P. J. Studies of Platinum (II) Methionine Complexes : Metabolites of Cisplatin. *Inorg. Chem.* **31,** 877–888 (1992).

38. Munk, V. P., Sadler, P. J. Palladium(II) diamine complex induces reduction of glutathione disulfide. *Chem. Commun. (Camb).* **1,** 1788–1789 (2004).

39. York, N. Hard and Soft Acids and Bases. *J. Am. Chem. Soc.* **85,** 3533–3539 (1963).

40. *F.A. Cotton (Ed.), Inorganic Syntheses, Vol. XII, McGraw-HILL Book CO, 1972, p. 216.*

41. Mirzahosseini, A., Somlyay, M., Noszál, B. The comprehensive acid–base characterization of glutathione. *Chem. Phys. Lett.* **622,** 50–56 (2015).

42. Breet, E. L., Van Eldik, R. The Isolation and Identification of an Unusual Palladium (II) Substituted Dien Complex. *Inorganica Chim. Acta* **76,** 301–303 (1983).

43. Zhao, G. Chen, Y. Ethylenediamine-palladium (II) complexes with pyridine and its derivatives: synthesis, molecular structure and initial antitumor studies. *J. Inorg. Biochem.* **73,** 145–149 (1999).

Appendix

Appendix A

^{1}H NMR spectrum of H-Ala-Gly–OMe (**2**)

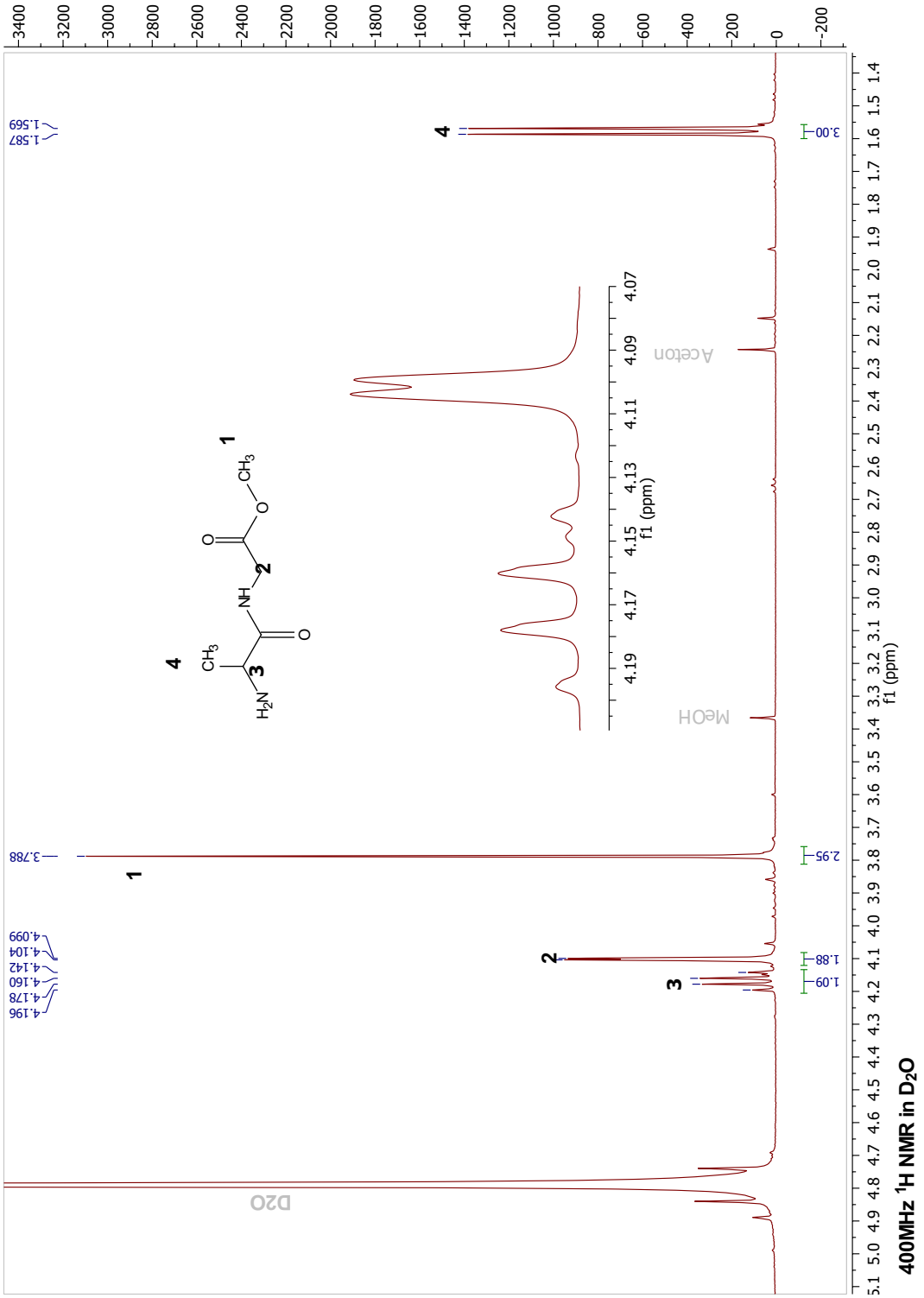

^{13}C NMR spectrum of H-Ala-Gly–OMe (**2**)

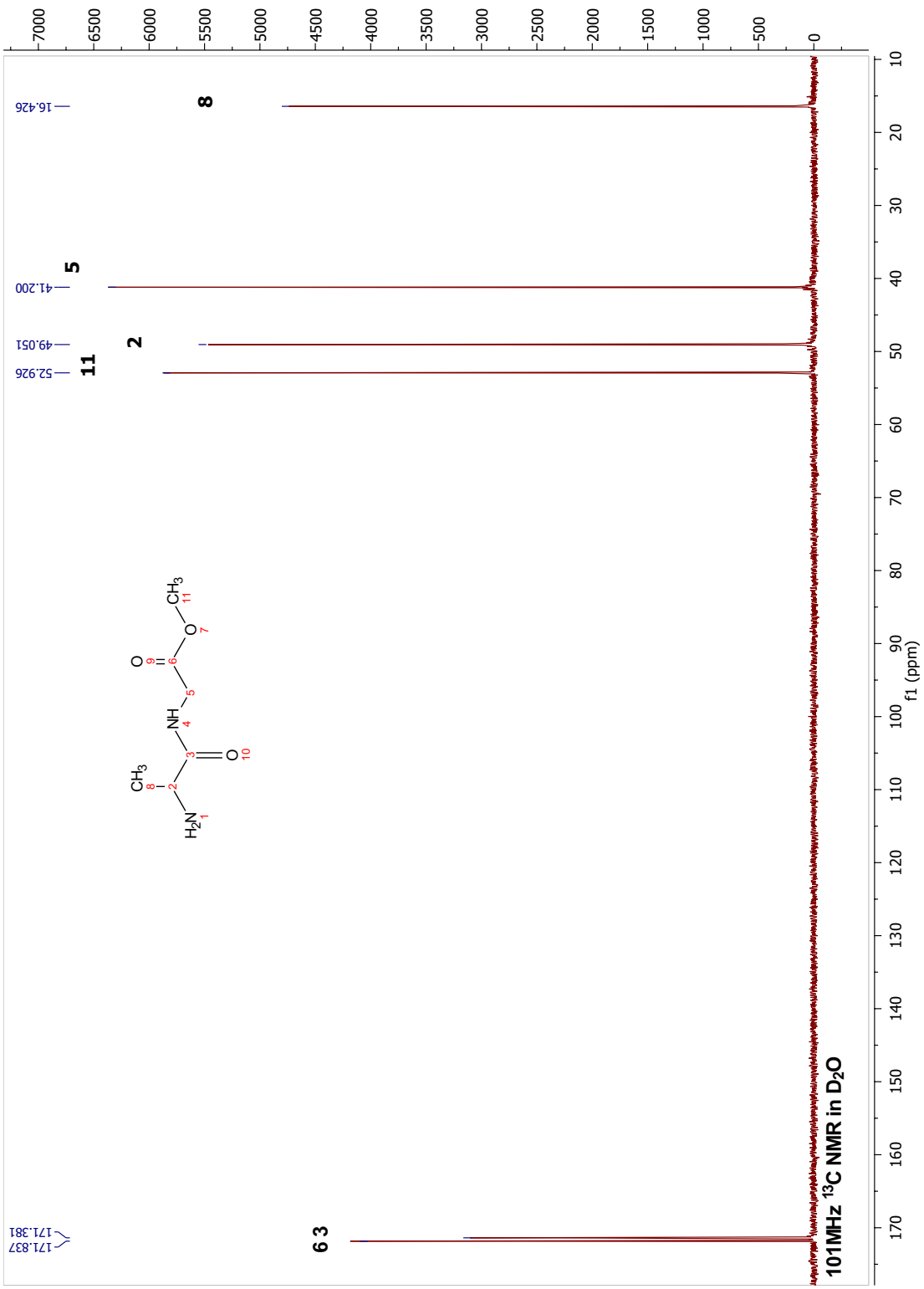

Appendix B

^{1}H NMR spectrum of O^{t}Bu-Fmoc-*iso*Asp-Ala-Gly-OMe (**4**)

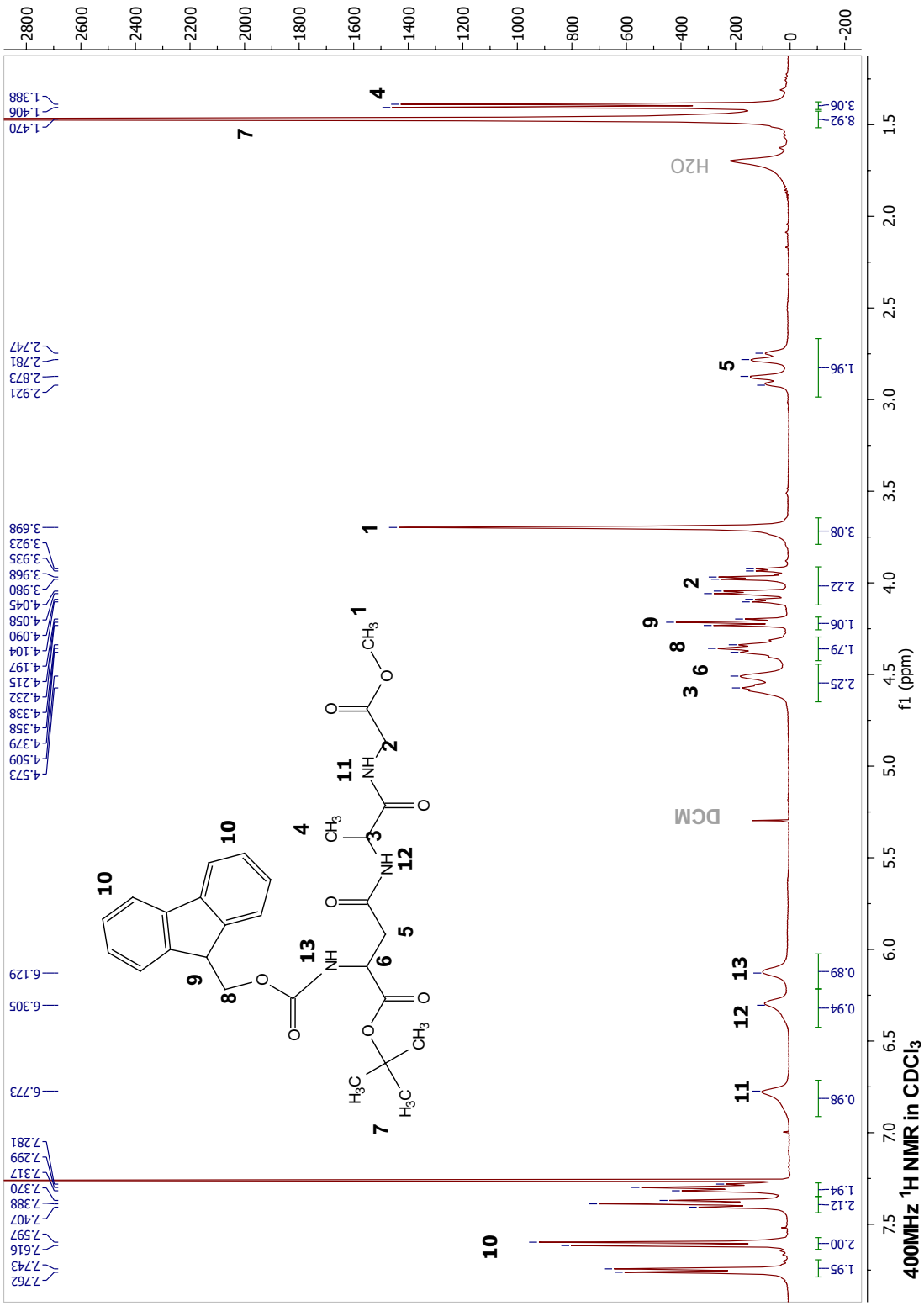

^{1}H COSY spectrum of O^{t}Bu-Fmoc-*iso*Asp-Ala-Gly-OMe (**4**)

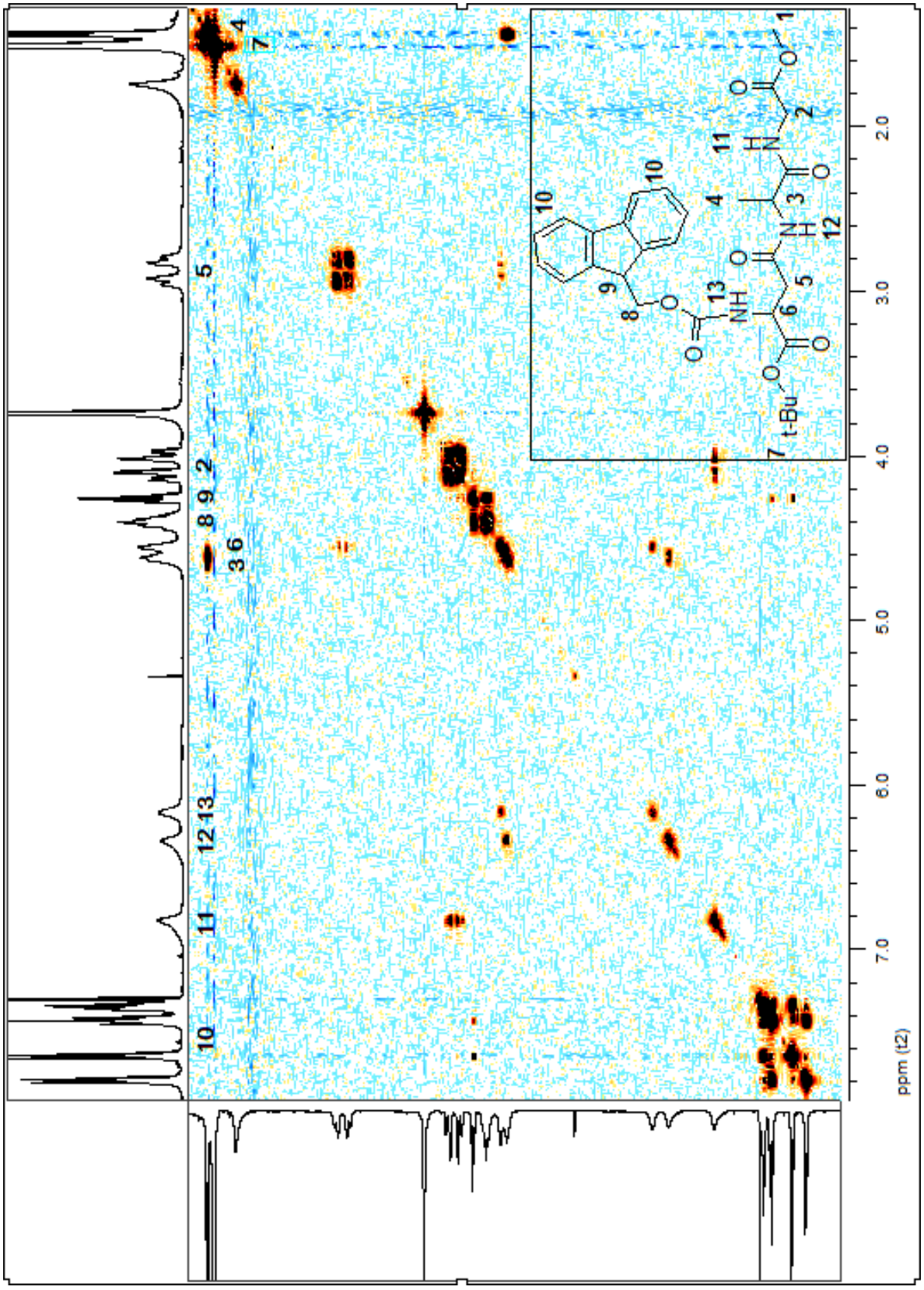

^{13}C NMR spectrum of O^{t}Bu-Fmoc-*iso*Asp-Ala-Gly-OMe (**4**)

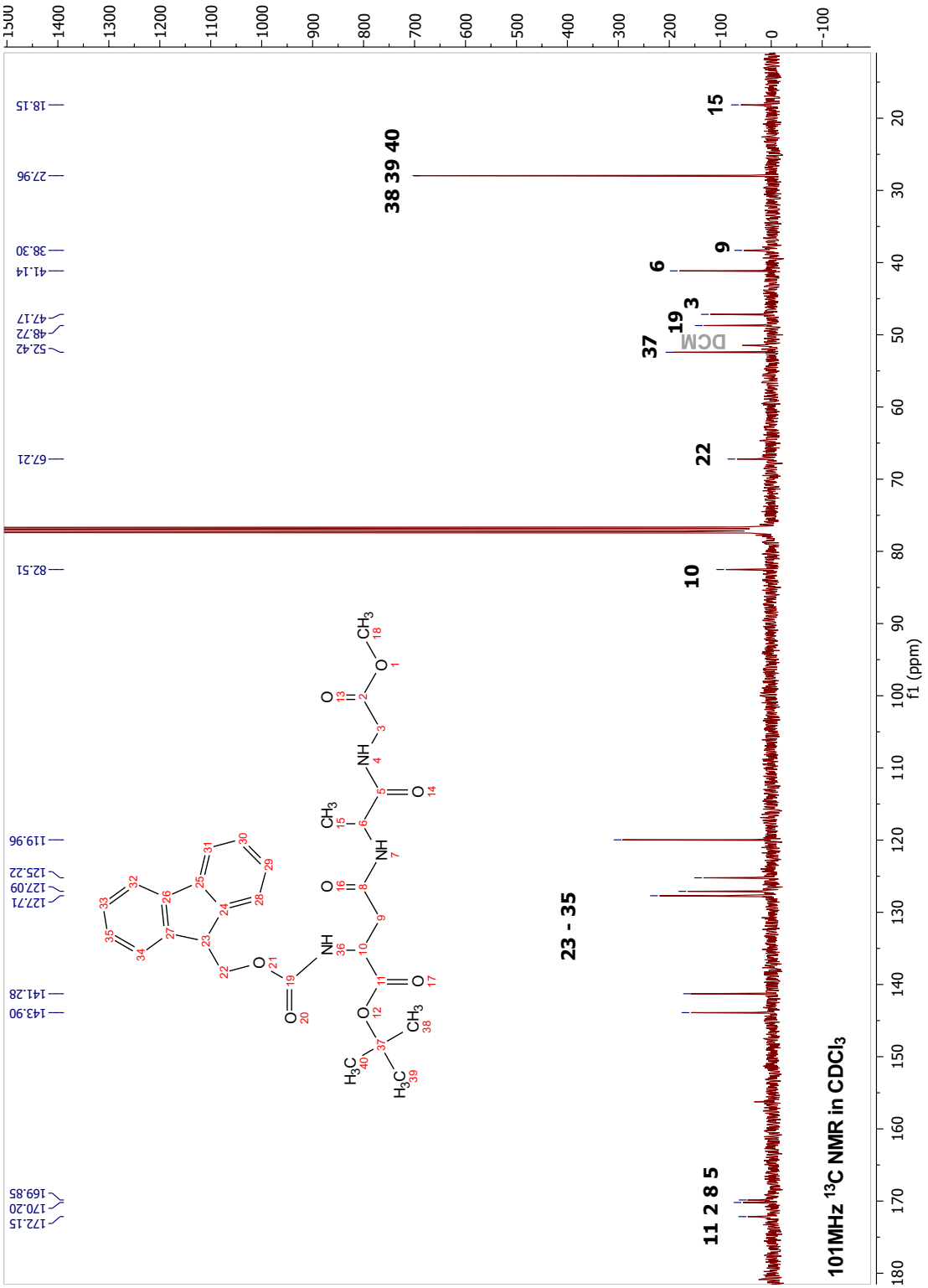

IR spectrum of O^{t}Bu-Fmoc-*iso*Asp-Ala-Gly-OMe (**4**)

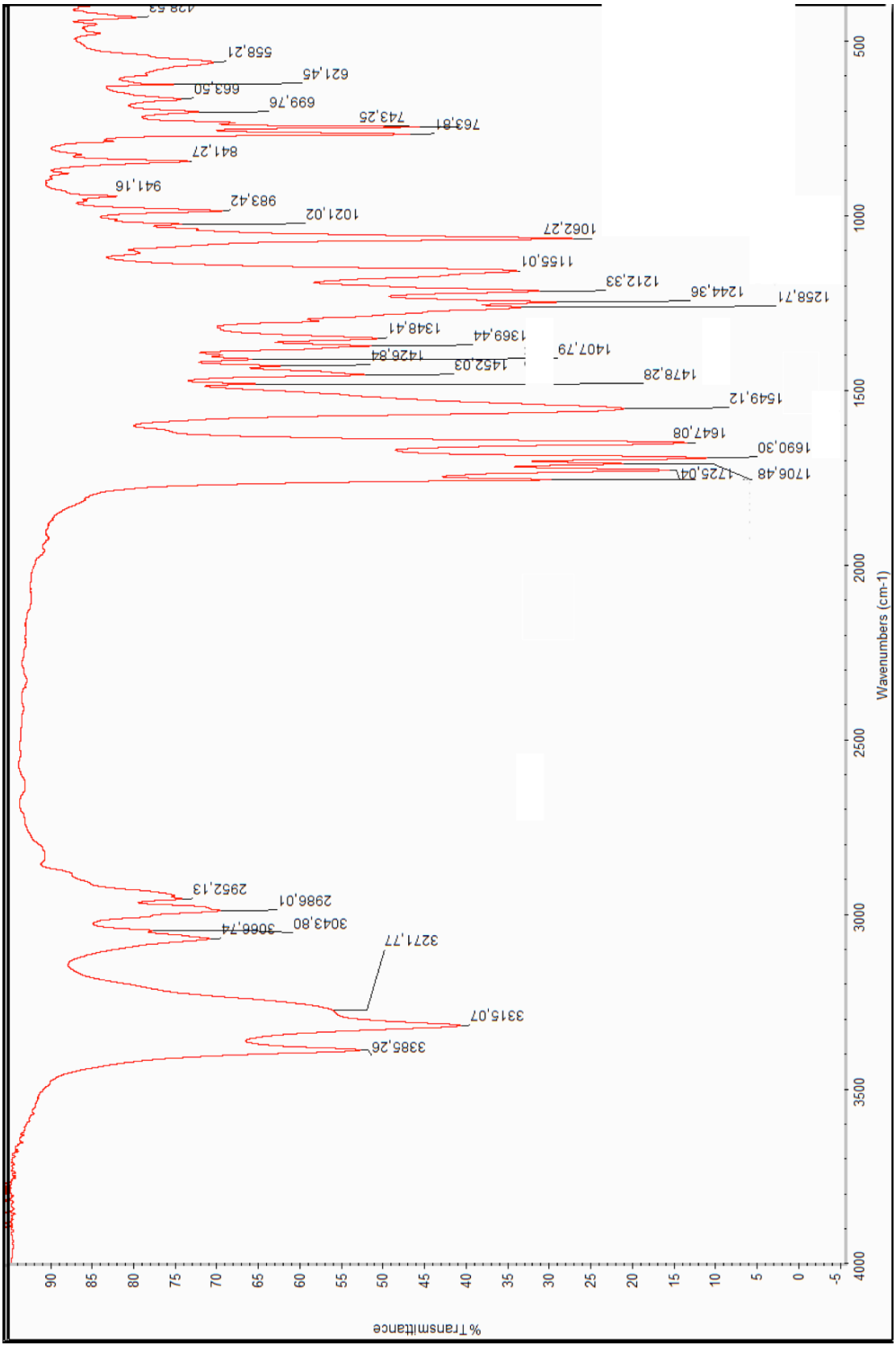

Appendix C

^{1}H NMR spectrum of O^{t}Bu-*iso*Asp-Ala-Gly-OMe (**5**)

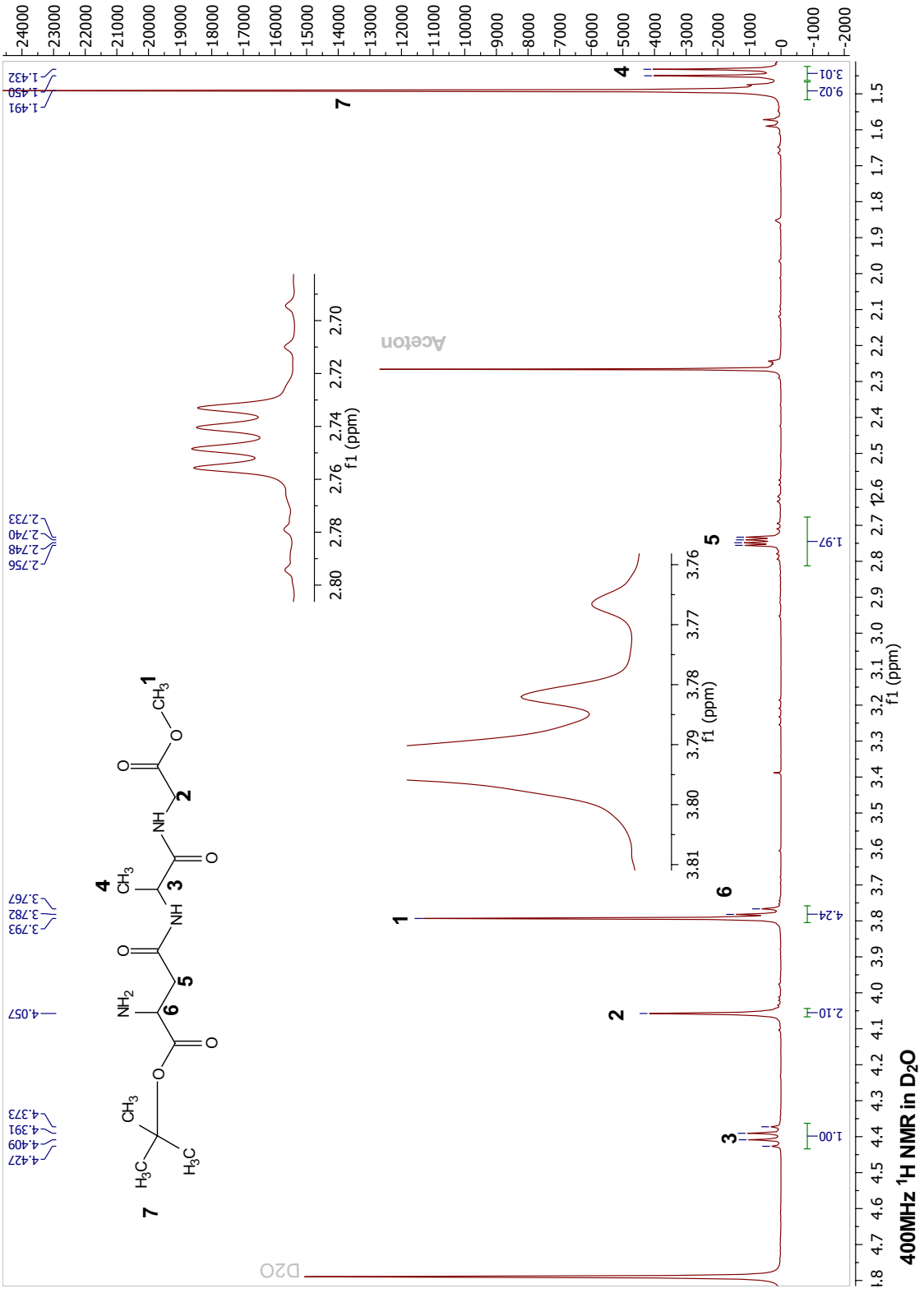

^{13}C NMR spectrum of O^{t}Bu-*iso*Asp-Ala-Gly-OMe (**4**)

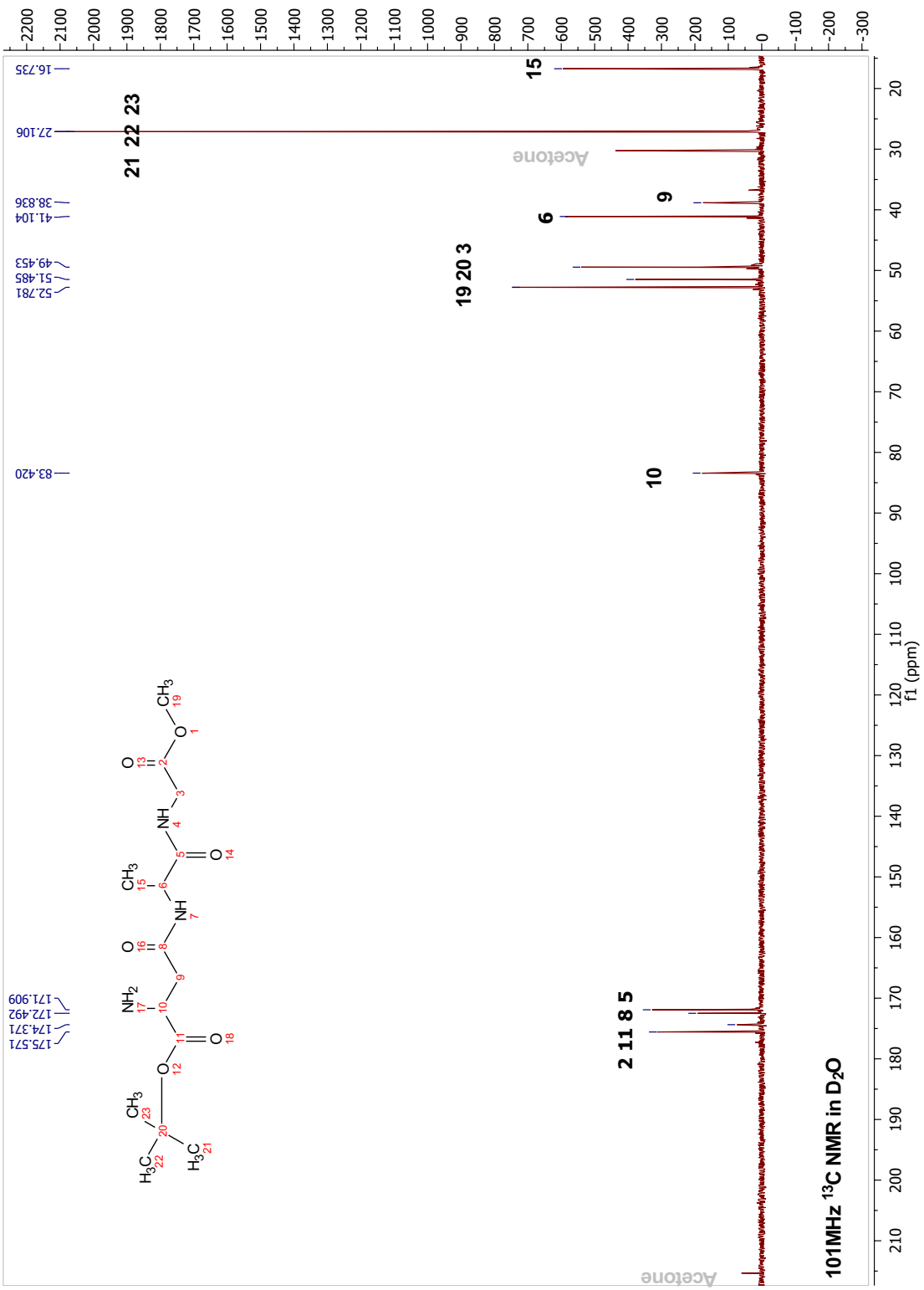

IR spectrum of O^{t}Bu-*iso*Asp-Ala-Gly-OMe (**4**)

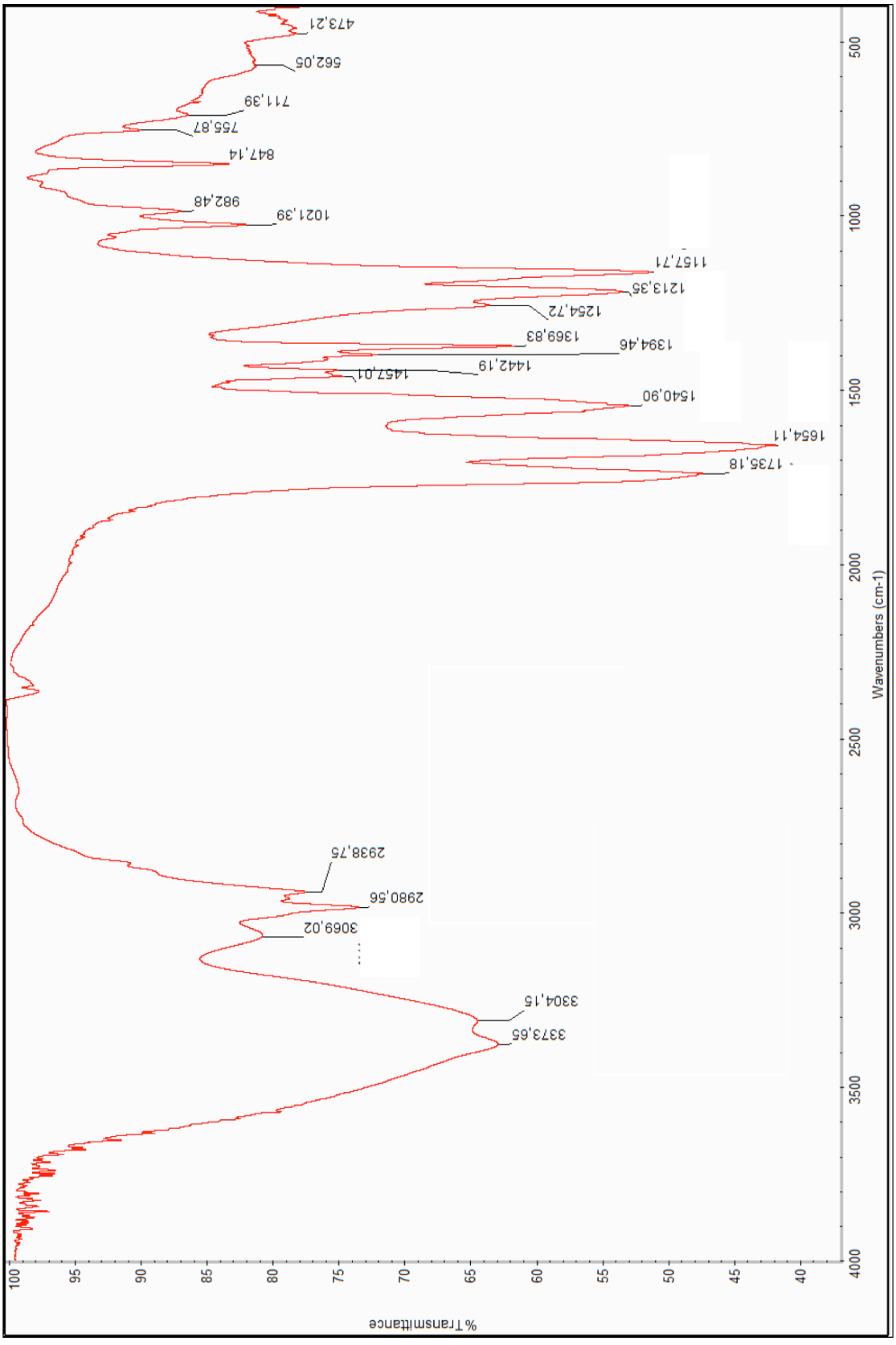

Appendix D

Uv-Vis spectrum of Pd-O^{t}Bu-*iso*Asp-Ala-Gly-OMe (**8**) and (**9**)

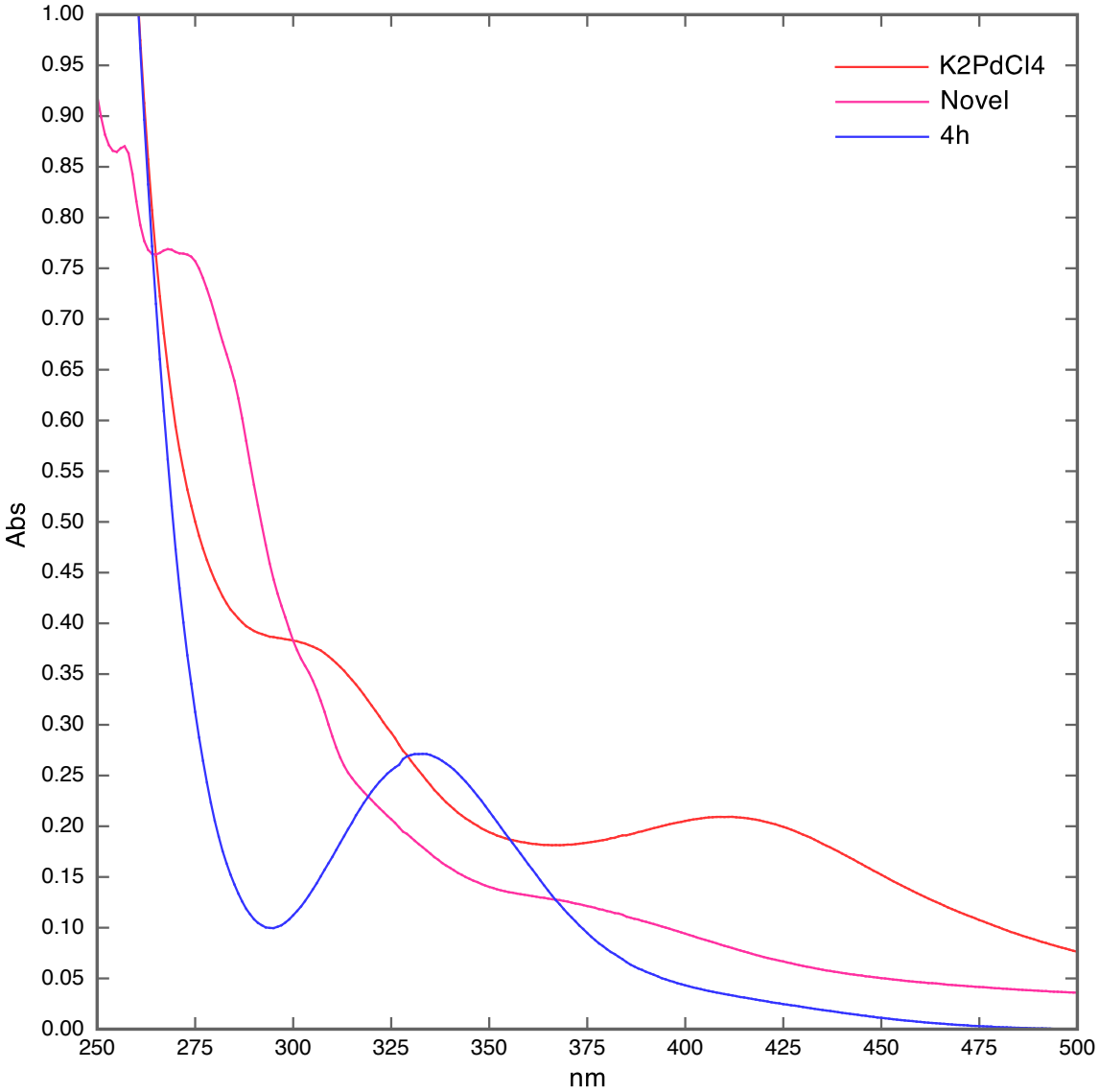

IR spectrum of Pd-O^{t}Bu-*iso*Asp-Ala-Gly-OMe (8) and (9)

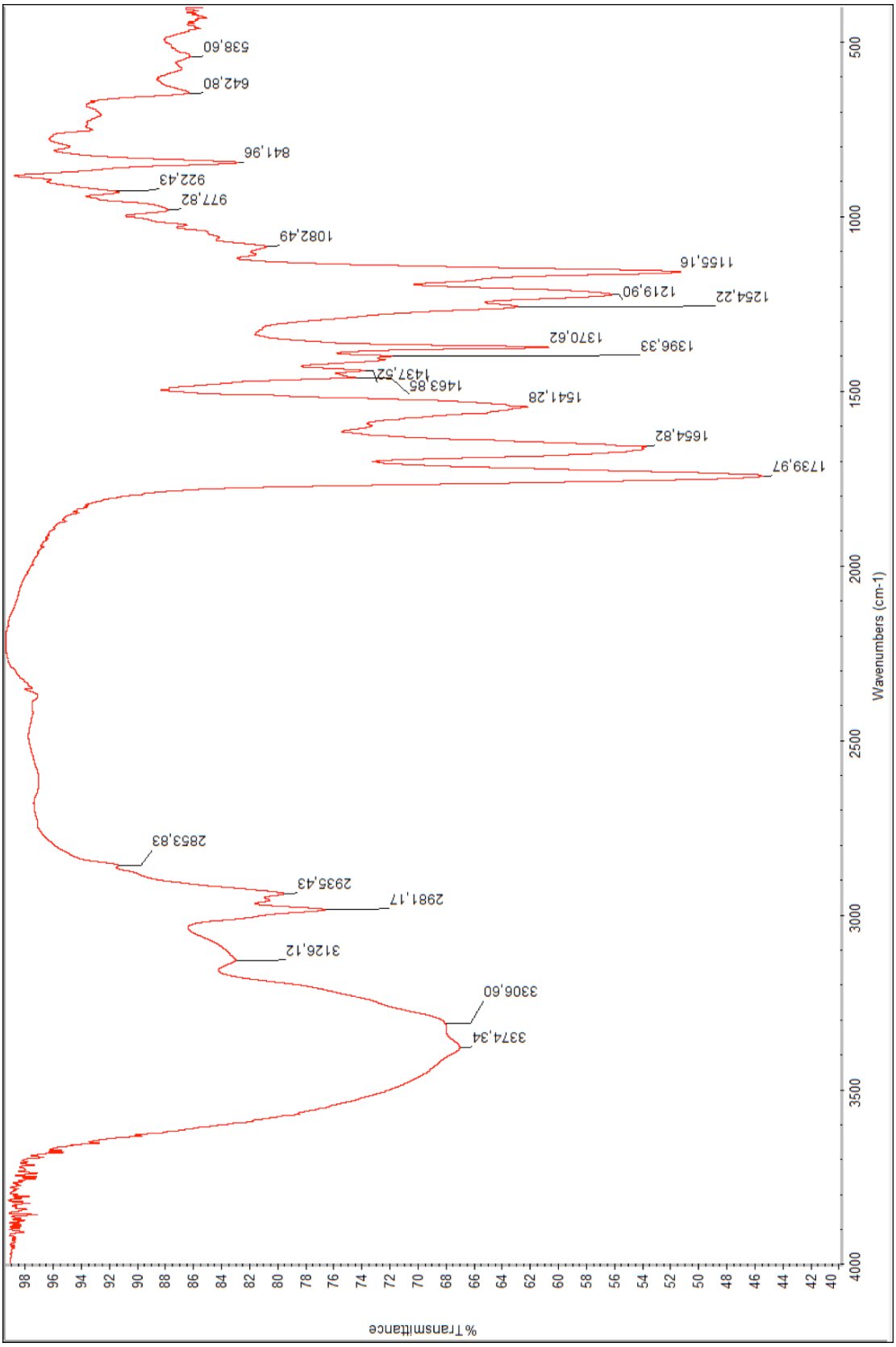

Appendix E

^{1}H NMR spectrum of GSH(SMe)(**13**)

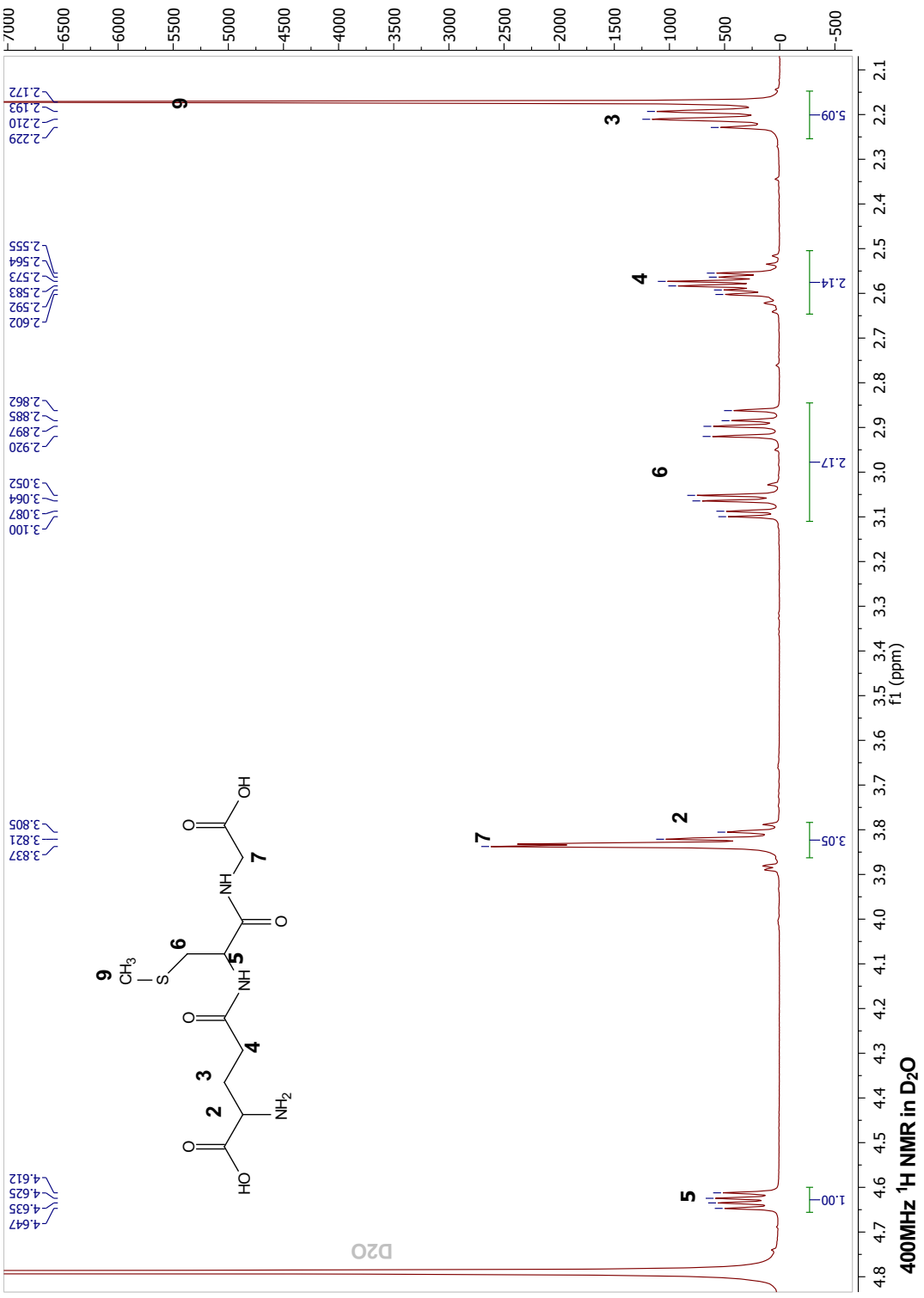

^{13}C NMR spectrum of GSH(SMe)(**13**)

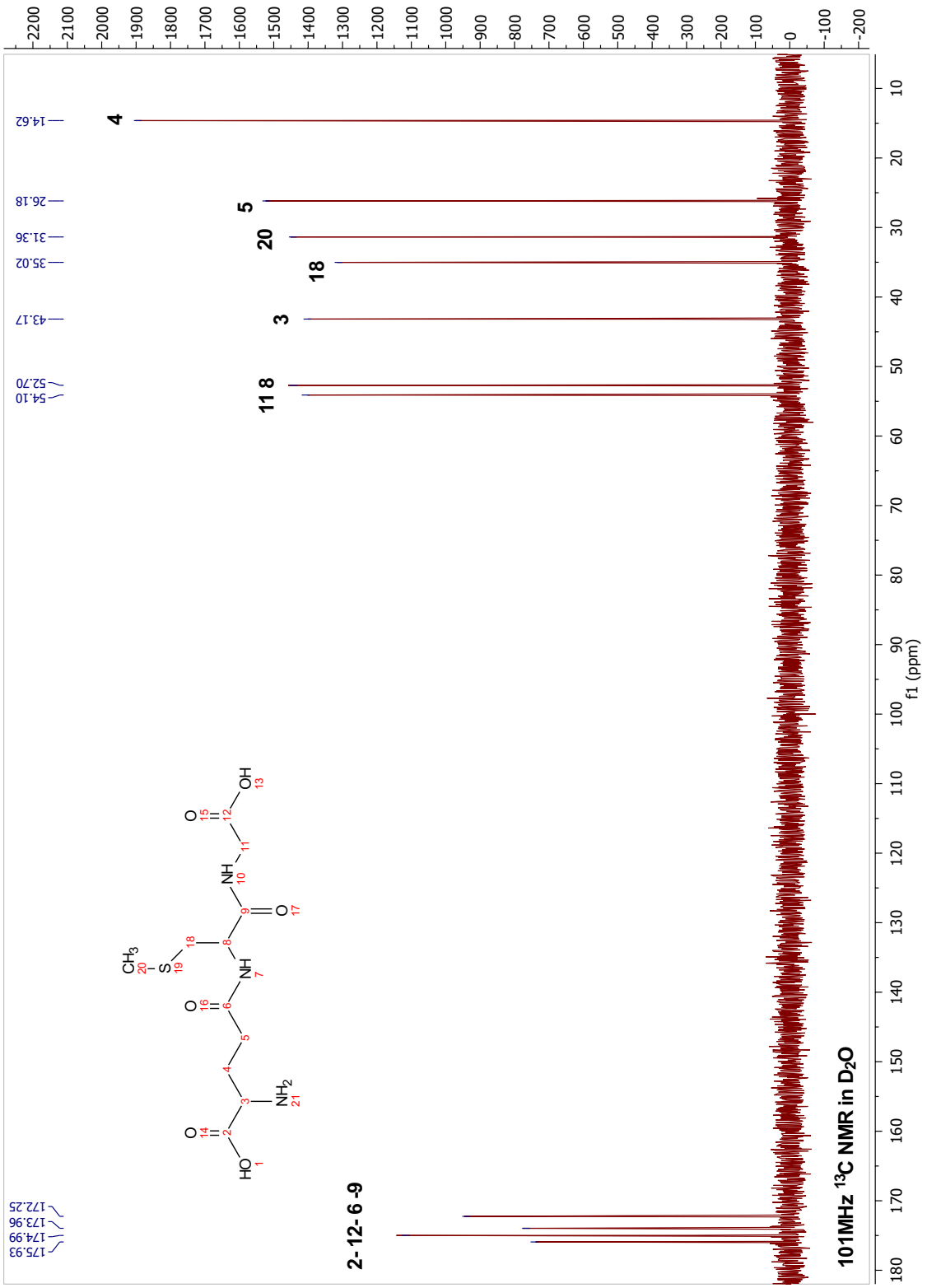

Appendix F

^{1}H NMR spectrum of {GSH(OMe)$_2$(SMe)} (**12**)

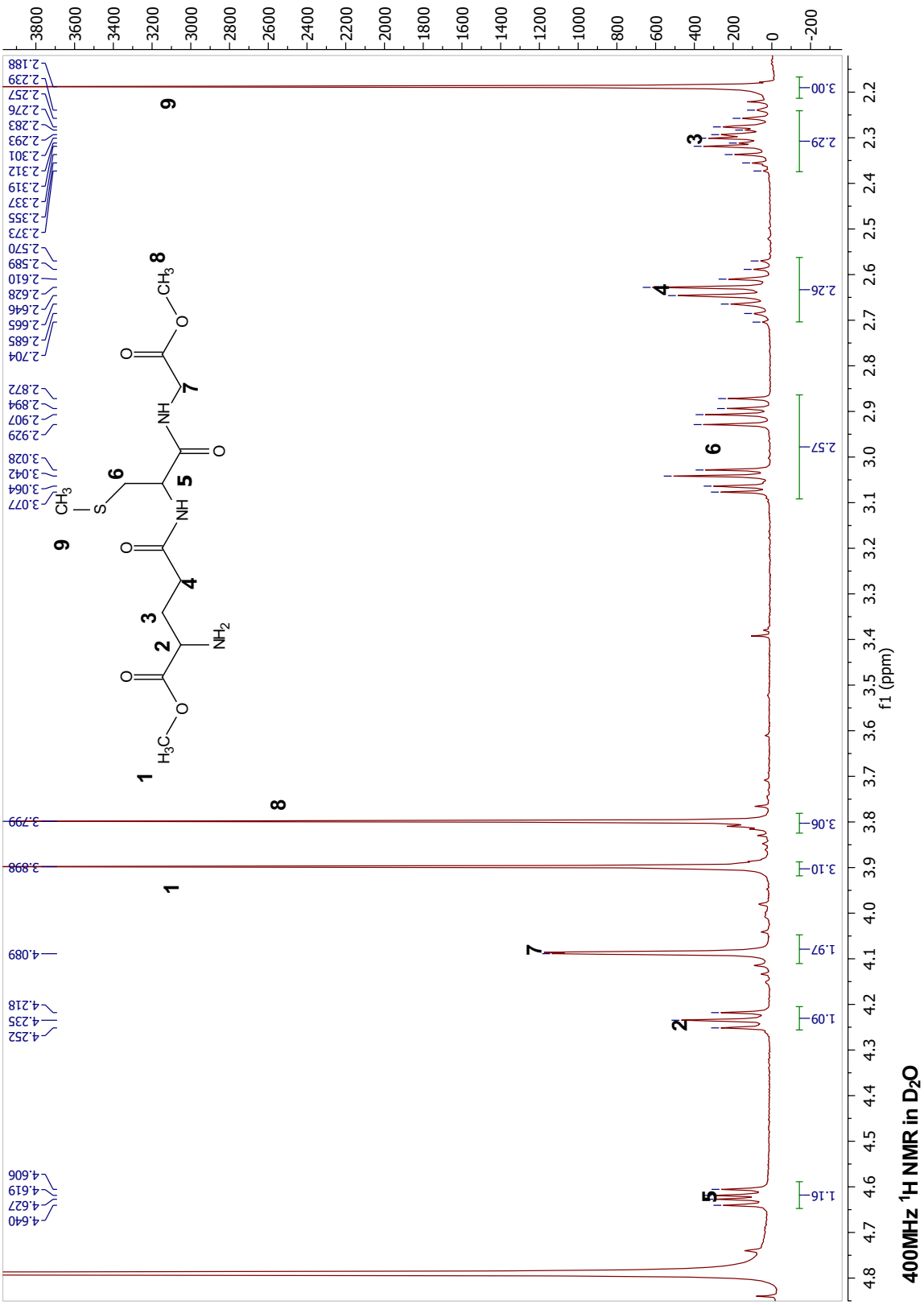

^{13}C NMR spectrum of {GSH(OMe)$_2$(SMe)} (**12**)

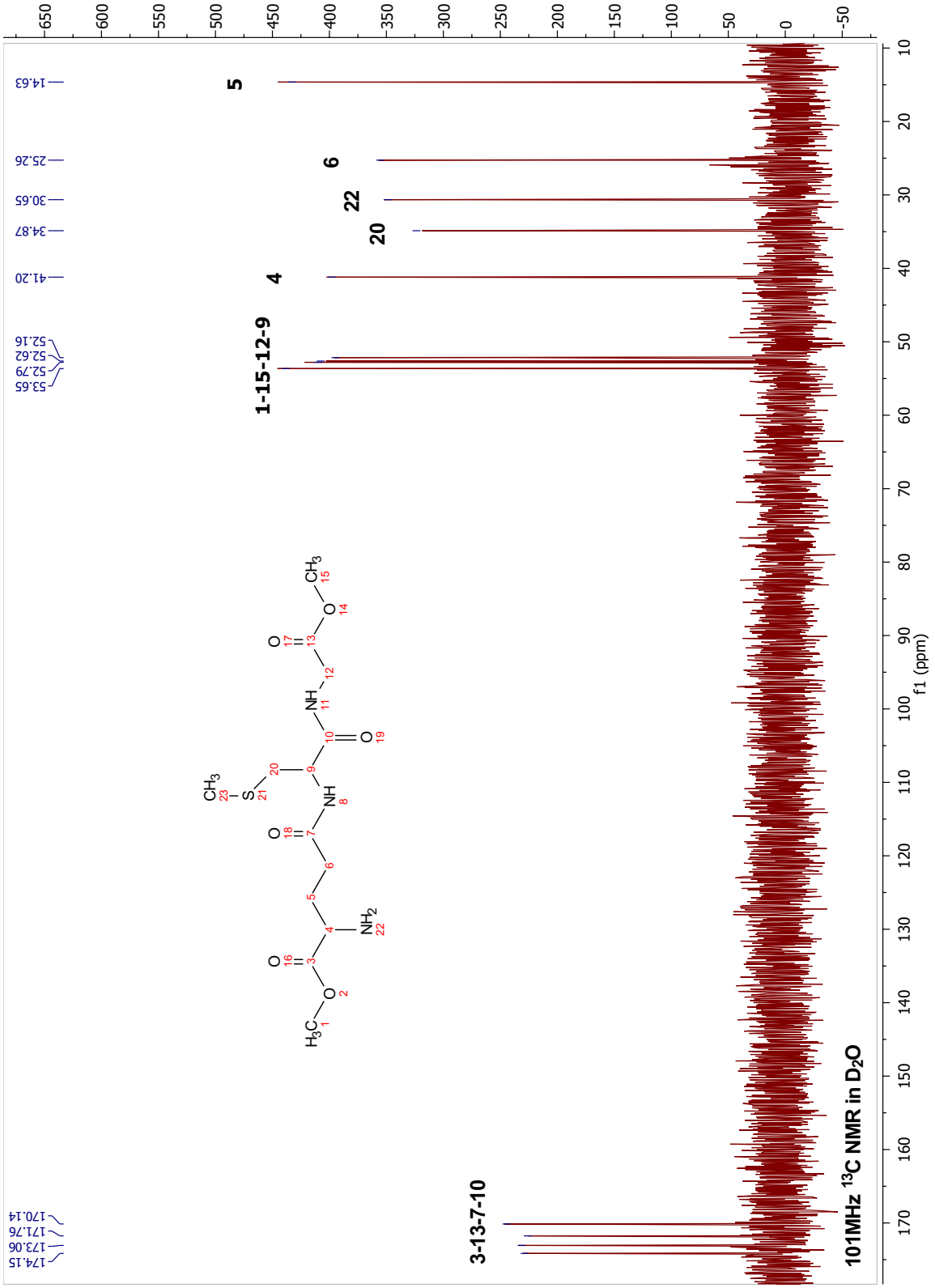

IR spectrum of {GSH(OMe)$_2$(SMe)} (**12**)

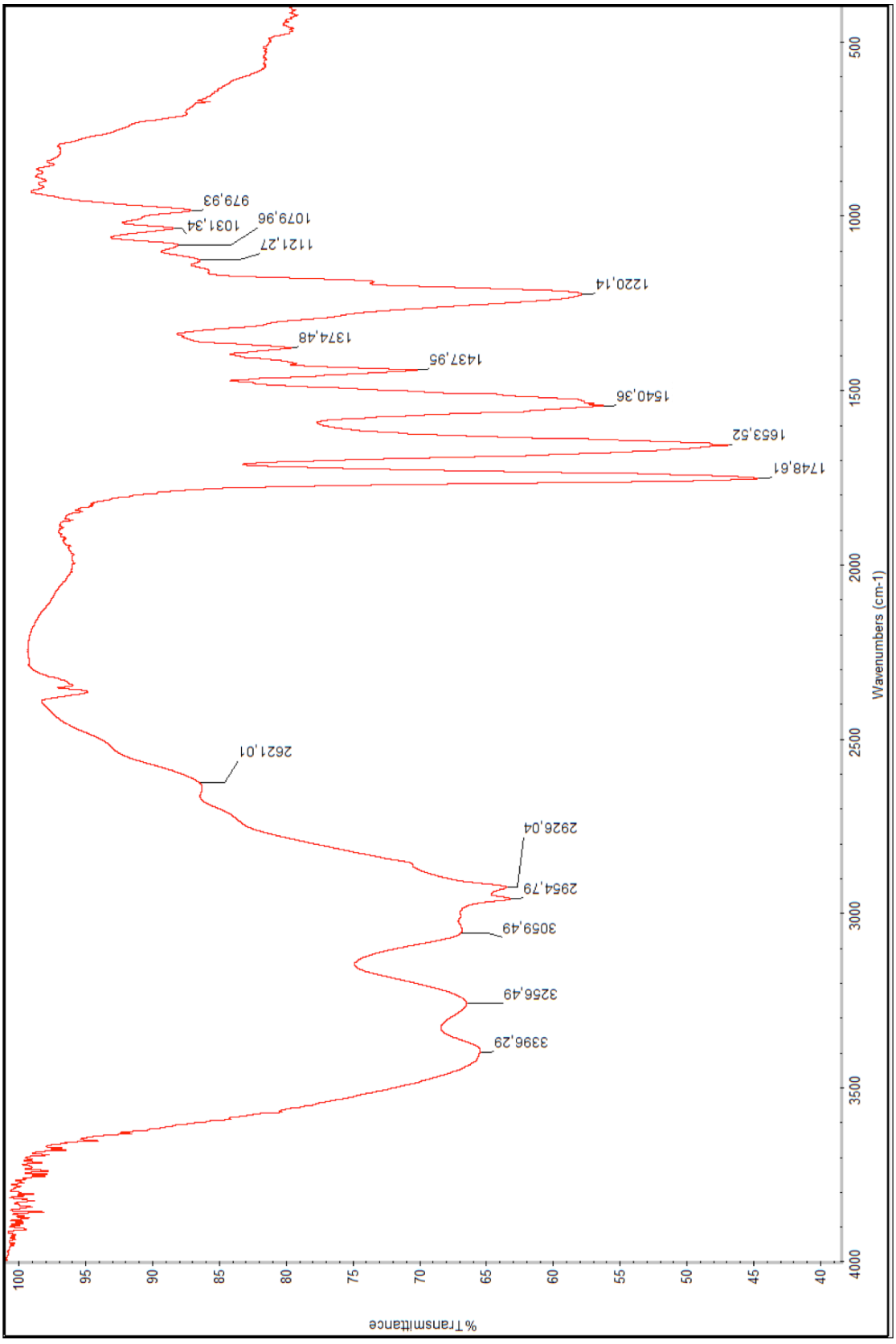

Appendix G

^{1}H NMR spectrum of $[Pd(en)Cl_2]$

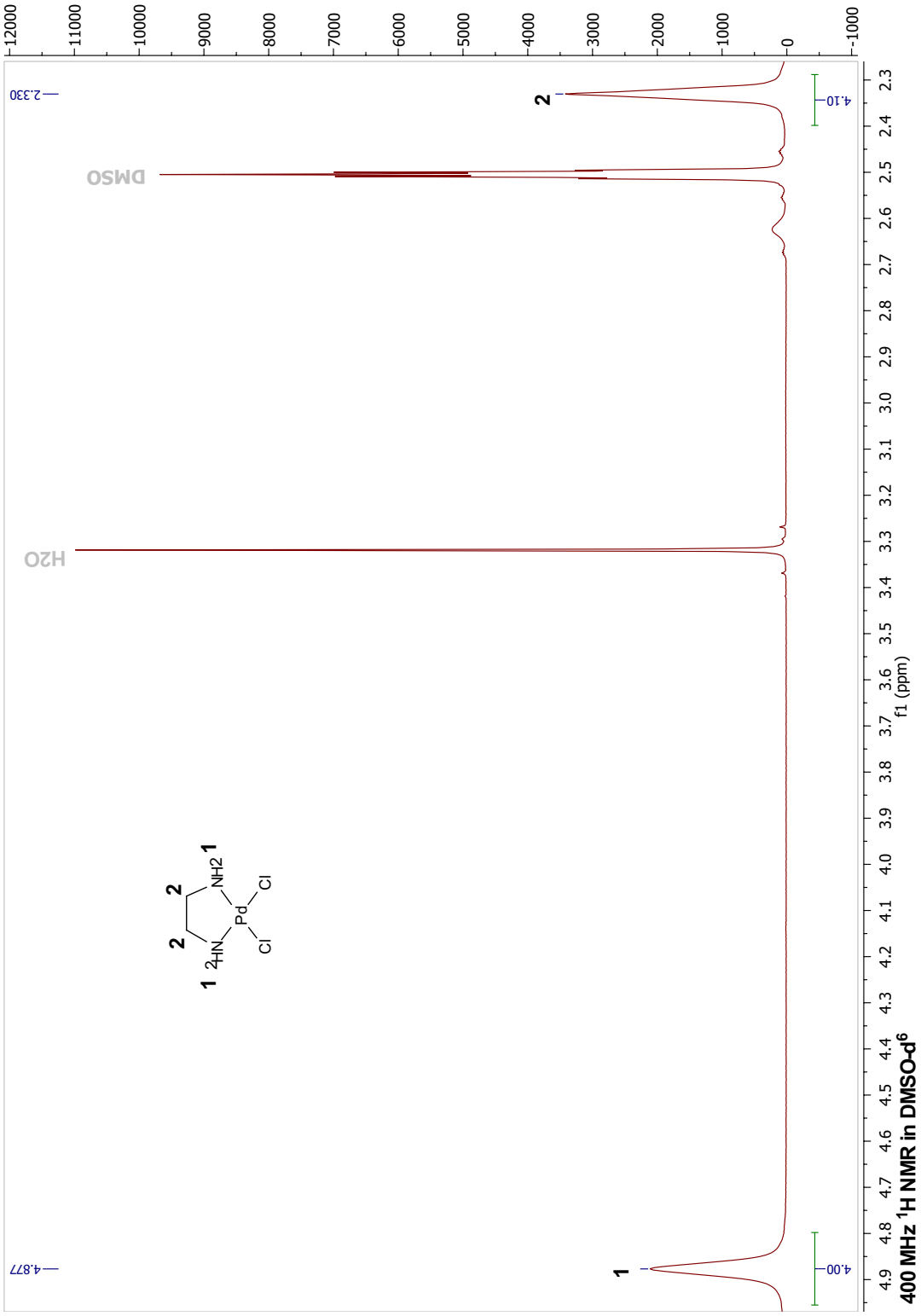

IR spectrum of $[Pd(en)Cl_2]$

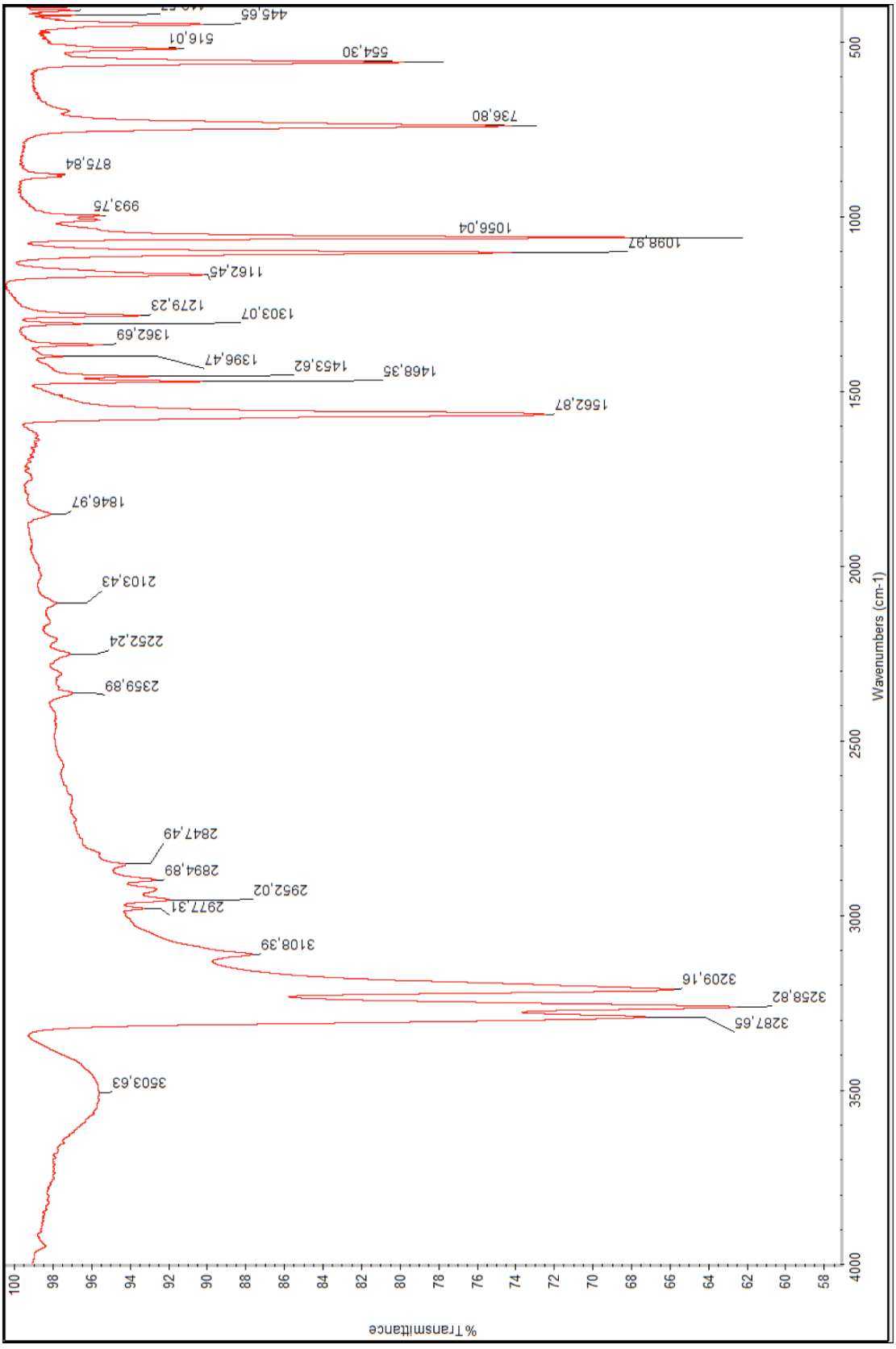

^{1}H NMR spectrum of $[Pd(en)(H_{2O})](NO_3)_2$

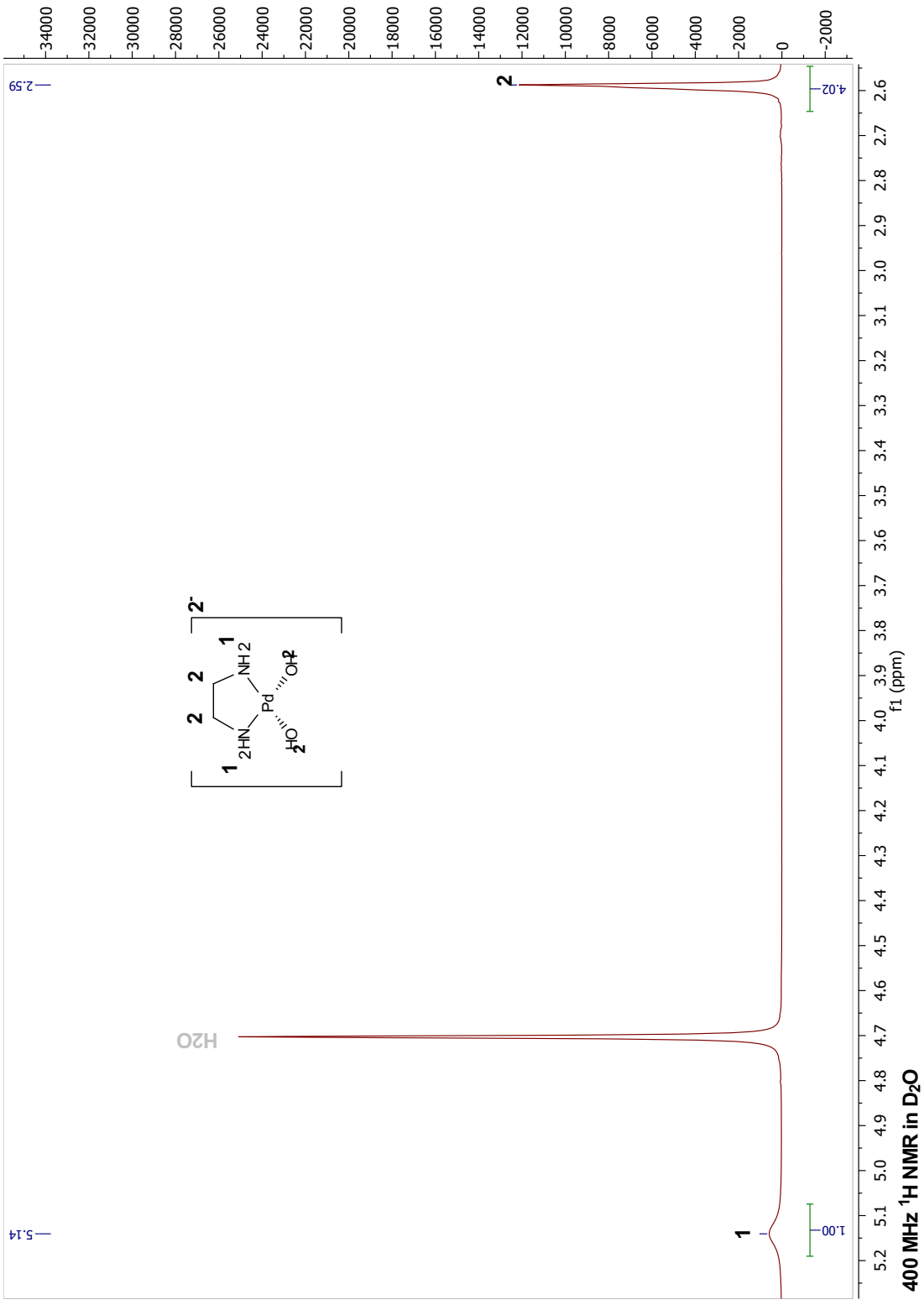

IR spectrum of $[Pd(en)(H_2O)](NO_3)_2$

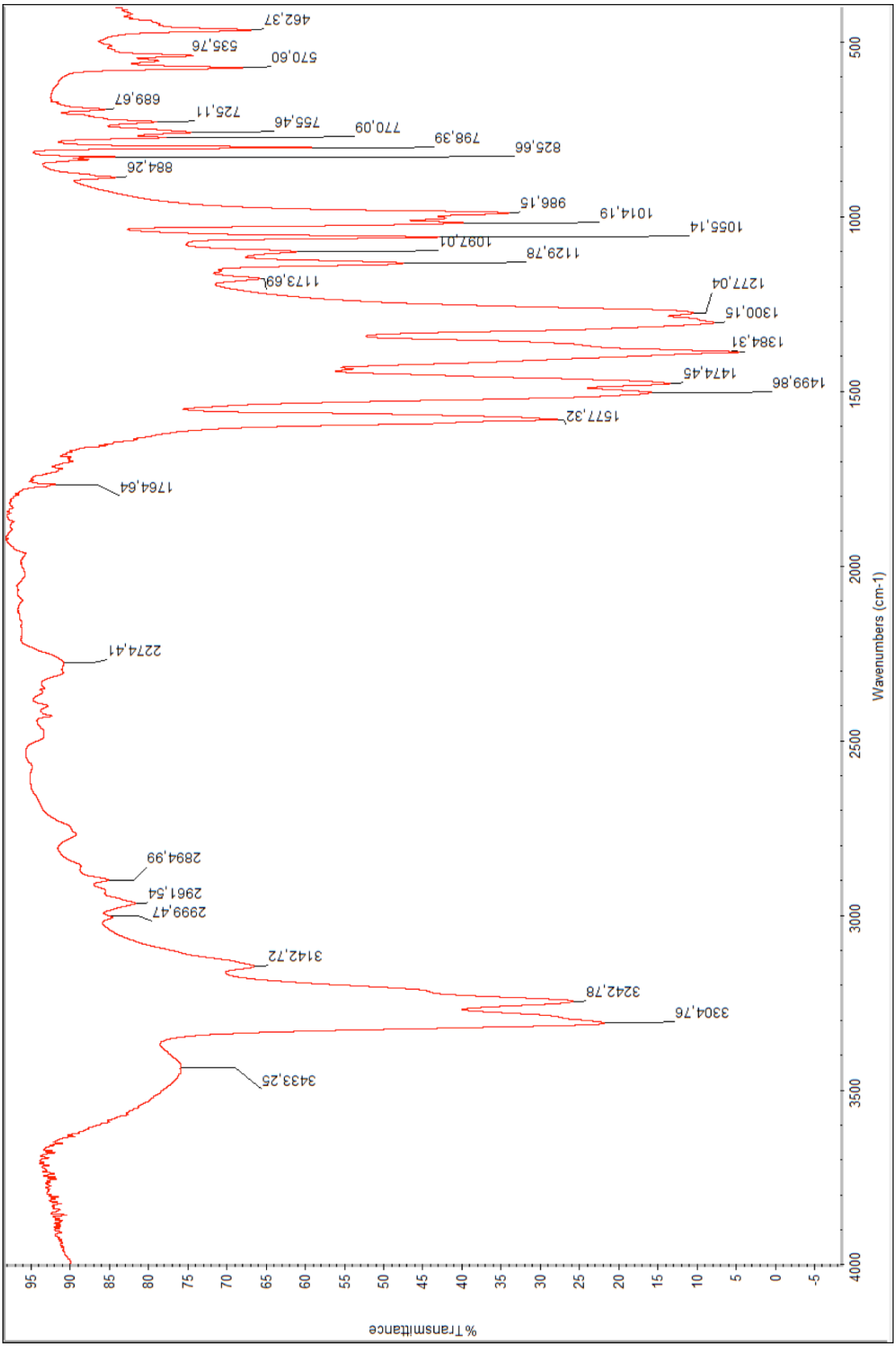

^{1}H NMR spectrum of [Pd(dien)Cl]Cl

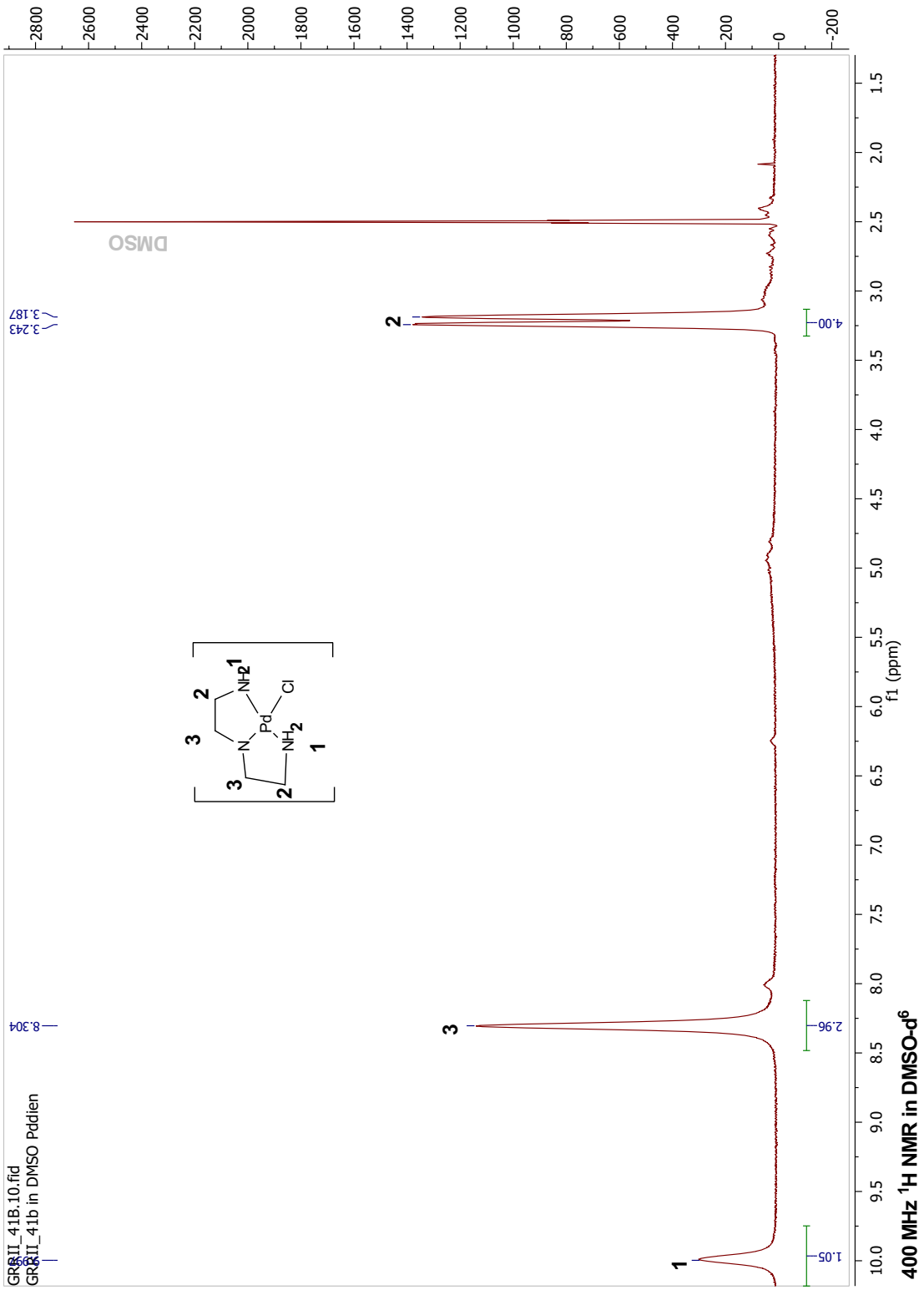

IR spectrum of [Pd(dien)Cl]Cl